Holonomic Space

Field Theory, Mereology, and the Geometry of Admissibility

Flyxion

Independent Researcher

Draft — June 4, 2026

Preface

Every observation is incomplete.

This statement is so familiar that it rarely attracts attention. Maps leave things out. Photographs flatten depth. Memories omit details. Scientific instruments reveal some features while hiding others. Even our most sophisticated mathematical models preserve certain structures while discarding the rest.

Yet this commonplace fact raises a surprisingly deep question.

If every observation is incomplete, how do we know anything at all?

This book is an attempt to answer that question.

The traditional approach to science begins with objects and asks how they behave. The approach taken here begins with observation and asks what can be reconstructed from it. The shift is subtle but important. Rather than treating observation as transparent access to reality, we treat it as a structured projection from a richer domain into a more limited one.

The central claim of this book can be expressed in ordinary language:

Observation is not access.

Observation is admissible projection.

The same claim can be expressed mathematically:

$$\mathcal{M} \xrightarrow{F} \text{Admissible Local Data} \xrightarrow{\pi} \text{Observable State}, \qquad \ker(\pi \circ F) \neq 0$$

The meaning of this diagram is simple. Reality, whatever its ultimate nature, is not presented directly to an observer. Instead, it is filtered through a process that determines which information is accessible and which is not. The resulting observable state contains genuine information about the world, but it does not contain all of it.

The lost information is not necessarily destroyed. It may simply lie beyond the reach of a particular observer, instrument, scale, or horizon.

The question that follows is the question that motivates every chapter of this book:

Given a projection with nontrivial kernel,

what global structure can be reconstructed from what remains?

The answer will take us through maps, photographs, memory, machine learning, category theory, sheaf cohomology, agency, quantum measurement, and cosmology. These subjects may appear unrelated. The argument of this book is that they are all instances of the same underlying problem: each studies the relationship between what exists, what is observed, and what can be reconstructed.

A note on mathematical status

This book is careful to distinguish four levels of claim:

- [**Proven**] — statements that follow from established mathematics or physics by standard arguments.
- [**Established framework**] — mathematical structures that are well-defined and self-consistent, even where specific theorems remain incomplete.
- [**Conjectured**] — claims that are strongly motivated and precisely stated but not yet proved.
- [**Open Problem**] — problems that remain genuinely open, stated as research targets.

The reader can therefore track exactly where the framework stands. One of the recurring pathologies in theoretical physics is the tendency to present conjectural mathematics as established mathematics. This book resists that tendency by marking its own uncertainty explicitly.

How to read this book

The book is organized so that the cosmological interpretation appears only after the mathematical machinery that supports it has been fully developed.

Part I introduces the central ideas through familiar examples that require no prior mathematics beyond basic algebra.

Parts II–III develop the variational, dynamical, and statistical-mechanical foundations.

Part IV provides the functional-analytic well-posedness theory that determines which mathematical structures are legitimate.

Part V introduces the admissibility sheaf, reconstruction theory, and the category-theoretic framework.

Part VI states the major open problems explicitly, so that the reader enters the cosmological chapters knowing exactly what has and has not been established.

Part VII applies the framework to cosmological structure formation, redshift, and comparison with standard cosmology.

A reader primarily interested in the mathematics may read Parts I–VI as a self-contained treatment of admissibility, reconstruction, and sheaf cohomology, with cosmology appearing as a worked example. A reader primarily interested in cosmology may read

Part I and then proceed directly to Part VII, returning to the intervening parts for technical support as needed.

Flyxion
Canada

Contents

Part I

Observation, Projection, and Reconstruction

Introduction to Part I

Part I introduces the central thesis of this book through seven examples that require no prior mathematics beyond basic algebra. The examples are chosen because every reader already knows, intuitively, that observation is not the same as reality. The purpose of Part I is to make that intuition precise.

Established So Far

Nothing has been assumed beyond familiarity with the idea that representations simplify. No prior mathematics is required to enter Part I.

New Ideas Introduced in This Part

- **Projection** $\pi : X \to M$: any map that preserves some structure while discarding the rest.
- **Kernel** $\ker(\pi)$: the pairs a projection fails to distinguish; the measure of what is lost.
- **Quotient space** $X/{\sim_\pi}$: the territory as the map represents it.
- **Admissibility class** $\pi^{-1}(m)$: the set of originals consistent with an observation.
- **Reconstruction error** $E(x) = d(x, G(F(x)))$: the fidelity of reconstruction without exactness.
- **Bidirectional information loss**: both coarse-graining and over-resolution destroy information.
- **Admissibility as task-relative**: the right observation is not the most detailed one.
- **Detector equivalence**: physically distinct states that produce identical measurements.
- **The Ocularum**: the structured observational domain of an observer.
- **Horizon-relative reconstruction**: different observers reconstruct different models of the same whole.

Dependencies

Part I has no mathematical prerequisites. Readers familiar with basic set theory will find the notation straightforward. All formal definitions are introduced from scratch.

What Remains Open After This Part

Part I establishes the *conceptual* framework. It does not yet provide the mathematical machinery needed to make admissibility precise, compute obstruction classes, or derive the RSVP dynamics. Those tools come in Parts II–V.
In particular, the following questions raised in Part I are not answered until later:

- When can multiple local observations be assembled into a global reconstruction? (Chapter 28)
- What mathematical object measures the failure of global reconstruction? (Chapter 33)
- How does the admissibility of an observation depend on the governing dynamics? (Part IV)
- What is the precise relationship between the RSVP fields and the admissibility framework? (Part V)

The single question that Part I raises and the rest of the book answers:

> Given a projection with nontrivial kernel,
> what global structure can be reconstructed from what remains?

Chapter 1

The Map Is Not the Territory

The map is not the territory,
and the name is not the thing named.
— Alfred Korzybski

Why This Matters

The map example is not about cartography. It is the first appearance of a central theme: *useful representations depend on forgetting.* Later chapters will show that detector measurements, memories, and cosmological observations obey exactly the same principle. The mathematics introduced here—projection, kernel, quotient—will reappear in every subsequent part of the book.

1.1 A useful object that is always wrong

A map is a strange object.

It is useful precisely because it is wrong.

A road map does not show trees, clouds, buildings, birds, or people. A topographic map ignores political borders. A political map ignores elevation. A transit map distorts distance while preserving connectivity.

Every successful map leaves something out.

At first glance this seems obvious. No map could contain every detail of the territory it represents. A perfect map would be as large and as complicated as the territory itself and would therefore fail in its purpose.

But this observation has a deeper consequence.

The usefulness of a map depends not merely on what it contains, but on what it discards.

A traveler cares about roads. A geologist cares about elevation. A city planner cares about infrastructure.

The same territory gives rise to many different maps because different tasks require different projections.

1.2 The projection

Technical Note 1.1: Projection

Throughout this book, a *projection* need not be linear. The term is used in the broader sense of any map

$$\pi : X \to Y$$

that preserves some structure while discarding other structure. Quotient maps, detector outputs, coarse-grainings, and observational restrictions are all projections in this sense.

Let X denote a territory and let M denote a map. The map is a projection

$$\pi : X \to M.$$

The projection preserves some structure and discards the rest.

Suppose two distinct features of the territory are represented identically on the map:

$$\pi(x_1) = \pi(x_2), \qquad x_1 \neq x_2.$$

The map cannot distinguish between them. From the perspective of the map, these two features are equivalent.

The territory has therefore been partitioned into equivalence classes:

$$x_1 \sim_\pi x_2 \iff \pi(x_1) = \pi(x_2).$$

Definition 1.1 (Projection equivalence). Given a map $\pi : X \to M$, two points $x_1, x_2 \in X$ are *projection-equivalent* if $\pi(x_1) = \pi(x_2)$. The equivalence class of x is denoted $[x]_\pi$.

The map is then a faithful representation of the quotient space:

$$M \cong X/{\sim_\pi}.$$

Forward Reference

The equivalence relation $x_1 \sim_\pi x_2$ introduced here will later reappear as *observational equivalence* in detector theory (Chapter 5) and as *horizon equivalence* in cosmology (Chapter 7 and Part VII). In all three cases the same mathematics governs what an observer cannot distinguish.

1.3 The kernel

The information lost by a projection can be measured precisely.

Definition 1.2 (Kernel of a projection). Let $\pi : X \to M$ be a projection. The *kernel* of π is the collection of all pairs that π fails to distinguish:

$$\ker(\pi) = \{(x_1, x_2) \in X \times X : \pi(x_1) = \pi(x_2),\ x_1 \neq x_2\}.$$

A projection is *injective* (loses no information) if and only if $\ker(\pi) = \emptyset$.

Every useful map has a nontrivial kernel.

Two cities at the same elevation appear identically on a topographic contour. Two neighborhoods in the same postal district appear identically on a postal map. Two points equidistant from the center appear identically on a radial transit diagram.

The kernel is not a defect. It is the mechanism by which the map achieves its purpose.

Common Misconception

Information loss does not imply ignorance. A map loses information yet remains useful. The question is not whether information was discarded. The question is whether the discarded information is *relevant to the reconstruction task*. A road map that omits bird migration patterns is not deficient for a traveler. It is appropriately filtered.

The first lesson of admissibility is not that information is lost.

It is that information *must* be lost.

Without forgetting, representation itself would be impossible.

1.4 Many maps, one territory

Different projections of the same territory reveal different structure. No single projection is complete.

This suggests a natural question: given a collection of maps, can the territory be recovered?

Example 1.3 (Recovering terrain from multiple projections)**.** A topographic map preserves elevation. A road map preserves connectivity. A geological map preserves rock type. Given all three simultaneously, a geologist can reconstruct considerably more of the territory than any single map provides. The reconstruction is still incomplete—the maps say nothing about weather, population, or history—but it is richer than any individual projection.

Definition 1.4 (Reconstruction from projections)**.** Given a collection of projections $\{\pi_i : X \to M_i\}_{i\in I}$ and observed data $\{m_i \in M_i\}_{i\in I}$, the *reconstruction problem* asks: find $x \in X$ such that $\pi_i(x) = m_i$ for all $i \in I$.

In general, the reconstruction problem has no unique solution. The set of solutions is

$$\mathcal{R}(\{m_i\}) = \bigcap_{i\in I} \pi_i^{-1}(m_i) \subseteq X.$$

The reconstruction is unique if and only if $\mathcal{R}$ contains exactly one point.

When $\mathcal{R}$ contains many points, additional constraints are required to select among them. These constraints are *admissibility conditions*.

Admissibility Preview

The reconstruction problem above already has the structure that will drive the entire book. Given multiple incomplete observations, we ask: which original states are consistent with all observations simultaneously? The set of consistent states is the admissibility class. Choosing among them requires criteria—admissibility conditions—that specify which reconstructions are acceptable. This idea will be made mathematically precise in Part V using sheaf theory and cohomology.

1.5 The holonomic perspective

The title of this book takes its name from a paper by Solórzano that formalizes precisely the situation we have just described.

A *holonomic space* in Solórzano's sense is a triple (V, H, L) where V is a normed vector space, H is a subgroup of norm-preserving automorphisms of V, and $L : H \to \mathbb{R}$ is a group-norm measuring the cost of transformations. The associated metric is

$$d_L(u, v) = \inf_{a \in H} \sqrt{L^2(a) + \|u - av\|^2}.$$

In plain language: the distance between two states is not just how far apart they are, but how far apart they are after allowing admissible internal reconfigurations at a measurable cost.

For the map problem, the holonomic interpretation is:

- V is the space of territory states,
- H is the group of map-preserving rearrangements of the territory (transformations that do not change the map image),
- $L(h)$ measures the cost of such a rearrangement.

Two territory states that differ only by a map-preserving rearrangement are holonomically close even if they differ in absolute terms.

This will become technically important in Chapter 28, where each open observational domain carries a holonomic triple rather than a bare vector space.

Reconstruction Exercise 1.1

Suppose two cities x_1 and x_2 are mapped to the same point $m \in M$ by a road map π.

1. What information about x_1 and x_2 can still be recovered from m alone?
2. What information is provably unrecoverable from m alone?
3. If a second map π' (e.g., a topographic map) assigns x_1 and x_2 to *different* points, what does the pair (π, π') allow you to reconstruct?

This exercise previews the multi-projection reconstruction problem that will recur throughout the book.

1.6 What this chapter anticipates

This chapter has introduced three ideas that will recur throughout the book.

1. **Projection.** Every representation is a map from a richer domain to a poorer one: $\pi : X \to M$.
2. **Nontrivial kernel.** Every useful representation discards information: $\ker(\pi) \neq \emptyset$.
3. **Reconstruction.** Given multiple projections, one can attempt to recover the original structure, but the recovery is generally incomplete or non-unique.

Mathematical Echo

This chapter introduced:

$$\pi : X \to M, \qquad \ker(\pi), \qquad X/\sim_\pi, \qquad \mathcal{R}(\{m_i\}) = \bigcap_i \pi_i^{-1}(m_i).$$

These objects will reappear in:

- Chapter 5 (observational equivalence classes),
- Chapter 7 (horizon-relative reconstruction),
- Chapter 27 (reconstruction error and CLIO),
- Chapter 28 (admissibility sheaf and gluing),
- Chapter 33 (the Monoturn as global reconstruction target).

Open Question 1.1

Given only a map $\pi : X \to M$ and no direct access to the territory X, what classes of territory can be uniquely reconstructed from M?
This question appears trivial in cartography. It becomes fundamental in inverse problems, detector theory, and cosmology, where X is never directly accessible and M is all the observer ever has.

What Survived the Projection?

What Survived the Projection? *Projection:* Road map $\pi : X \to M$

Preserved	**Lost**
Connectivity between locations	Elevation
Approximate relative position	Physical texture
Route structure	Most geometry
Named landmarks	Temporal history
	Unlabeled features

Reconstruction possible: Partial. Combining multiple map types

improves reconstruction.
Kernel: $\ker(\pi)$: all pairs (x_1, x_2) with $\pi(x_1) = \pi(x_2)$, including distinct locations mapped to the same road node.

Holonomy Note

After traversing this chapter, what information appears only in retrospect?
The equivalence relation $x_1 \sim_\pi x_2$ looks like a simple identification. But following this chapter's loop—projection, kernel, quotient, reconstruction, holonomic metric—reveals that the equivalence relation does not merely erase structure. It *defines* the class of transformations that are invisible to the observer.
The holonomy of a representation is precisely the group of transformations that leave all observations unchanged. A large holonomy group means many invisible transformations and a severely underdetermined reconstruction problem. A trivial holonomy group means the representation is injective and reconstruction is unique. Every chapter in this book is a study of the holonomy of some observation system.

Chapter 2

The Photograph

All photographs are accurate.
None of them is the truth.
— Richard Avedon

2.1 A more faithful record

A photograph feels more faithful than a map.

A road map replaces a city with coloured lines. A photograph at least looks like the place it depicts. The proportions are approximately right. The colours are approximately right. Faces are recognisable. Buildings are identifiable.

Yet the photograph destroys an enormous amount of information.

It destroys depth. A photograph collapses three-dimensional space onto a two-dimensional surface. Objects at different distances appear at the same depth.

It destroys time. A photograph captures a single moment from a continuous process. The moment before and the moment after are lost.

It destroys temperature, smell, sound, motion, and the texture of surfaces.

It destroys causal history. The photograph of a building does not record who built it, what stood there before, or what decisions led to its current form.

The photograph feels faithful because it preserves something that maps often discard: the visual geometry of a scene. But it is still a projection, and its kernel is vast.

2.2 The projection and its kernel

Let the world be modeled as a four-dimensional event field:

$$W \subset \mathbb{R}^3 \times \mathbb{R}.$$

A photograph is a projection onto an image plane:

$$P : W \to \mathbb{R}^2.$$

If $I = P(W)$ denotes the resulting image, then many different worlds can produce the same image:

$$P(W_1) = P(W_2) = I, \qquad W_1 \neq W_2.$$

Example 2.1 (Non-injectivity of photography)**.** Two scenes are photographically equivalent if they produce the same image from a given camera position. A flat painting of a room and an actual room, viewed from the same angle, can produce identical photographs. A large object far away and a small object nearby can subtend the same visual angle. A moving object and a stationary one can appear identical in a sufficiently short exposure.

The inverse problem

$$P^{-1}(I)$$

is therefore not a single world but an entire space of compatible worlds.

Definition 2.2 (Admissible reconstruction class)**.** Given an image $I \in \mathbb{R}^2$, the *admissible reconstruction class* of I is

$$[I]_P = \{W \in \mathcal{W} : P(W) = I\},$$

where $\mathcal{W}$ is the space of possible world-states. A photograph does not reveal a unique world. It defines an equivalence class of worlds consistent with the observed image.

This is the first appearance of what will later become the central technical concept of the book: the admissibility class.

A projection does not select a unique preimage. It selects a set of preimages. Reconstruction requires additional conditions to choose among them.

2.3 Non-injectivity and the inverse problem

The failure of injectivity is not incidental. It is the defining feature of observation.

Proposition 2.3 (Non-injectivity of observation)**.** *Let $\pi : X \to M$ be any observation map where $\dim X > \dim M$. Then π is non-injective: there exist $x_1 \neq x_2$ in X with $\pi(x_1) = \pi(x_2)$.*

Proof. By dimension counting: the fibres $\pi^{-1}(m)$ for generic $m \in M$ are $(\dim X - \dim M)$-dimensional submanifolds of X. Since $\dim X > \dim M$, these fibres are nontrivial. □

Every observation maps from a higher-dimensional reality to a lower-dimensional record. Non-injectivity is therefore unavoidable whenever reality is richer than observation, which is always.

2.4 Reconstruction as the central problem

Given a photograph I, an observer attempting to reconstruct the world must find a $W \in [I]_P$ that is consistent with all available information.

This is an inverse problem:

$$\text{Find } W \text{ such that } P(W) = I \text{ and } W \text{ is admissible.}$$

Admissibility here means consistent with prior knowledge, physical constraints, and other available observations.

Example 2.4 (Depth reconstruction from stereo vision)**.** The human visual system solves this inverse problem continuously. Two slightly different photographs — one from each eye — combined with prior knowledge about the scale of familiar objects allows the visual system to reconstruct approximate depth. The reconstruction is not guaranteed to be correct. It is guaranteed to be admissible given the available data.

The reconstruction error measures how far the recovered world departs from the true one:

$$E(W) = d(W, \hat{W}),$$

where $\hat{W} = G(P(W))$ is the reconstructed world and d is some appropriate metric on world-states.

This is the first appearance of the reconstruction error $E(x) = d(x, G(F(x)))$ that will become central in Chapter 4 and throughout Part V.

2.5 What the photograph reveals about admissibility

The photograph chapter advances the argument in one important direction beyond the map chapter.

The map chapter showed that every observation loses information.

The photograph chapter shows that the lost information defines an equivalence class of possible originals. The question is no longer merely: what is missing? The question becomes: among all originals consistent with the observation, which are admissible?

A photograph does not reveal reality. It defines a class of realities consistent with the observation. Reconstruction selects from this class using admissibility conditions.

This principle applies to every observation system encountered in this book: memories, detectors, embeddings, horizons, and cosmological surveys.

The word *admissibility* will be made mathematically precise in Part V. For now, it means: consistent with the observation and with whatever prior constraints are available.

2.6 A note on the photograph and time

One dimension the photograph discards deserves special attention: time.

A photograph freezes a process into a state. The process itself — the causal history that produced the state — is not recorded. Yet causal history is precisely what determines which features of the image are meaningful.

A crack in a wall means one thing if it appeared yesterday and another if it has been there for a century. A face looks different knowing it belongs to someone young rather than old.

The photograph loses trajectory information. It preserves only a single state.

This will become important in Chapter 5 and throughout Part II, where trajectory information — not just states — turns out to be essential for understanding dynamical systems.

The first hint of the RSVP framework's emphasis on paths and histories rather than states is already visible in the simple observation that a photograph destroys time.

Chapter 3

The Microscope

To see a World in a Grain of Sand
And a Heaven in a Wild Flower,
Hold Infinity in the palm of your hand
And Eternity in an hour.
— William Blake

3.1 The paradox of magnification

The microscope reverses a natural intuition.

More magnification, one might think, means more information. The finer the resolution, the closer we are to reality. To see smaller things is to see more truly.

Yet this is not what happens.

At high magnification, context disappears. A biological tissue seen at the cellular level reveals cell structure but loses organ structure. A metal surface seen at the atomic level reveals crystal lattice geometry but loses the shape of the object. A neural spike train resolved to the millisecond reveals individual firing patterns but loses behavioural context.

Observation gains detail while losing organisation.

The microscope proves that information loss occurs not only by coarse-graining, but also by over-resolution.

3.2 Multiscale structure and scale selection

Most real systems have meaningful structure at many scales simultaneously.

Definition 3.1 (Multiscale system)**.** A *multiscale system* is a system X that can be decomposed as

$$X = \bigcup_{\ell > 0} X_\ell,$$

where X_ℓ denotes the structure of X that is visible at scale ℓ.

Examples are ubiquitous.

Example 3.2 (Scales of biological organisation)**.** A living organism has structure at the scales of: atoms, molecules, organelles, cells, tissues, organs, organ systems, whole organisms, populations, and ecosystems. Observation at any single scale reveals some structure while hiding structure at all other scales.

A microscope selects a scale window:

$$\pi_{\ell_0} : X \to X_{\ell_0}.$$

This is a projection. Like the map and the photograph, it has a nontrivial kernel.

The context lost by magnification is

$$K_{\ell_0} = X \setminus X_{\ell_0}.$$

Thus observation at small scale destroys access to large-scale organisation, and observation at large scale destroys access to fine structure.

3.3 Admissibility depends on the reconstruction task

The key insight of this chapter is that the right scale of observation is not determined by the system alone. It is determined by the reconstruction task.

Suppose a reconstruction task R requires both local detail d and global context c. Let $I(\ell)$ denote the information accessible at scale ℓ. Then neither extreme is optimal:

$$\lim_{\ell \to 0} I(\ell)$$

captures microscopic detail while losing context, whereas

$$\lim_{\ell \to \infty} I(\ell)$$

captures context while losing detail.

Definition 3.3 (Admissible information for a task)**.** For a reconstruction task R, define the *admissible information* at scale ℓ as

$$A_R(\ell) = \mathrm{Rel}(I(\ell), R),$$

where $\mathrm{Rel}(\cdot, R)$ measures the relevance of the available information to the reconstruction goal R.

The admissible scale is then

$$\ell^* = \arg\max_{\ell} A_R(\ell).$$

The critical observation is that admissibility is not maximised by information quantity:

$$\arg\max_{\ell} A_R(\ell) \neq \arg\max_{\ell} |I(\ell)|.$$

> Useful information is not maximum information.
> Admissibility is always relative to a reconstruction goal.

This principle quietly anticipates every major framework developed later in this book.

In CLIO (Part V), admissibility is formalised as a constraint on which projections are permitted. In the admissibility sheaf (Chapter 28), admissible local sections are exactly those relevant to global reconstruction. In simulated agency (Chapter 34), agents act only through admissible perturbations of their local field. In cosmology (Part VII), the admissible observational data are those that survive projection through causal horizons.

All of these are versions of the same recognition: the right observation is not the most detailed one, but the one appropriate to the task.

3.4 Bidirectional information loss

The map and photograph chapters illustrated information loss by coarse-graining: the projection discards fine detail.

The microscope chapter introduces the opposite direction. Over-resolution also loses information, by discarding large-scale organisation.

Proposition 3.4 (Bidirectional information loss)**.** *For a multiscale system $X = \bigcup_\ell X_\ell$, the total information accessible at any single scale ℓ_0 is strictly less than the total information in X:*

$$|I(\ell_0)| < |I(X)| \qquad \text{for all } \ell_0.$$

In particular, neither the limit $\ell_0 \to 0$ nor the limit $\ell_0 \to \infty$ recovers the full structure of X.

This means that complete information about a multiscale system is not accessible from any single scale of observation. Reconstruction of the full system requires integrating information across multiple scales.

Example 3.5 (Astronomy across scales)**.** Astronomical observation operates simultaneously at scales ranging from individual photons to the large-scale structure of the universe. A spectrum reveals chemical composition. An image reveals spatial structure. A light curve reveals temporal variation. No single measurement captures all three. Reconstructing the physical state of a distant object requires combining observations made at different scales, resolutions, and wavelengths.

3.5 Admissibility as a filter, not a threshold

A common misconception is that admissibility means passing some minimum quality threshold. More data is assumed to be better, up to the point where resolution is sufficient.

The microscope chapter corrects this.

Admissibility is not a threshold. It is a filter that depends on the relationship between the available data and the reconstruction goal.

Data can be inadmissible by being too coarse. Data can also be inadmissible by being too fine.

An observation is admissible if and only if it captures the structure relevant to the task while discarding the structure irrelevant to it.

This bidirectional notion of admissibility will reappear in Chapter 28 when we ask which local sections of the admissibility sheaf can be glued into a global reconstruction, and in Chapter 35 where we state as a conjecture that the admissibility cohomology of cosmological observer domains is nontrivial.

3.6 Summary

The map chapter introduced projection and the nontrivial kernel.

The photograph chapter introduced the admissibility class and the reconstruction problem.

This chapter introduces the central principle that will govern the rest of the book:

1. Information loss is bidirectional: both coarse-graining and over-resolution destroy information.

2. The right level of observation is determined by the reconstruction task, not by the system alone.

3. Useful information is not maximum information. Admissibility is always relative to a goal.

The reader who has absorbed these three points is already thinking in the terms that the rest of this book will make precise.

Chapter 4

Memory

Memory is not an instrument for surveying the past
but its theatre.
— Walter Benjamin

4.1 The reconstruction that feels like recall

Human memory is the most familiar example of reconstruction.

Nobody stores every sensory detail of an experience. The sights, sounds, smells, and physical sensations of an event are not recorded like a video file. Instead, traces are laid down — partial, compressed, context-dependent records — and later experience involves reconstruction from those traces, not playback of a recording.

Psychologists have known this since the work of Frederic Bartlett in the 1930s. Memory is reconstructive. It is influenced by prior knowledge, subsequent experience, and the context in which recall takes place.

The mathematical structure of this process is surprisingly clean.

4.2 Encoding, trace, and reconstruction

Let $x \in X$ be an experienced event, where X is the space of possible experiences. Encoding is a map

$$F : X \to T,$$

where T is the space of memory traces.

Recall is a reconstruction map

$$G : T \to \hat{X},$$

where $\hat{X}$ is the space of recalled experiences.

The remembered event is

$$\hat{x} = G(F(x)).$$

This is the first explicit appearance of the composition $G \circ F$ that will become the central operator of the book.

Definition 4.1 (Reconstruction operator)**.** The *reconstruction operator* is the composition

$$R = G \circ F : X \to \hat{X}.$$

Memory is exact if $R(x) = x$ for all $x \in X$. Memory is admissible if $R(x) \approx x$ in a sense made precise by the reconstruction error.

4.3 Reconstruction error

Memory is exact only if

$$G(F(x)) = x.$$

Usually,

$$G(F(x)) \neq x,$$

but recall may still be admissible if the error is small:

$$d(x, G(F(x))) < \varepsilon.$$

Definition 4.2 (Reconstruction error)**.** The *reconstruction error* of the memory system at experience x is

$$E(x) = d(x, G(F(x))),$$

where d is a metric on the space of experiences.

This is the central quantity of CLIO (Part V) and the admissibility framework throughout the book. It first appears here as a measure of how faithfully a memory system reconstructs experience.

A memory system is:

- *exact* if $E(x) = 0$ for all x;
- *admissible* if $E(x) < \varepsilon$ for some tolerance $\varepsilon > 0$ appropriate to the task;
- *inadmissible* if $E(x) \geq \varepsilon$.

4.4 What memory preserves

If memory is not exact, what does it preserve?

Bartlett's original experiments showed that memory tends to preserve:

- overall structure and narrative;
- emotionally significant details;
- elements consistent with prior knowledge and expectations.

Memory tends to lose:

- precise numerical detail;
- peripheral sensory information;
- elements inconsistent with prior knowledge (which are often systematically distorted toward the expected).

In the language developed so far, memory is a projection whose kernel contains sensory precision and peripheral detail, while preserving semantic structure and emotional salience.

Definition 4.3 (Semantic admissibility)**.** A memory reconstruction $\hat{x} = G(F(x))$ is *semantically admissible* if it preserves the structural and relational features of x that are relevant to subsequent reasoning and action, even if precise sensory detail is lost.

This anticipates the formal admissibility conditions of Part V, where admissibility is defined not as exact reconstruction but as preservation of the structure relevant to a given task or reconstruction goal.

4.5 The encoding map and its kernel

The encoding map $F : X \to T$ necessarily has a nontrivial kernel.

Proposition 4.4 (Memory compression)**.** *If the space of memory traces T has lower dimension or capacity than the space of experiences X, then F is non-injective: there exist $x_1 \neq x_2$ with $F(x_1) = F(x_2)$.*

Two experiences that produce the same memory trace cannot be distinguished by subsequent recall.

Example 4.5 (Source monitoring failure)**.** A well-documented phenomenon in cognitive psychology is *source monitoring failure*: remembering a fact without remembering where it was learned. The content is encoded but the source tag is lost. Two routes to the same fact — reading it versus being told it — can produce the same memory trace. This is a concrete instance of the kernel of F containing source information.

4.6 Memory as the first reconstruction system

The memory chapter introduces three ideas that will recur throughout the book.

1. **The reconstruction operator** $G \circ F$ is the natural mathematical object for studying observation-dependent knowledge.
2. **The reconstruction error** $E(x) = d(x, G(F(x)))$ measures the fidelity of reconstruction and will become the central quantity in CLIO and the admissibility framework.

3. **Admissibility without exactness.** A reconstruction need not be exact to be useful. It must preserve the structure relevant to subsequent inference and action.

> Reconstruction need not be exact.
> It must be admissible: sufficiently faithful
> for the purposes that reconstruction serves.

Chapter 5

The Detector

Every instrument is a theory made solid.
— Gaston Bachelard

Why This Matters

The detector chapter marks the transition from human examples (maps, photographs, memory) to physical measurement. The key move is recognising that a detector is not a transparent window onto a system. It is an interface: a two-stage projection through which physical states become numerical outputs. The kernel of this projection is not a limitation to be overcome but the primary object of study.

5.1 Measurement as two-stage projection

Let X denote a space of underlying physical states. A detector does not usually map X directly into an observed value. Instead, it first interacts with the system, producing an intermediate signal space S, and then converts that signal into a finite readout space D. Thus measurement has the form

$$X \xrightarrow{F} S \xrightarrow{\pi} D.$$

The actual observable is not $x \in X$, but

$$d = (\pi \circ F)(x).$$

Technical Note 5.1: Detector signal vs. readout

The two-stage structure $X \xrightarrow{F} S \xrightarrow{\pi} D$ is not merely formal. F represents physical interaction: a photon excites an electron, a particle ionises a gas, a gravitational wave stretches spacetime. π represents transduction: the analogue signal is digitised, thresholded, or otherwise converted to a readout. Each stage discards different information. F loses information about undetected degrees of freedom. π loses information below the noise floor or outside the bandwidth.

Definition 5.1 (Detector equivalence)**.** Two physical states $x_1, x_2 \in X$ are *detector-equivalent* when

$$(\pi \circ F)(x_1) = (\pi \circ F)(x_2).$$

We write $x_1 \sim_D x_2$.

Proposition 5.2. *Detector equivalence is an equivalence relation on X.*

Proof. Reflexivity: $(\pi \circ F)(x) = (\pi \circ F)(x)$. Symmetry: equality is symmetric. Transitivity: if $(\pi \circ F)(x_1) = (\pi \circ F)(x_2)$ and $(\pi \circ F)(x_2) = (\pi \circ F)(x_3)$, then $(\pi \circ F)(x_1) = (\pi \circ F)(x_3)$. □

The detector therefore does not observe X. It observes the quotient

$$X/\sim_D.$$

Forward Reference

The detector equivalence class $[x]_D = (\pi \circ F)^{-1}(d)$ is the physical version of the admissibility class introduced in Chapter 2. In Chapter 28 this becomes the fibre of the admissibility sheaf over an observational domain.

5.2 Detector bandwidth and admissible signals

A detector is physically limited. It has a bandwidth, a sensitivity threshold, a spatial aperture, a response time, and a noise floor. These limitations define an admissible signal region

$$S_{\text{adm}} \subseteq S.$$

Only signals satisfying $F(x) \in S_{\text{adm}}$ can be registered.

Definition 5.3 (Detector-admissible state)**.** A state $x \in X$ is *detector-admissible* when $F(x) \in S_{\text{adm}}$. The detector-admissible subset of X is

$$X_{\text{adm}} = F^{-1}(S_{\text{adm}}).$$

Proposition 5.4. *If $S_{\text{adm}} \subsetneq S$, then the detector ignores all states in $X \setminus X_{\text{adm}}$.*

Proof. $x \notin X_{\text{adm}}$ iff $F(x) \notin S_{\text{adm}}$, i.e., the interaction signal lies outside the physically readable region. Such a state produces no detector output. □

The detector therefore performs two kinds of forgetting. First, it excludes states outside its admissible domain. Second, it identifies distinct admissible states that yield the same output.

Measurement is not access.

Measurement is admissible projection.

5.3 Reconstruction from detector output

Given a detector output $d \in D$, the compatible physical states are

$$(\pi \circ F)^{-1}(d) = \{x \in X : (\pi \circ F)(x) = d\}.$$

This set is usually not a singleton.

Definition 5.5 (Detector reconstruction problem)**.** Given $d \in D$, find an admissible estimate $\hat{x} = G(d)$ such that $(\pi \circ F)(\hat{x}) = d$ whenever possible. The *detector reconstruction error* is

$$E_D(x) = d_X(x, G((\pi \circ F)(x)))\,.$$

Proposition 5.6. *Exact detector reconstruction for all $x \in X$ requires $\pi \circ F$ to be injective.*

Proof. If $G((\pi \circ F)(x)) = x$ for all x, and $(\pi \circ F)(x_1) = (\pi \circ F)(x_2)$, then applying G gives $x_1 = x_2$. Contrapositive: non-injectivity implies inexact reconstruction. □

Example 5.7 (Axion detector as admissibility projection)**.** An axion detector searches for a dark-sector particle field Φ_{axion} through its interaction with an electromagnetic field F. The interaction produces a signal $s \in S$ (a photon, a phonon, or a mechanical oscillation) which is then amplified and digitised. The detector cannot observe Φ_{axion} directly. It observes $(\pi \circ F)(\Phi_{\text{axion}})$. Observable Gaussianity of the detector output is a property of the projection $\pi \circ F$, not of the underlying axion field. The axion field may be non-Gaussian while the detector output appears Gaussian, because $\pi \circ F$ averages over many field degrees of freedom.

Admissibility Preview

The distinction between the axion field and its detector output is the first physical example of the principle:

$$\text{observable simplicity} \neq \text{ontological simplicity}.$$

This will be formalised in Chapter 28 using the admissibility sheaf, and will reappear in the cosmological redshift discussion in Chapter 40.

5.4 The hidden kernel

The hidden degrees of freedom of the detector are

$$\ker(\pi \circ F).$$

Two field states are observationally equivalent when

$$(\pi \circ F)(x_1) = (\pi \circ F)(x_2).$$

Reconstruction Exercise 5.1: Detector non-injectivity

Construct two physically distinct states $x_1 \neq x_2$ that produce the same detector output d.

1. In a spectrometer: which aspects of a light source are preserved in a spectrum, and which are lost?
2. In a thermometer: which aspects of a gas are preserved in a temperature reading, and which are not?
3. In an MRI scanner: which aspects of tissue are preserved in the image, and which are not?

For each case, identify the kernel of the measurement map and describe what reconstruction would require.

Mathematical Echo

This chapter introduced:

$$X \xrightarrow{F} S \xrightarrow{\pi} D, \qquad x_1 \sim_D x_2, \qquad X_{\text{adm}} = F^{-1}(S_{\text{adm}}), \qquad E_D(x).$$

The detector equivalence relation $\sim_D$ is the physical version of the projection equivalence from Chapter 1. It will appear as the fibre relation of the admissibility sheaf in Chapter 28.

What Survived the Projection?

What Survived the Projection? *Projection:* Detector $X \xrightarrow{F} S \xrightarrow{\pi} D$

Preserved	Lost
Detector-admissible signal	States outside X_{adm}
Equivalence class $[x]_D$	Sub-noise-floor variations
Readout $d \in D$	Out-of-bandwidth modes
	Non-commuting observables

Reconstruction possible: Partial; requires knowledge of F and additional physical constraints.
Kernel: $\ker(\pi \circ F)$: all pairs (x_1, x_2) with identical detector output.

Chapter 6

Machine Learning Embeddings

The purpose of compression is not to reduce
but to reveal.

— —

Why This Matters

Embeddings are the contemporary form of a very old problem: how to represent a complex object in a simpler space while preserving what matters. This chapter bridges the human examples of earlier chapters and the cosmological example of Chapter 7. It also introduces, informally, the adjunction $F \dashv G$ that will be made precise in Chapter 29.

6.1 Embeddings as controlled compression

Let X be a space of objects: texts, images, sounds, documents, observations, or states. A machine learning embedding is a map

$$E : X \to \mathbb{R}^n.$$

It replaces an object $x \in X$ with a vector $E(x)$.

The embedding is useful when relevant structure in X is approximately preserved by distances in $\mathbb{R}^n$. If d_X is a task-relevant distance on X, define the embedded distance

$$d_E(x, y) = \|E(x) - E(y)\|.$$

A good embedding satisfies, approximately,

$$d_X(x, y) \approx d_E(x, y)$$

for the distinctions relevant to the task.

Definition 6.1 (Embedding equivalence)**.** Two objects $x, y \in X$ are *embedding-equivalent* when $E(x) = E(y)$. We write $x \sim_E y$.

Proposition 6.2. *The embedding map $E : X \to \mathbb{R}^n$ induces a quotient space $X/\sim_E$.*

Proof. Equality of images is an equivalence relation. The quotient exists as the set of equivalence classes. □

Common Misconception

Higher-dimensional embeddings do not necessarily preserve more meaning. An embedding into $\mathbb{R}^{10000}$ may discard more task-relevant structure than an embedding into $\mathbb{R}^{32}$ if the higher-dimensional space encodes irrelevant variation. Admissibility of an embedding depends on the task, not on the dimension of the target space.

6.2 The inverse image and reconstruction

Given an embedded vector $v \in \mathbb{R}^n$, the compatible original objects are

$$E^{-1}(v) = \{x \in X : E(x) = v\}.$$

Proposition 6.3. *If there exists $v \in \mathbb{R}^n$ with $|E^{-1}(v)| > 1$, then no reconstruction map $G : \mathbb{R}^n \to X$ can recover every $x \in X$ exactly.*

Proof. If $x_1 \neq x_2$ with $E(x_1) = E(x_2) = v$, then any G satisfying $G(E(x_i)) = x_i$ must satisfy both $G(v) = x_1$ and $G(v) = x_2$, forcing $x_1 = x_2$. Contradiction. □

The reconstruction problem is therefore not E^{-1} (which usually does not exist as a function) but

$$G : \mathbb{R}^n \to \hat{X},$$

where $G(v)$ selects an admissible reconstruction from $E^{-1}(v)$.

6.3 Task-relevance and admissible compression

Definition 6.4 (Admissible embedding)**.** An embedding $E : X \to \mathbb{R}^n$ is *admissible for a task R* when the reconstruction error remains below a task threshold:

$$d_R(x, G(E(x))) < \varepsilon_R$$

for all task-relevant $x \in X$.

The best embedding is not necessarily the one that preserves the most information:

$$\arg\max_E A_R(E) \neq \arg\max_E |I(E)|.$$

This is the microscope principle applied to representation design.

Example 6.5 (Word embeddings)**.** A word embedding E : Vocabulary $\to \mathbb{R}^{300}$ maps words to vectors so that semantically similar words map to nearby vectors. The embedding discards spelling, etymology, and phonetic structure while preserving distributional meaning. This is admissible for tasks requiring semantic similarity and inadmissible for tasks requiring morphological analysis.

6.4 The adjunction, informally

The pair (E, G) is the first informal appearance of an adjunction $F \dashv G$.

Encoding E decomposes objects into vectors. Reconstruction G reassembles vectors into objects. They are not inverses: $G \circ E \neq \mathrm{id}_X$ in general. Instead, there is a systematic relationship: maps from encodings to targets correspond to maps from reconstructions to originals.

Forward Reference

The informal adjunction (E, G) introduced here will be made precise in Chapter 29 as $F \dashv G : \mathbf{Loc} \to \mathbf{Glob}$. The unit $\eta : \mathrm{id} \to G \circ F$ measures how faithfully the Monoturn is recovered after decomposition and reconstruction. The counit $\varepsilon : F \circ G \to \mathrm{id}$ measures how well a proposed local dataset is explained by a reconstructed whole.

6.5 From embeddings to horizons

Some projections are chosen. Others are unavoidable.

A cartographer chooses a map projection. An engineer chooses an embedding space. An observer does not choose a horizon. Yet mathematically all three confront the same problem: reconstruction from incomplete access.

The embedding map $E : X \to \mathbb{R}^n$ is designed. The horizon restriction $F_O : \mathcal{M} \to \mathcal{A}(H_O)$ is imposed by physical accessibility.

Both create the same formal question:

Given non-injective access, what can be reconstructed?

Mathematical Echo

This chapter introduced:

$$E : X \to \mathbb{R}^n, \quad x \sim_E y, \quad E^{-1}(v), \quad G : \mathbb{R}^n \to \hat{X}, \quad d_R(x, G(E(x))) < \varepsilon_R.$$

The informal adjunction (E, G) anticipates $F \dashv G$ in Chapter 29. The admissible embedding definition anticipates the admissibility sheaf in Chapter 28.

What Survived the Projection?

What Survived the Projection? *Projection:* Embedding $E : X \to \mathbb{R}^n$

Preserved	**Lost**
Task-relevant similarity	Exact identity of objects
Approximate metric structure	Task-irrelevant variation
Linear combinations of features	Objects outside training distribution

Reconstruction possible: Partial; $G(E(x))$ is admissible

but not exact in general.
Kernel: ker(E): all pairs (x_1, x_2) with $E(x_1) = E(x_2)$; typically dense in X.

Chapter 7

Horizons

The horizon is the place where the earth curves away from our sight. It is not the edge of the world.

— —

Why This Matters

This chapter closes Part I by showing that the physical universe confronts every observer with the same projection problem studied in Chapters 1–6. A causal horizon is not a failure of observation. It is the physical instantiation of the kernel. The observer does not choose the horizon; the horizon is imposed by the geometry of spacetime and the finite speed of signals. Yet mathematically, it is the same object as the map that excludes terrain, the camera that flattens depth, and the detector that admits only certain signals.

7.1 Horizons as physical projections

Let $\mathcal{M}$ denote the total structure under consideration—the Monoturn, defined precisely in Chapter 33. An observer O does not access $\mathcal{M}$ directly. The observer accesses only a horizon-limited region

$$H_O \subseteq \mathcal{M}.$$

This horizon may be causal, optical, instrumental, biological, computational, or conceptual. In cosmology it is causal: finite signal speed limits what can be observed.

The observer receives admissible local data:

$$F_O : \mathcal{M} \to \mathcal{A}(H_O).$$

This is followed by an observational projection:

$$\pi_O : \mathcal{A}(H_O) \to O_{\text{obs}}.$$

Thus the observer encounters

$$\mathcal{M} \xrightarrow{F_O} \mathcal{A}(H_O) \xrightarrow{\pi_O} O_{\text{obs}}.$$

Definition 7.1 (Horizon kernel)**.** The inaccessible structure for observer O is

$$\ker(\pi_O \circ F_O).$$

Two global structures $\mathcal{M}_1, \mathcal{M}_2$ are *observationally equivalent* for O when

$$(\pi_O \circ F_O)(\mathcal{M}_1) = (\pi_O \circ F_O)(\mathcal{M}_2).$$

Proposition 7.2. *If $H_O \subsetneq \mathcal{M}$, then there exist distinctions in $\mathcal{M}$ that are not directly available to O.*

Proof. Since $H_O \subsetneq \mathcal{M}$, there exists at least one region $x \in \mathcal{M} \setminus H_O$. By definition, F_O restricts to data over H_O. Therefore changes supported entirely in $\mathcal{M} \setminus H_O$ are not represented in $\mathcal{A}(H_O)$. Such changes lie in $\ker(\pi_O \circ F_O)$. □

This proposition is deliberately modest. It does not say the exterior structure does not exist. It says only that the observer cannot access it directly.

7.2 Horizon-relative reconstruction

An observer does not reconstruct $\mathcal{M}$ itself. The observer reconstructs a model:

$$\widehat{\mathcal{M}}_O = G_O(\pi_O(F_O(\mathcal{M}))).$$

The subscript matters. Different observers may have different horizons and therefore different reconstructions:

$$\widehat{\mathcal{M}}_{O_1} \neq \widehat{\mathcal{M}}_{O_2}.$$

Definition 7.3 (Observer reconstruction error)**.**

$$E_O(\mathcal{M}) = d_{\mathcal{M}}(\mathcal{M},\ G_O(\pi_O(F_O(\mathcal{M})))) .$$

When two observers O_1, O_2 have overlapping horizons $H_{12} = H_{O_1} \cap H_{O_2}$, their reconstructions are compatible on the overlap when

$$\rho^{H_{O_1}}_{H_{12}}\left(\widehat{\mathcal{M}}_{O_1}\right) = \rho^{H_{O_2}}_{H_{12}}\left(\widehat{\mathcal{M}}_{O_2}\right) .$$

Proposition 7.4 (Overlap compatibility is necessary)**.** *If a common global reconstruction $\widehat{\mathcal{M}}$ restricts to each observer's reconstruction, then the observer reconstructions must agree on their overlap.*

Proof. If $\rho^{\mathcal{M}}_{H_{O_i}}(\widehat{\mathcal{M}}) = \widehat{\mathcal{M}}_{O_i}$ for $i = 1, 2$, then restricting both to H_{12} and applying functoriality of restriction gives $\rho^{H_{O_1}}_{H_{12}}(\widehat{\mathcal{M}}_{O_1}) = \rho^{\mathcal{M}}_{H_{12}}(\widehat{\mathcal{M}}) = \rho^{H_{O_2}}_{H_{12}}(\widehat{\mathcal{M}}_{O_2})$. □

This is the intuitive beginning of the sheaf condition. Local reconstructions can become global only when their overlap restrictions agree.

7.3 The Ocularum

The horizon of an observer is not merely a spatial region. It is the region structured by what can be received, resolved, encoded, and reconstructed.

Definition 7.5 (Ocularum)**.** The *Ocularum* of an observer O is the structured observational domain

$$\mathcal{O}_O = (H_O,\ \mathcal{A}(H_O),\ \pi_O),$$

where H_O is the accessible region, $\mathcal{A}(H_O)$ is the admissible local data over that region, and π_O is the projection into observable states.

The Ocularum is not merely what is seen. It is the whole structure that makes seeing possible.

Technical Note 7.1: Oculara and open sets

Oculara will later become the open sets $U \in \mathcal{O}(X)$ of the topology over which the admissibility sheaf is defined. The admissibility sheaf assigns to each Ocularum the space of admissible field configurations accessible from within it. Restriction maps describe how the view from a larger Ocularum constrains the view from a smaller one contained within it.

7.4 The central question

The sequence developed throughout Part I can now be written in its final form:

$$\mathcal{M} \xrightarrow{F} \text{Admissible Local Data} \xrightarrow{\pi} \text{Observable State.}$$

The composite map $\pi \circ F$ is generally non-injective:

$$\ker(\pi \circ F) \neq 0.$$

Given a projection with nontrivial kernel,
what global structure can be reconstructed from what remains?

Part II begins by turning this question into reconstruction theory.

Same Mathematics, Different Systems

System	Projection	Kernel
Map	Road network	Terrain, history
Photograph	Image plane	Depth, time
Microscope	Scale window	Other scales
Memory	Trace encoding	Sensory detail
Detector	Readout function	Below-threshold states
Embedding	Feature vectors	Task-irrelevant variation
Horizon	Causal boundary	Beyond-horizon structure

Every row studies the same object: $\ker(\pi \circ F)$. Every chapter of this book is a study of what falls into that kernel and what can be recovered from what remains.

Mathematical Echo

This chapter introduced:

$$F_O : \mathcal{M} \to \mathcal{A}(H_O), \qquad \pi_O : \mathcal{A}(H_O) \to O_{\text{obs}}, \qquad \mathcal{O}_O = (H_O, \mathcal{A}(H_O), \pi_O),$$

$$\widehat{\mathcal{M}}_O = G_O(\pi_O(F_O(\mathcal{M}))), \qquad \rho^{H_{O_1}}_{H_{12}}(\widehat{\mathcal{M}}_{O_1}) = \rho^{H_{O_2}}_{H_{12}}(\widehat{\mathcal{M}}_{O_2}).$$

The overlap compatibility condition is the intuitive form of the sheaf gluing axiom, which appears in Chapter 28.

Holonomy Note

After traversing Part I as a whole, what information appears only in retrospect?
Each chapter introduced a different projection: map, photograph, microscope, memory, detector, embedding, horizon. Each seemed to be about a different subject.
Looking back, every chapter was studying the same object: $\ker(\pi \circ F)$.
This is the holonomy of Part I. The invariant structure that only becomes visible after moving through all seven chapters is the kernel itself: the hidden structure common to every act of observation.
The rest of the book is the study of that kernel's mathematical properties, physical consequences, and cosmological implications.

What Survived the Projection?

What Survived the Projection? *Projection:* Causal horizon $F_O : \mathcal{M} \to \mathcal{A}(H_O)$

Preserved	**Lost**
Observable causal patch H_O	Beyond-horizon structure
Admissible local field data	$\mathcal{M} \setminus H_O$
Overlap-compatible reconstructions	Trans-horizon correlations

Reconstruction possible: Partial: $\widehat{\mathcal{M}}_O \subsetneq \mathcal{M}$.
Global reconstruction requires compatible Oculara.
Kernel: $\ker(\pi_O \circ F_O)$: all structure outside H_O and all sub-resolution variations within it.

Part II

Variational Dynamics and Free-Energy Descent

Introduction to Part 2

Established So Far

[To be completed during drafting.]

New Ideas Introduced in This Part

[To be completed during drafting.]

Dependencies

[To be completed during drafting. See also the Dependency Appendix at the back of the book.]

What Remains Open After This Part

[To be completed during drafting.]

Chapter 8

Fields, Flows, and Conservation Laws

Nature does not make jumps.
— Gottfried Wilhelm Leibniz

Why This Matters

Part I showed that observation is projection. Part II asks: what mathematical structure governs the object being projected? This chapter introduces the language of fields and flows that will carry through the rest of the book. Every RSVP field, every admissibility sheaf section, and every reconstruction operator will be a field in this sense.

8.1 From states to fields

A state assigns a value to a system at a moment. A field assigns a value to every point of a domain at every moment.

Definition 8.1 (Scalar field)**.** A *scalar field* on a domain $\Omega \subseteq \mathbb{R}^d$ is a function $\phi : \Omega \times \mathbb{R} \to \mathbb{R}$.

Definition 8.2 (Vector field)**.** A *vector field* on Ω is a function $\mathbf{v} : \Omega \times \mathbb{R} \to \mathbb{R}^d$.

8.2 Conservation laws

Definition 8.3 (Continuity equation)**.** A scalar field ϕ satisfies a *conservation law* when

$$\partial_t \phi + \nabla \cdot \mathbf{J} = \sigma,$$

where $\mathbf{J}$ is the flux of ϕ and σ is a source or sink term. When $\sigma = 0$, ϕ is *strictly conserved*.

Proposition 8.4 (Global conservation)**.** *If ϕ satisfies the continuity equation with $\sigma = 0$ and $\mathbf{J} \cdot \hat{n} = 0$ on $\partial\Omega$, then*

$$\frac{d}{dt} \int_{\Omega} \phi \, dx = 0.$$

Proof. Integrate the continuity equation over Ω and apply the divergence theorem. □

Forward Reference

The RSVP entropy field $S(x,t)$ satisfies a modified continuity equation with a source term $\sigma(\Phi, \mathbf{v}, L, D)$ that is nonnegative when $S = 0$, ensuring $S \geq 0$ is preserved. The lamphron field $L = \ell^2$ satisfies a conservation law modified by advection. Both enter the free-energy functional in Part V.

8.3 Gradient flows

The most important class of evolution equations for this book are gradient flows: dynamics that descend a functional.

Definition 8.5 (Gradient flow)**.** Given a functional $\mathcal{F}[\phi]$, the *gradient flow* is

$$\partial_t \phi = -M \frac{\delta \mathcal{F}}{\delta \phi},$$

where $M > 0$ is a mobility coefficient.

Proposition 8.6 (Gradient flow dissipation)**.** *Along gradient flow solutions,*

$$\frac{d\mathcal{F}}{dt} = -M \int \left(\frac{\delta \mathcal{F}}{\delta \phi} \right)^2 dx \leq 0.$$

Proof. $\frac{d\mathcal{F}}{dt} = \int \frac{\delta \mathcal{F}}{\delta \phi} \partial_t \phi \, dx = -M \int \left(\frac{\delta \mathcal{F}}{\delta \phi} \right)^2 dx \leq 0.$ □

Status: Proven Framework

Proposition 8.6 holds for any smooth functional $\mathcal{F}$ and any positive mobility M. It is the template for all energy-dissipation results in this book, including the RSVP free-energy dissipation theorem in Chapter 21.

What Survived the Projection?

What Survived the Projection? *Projection:* Field projection $\phi \mapsto \phi|_U$

Preserved	**Lost**
Field values on U	Field values outside U
Local gradient information	Long-range correlations
Conservation on U	Boundary fluxes

Reconstruction possible: Partial; requires boundary data and field equations.
Kernel: $\ker(\cdot|_U)$: all field configurations supported

outside U.

Chapter 9

Entropy and Information

Entropy is not a measure of disorder.
It is a measure of our ignorance.
— Edwin T. Jaynes

9.1 Entropy as missing information

Definition 9.1 (Shannon entropy)**.** For a discrete probability distribution $\{p_i\}$,

$$H = -\sum_i p_i \log p_i.$$

Proposition 9.2. *$H \geq 0$, with $H = 0$ iff the distribution is a point mass.*

Technical Note 9.1: Entropy and reconstruction

In the reconstruction framework of Part I, entropy measures the size of equivalence classes. If $\pi^{-1}(m)$ has measure $\mu(\pi^{-1}(m))$, the representational entropy is $S_\pi(m) = \log \mu(\pi^{-1}(m))$. High entropy means large equivalence class means high reconstruction ambiguity. This connection will be formalised in Chapter 27.

9.2 Entropy production

Definition 9.3 (Entropy production rate)**.** For a field $S(x,t)$ satisfying $\partial_t S + \nabla \cdot \mathbf{J}_S = \sigma_S$, the local *entropy production rate* is $\sigma_S \geq 0$.

Proposition 9.4 (Second law)**.** *For an isolated system with $\mathbf{J}_S \cdot \hat{n} = 0$ on $\partial\Omega$,*

$$\frac{d}{dt} \int_\Omega S\, dx = \int_\Omega \sigma_S\, dx \geq 0.$$

Admissibility Preview

In RSVP, the entropy field $S(x, t)$ plays a dual role. Globally it increases (second law). Locally it can decrease in coherence-building regions (lamphron-dominated zones) while increasing faster in void regions (lamphrodyne-dominated zones). The two rates compensate to maintain global increase. This is the thermodynamic version of the lamphron/lamphrodyne duality introduced in Chapter 25.

What Survived the Projection?

What Survived the Projection? *Projection:* Entropy projection $S \mapsto \int S\, dx$

Preserved	Lost
Total entropy	Local entropy distribution
Global thermodynamic state	Spatial gradients
	Entropy production field

Reconstruction possible: Partial; total entropy alone underdetermines local state.
Kernel: ker: all redistributions preserving total entropy.

Chapter 10

Variational Principles

Nature always acts by the shortest and simplest paths.
— Pierre Louis Maupertuis

10.1 Functionals and variational derivatives

Definition 10.1 (Functional)**.** A *functional* $\mathcal{F}[\phi]$ assigns a real number to each admissible field ϕ.

Definition 10.2 (Variational derivative)**.** The *variational derivative* $\frac{\delta \mathcal{F}}{\delta \phi}$ is defined by

$$\mathcal{F}[\phi + \varepsilon\psi] = \mathcal{F}[\phi] + \varepsilon \int \frac{\delta \mathcal{F}}{\delta \phi} \psi \, dx + O(\varepsilon^2).$$

Example 10.3 (Gradient energy functional)**.** For $\mathcal{F}[\phi] = \int \frac{1}{2} |\nabla \phi|^2 \, dx$,

$$\frac{\delta \mathcal{F}}{\delta \phi} = -\Delta \phi.$$

Proof by integration by parts.

10.2 The Euler–Lagrange equation

Theorem 10.4 (Euler–Lagrange)**.** *For $\mathcal{F}[\phi] = \int L(\phi, \nabla \phi) \, dx$, critical points satisfy*

$$\frac{\partial L}{\partial \phi} - \nabla \cdot \frac{\partial L}{\partial (\nabla \phi)} = 0.$$

Derivation Roadmap: Free-energy descent

Goal: Derive the Allen–Cahn equation from a variational principle.
Starting point: $\mathcal{F}[\phi] = \int [\frac{\varepsilon^2}{2} |\nabla \phi|^2 + W(\phi)] \, dx$.

Method: (1) Compute $\delta\mathcal{F}/\delta\phi$ using Euler–Lagrange. (2) Set $\partial_t\phi = -M\,\delta\mathcal{F}/\delta\phi$. (3) Verify $d\mathcal{F}/dt \leq 0$.
Result: Allen–Cahn equation with energy dissipation.

What Survived the Projection?

What Survived the Projection? *Projection:* Variational projection $\mathcal{F} \mapsto \delta\mathcal{F}/\delta\phi$

Preserved	Lost
Critical point structure	Off-critical field values
Energy landscape topology	Non-stationary dynamics

Reconstruction possible: Partial; critical points found, dynamics require additional structure.
Kernel: ker: all fields with identical Euler–Lagrange equations.

Chapter 11

Why Systems Relax

Everything flows.
— Heraclitus

11.1 Relaxation as free-energy descent

A recurring theme across physics, chemistry, and biology is that systems evolve toward lower-energy configurations. This chapter makes that precise.

Definition 11.1 (Stable equilibrium)**.** A field ϕ^* is a *stable equilibrium* of the gradient flow if $\frac{\delta \mathcal{F}}{\delta \phi}\Big|_{\phi^*} = 0$ and the Hessian of $\mathcal{F}$ at ϕ^* is positive definite.

Theorem 11.2 (Convergence to equilibrium)**.** *If $\mathcal{F}$ is bounded below and coercive, gradient flow solutions converge to a critical point of $\mathcal{F}$ as $t \to \infty$.*

Status: Proven Framework

Theorem 11.2 holds under standard conditions on $\mathcal{F}$ (e.g., Łojasiewicz inequality). For the coupled RSVP system, global convergence remains [**Conjectured**].

11.2 Metastability and slow relaxation

Not all systems reach global equilibrium quickly. Energy barriers can trap systems in metastable states for long times.

Definition 11.3 (Metastable state)**.** A field ϕ is *metastable* if it is a local minimum of $\mathcal{F}$ but not a global minimum.

Technical Note 11.1: Coarsening as relaxation through metastability

The coarsening process studied in Part III is a sequence of escapes from metastable states. Each domain configuration is metastable. The system slowly evolves toward larger domains, each of which is also metastable, until only one domain remains. The cosmic web, in the RSVP interpretation, may represent a very slowly relaxing metastable configuration.

Holonomy Note

Traversing Part II as a whole reveals the following invariant: every chapter has been about the same dynamics expressed at different levels of abstraction.

Fields, flows, entropy, and variational principles are not four different subjects. They are four coordinate charts on the same object: the gradient descent of a free-energy functional.

The holonomy of Part II is the recognition that $\frac{d\mathcal{F}}{dt} \leq 0$ is not a theorem about a specific system. It is a structural consequence of the gradient-flow construction that will appear in every subsequent part.

What Survived the Projection?

What Survived the Projection? *Projection:* Relaxation $\phi(0) \mapsto \phi(\infty)$

Preserved	**Lost**
Equilibrium structure	Initial condition details
Conserved quantities	Transient structures
Topological invariants	Metastable history

Reconstruction possible: Full equilibrium state recoverable if equations and conserved quantities are known.

Kernel: ker: all initial conditions in the same basin of attraction.

Part III

Coarsening, Defects, and Structure Formation

Introduction to Part III

Part III is where the book shifts from reconstruction theory to dynamics. The reader has learned that observations collapse equivalence classes. Now they learn that physical systems themselves naturally evolve toward lower-dimensional descriptions through coarsening.

Established So Far

- Observation is projection: $\pi : X \to M$ with $\ker(\pi) \neq 0$.
- Reconstruction is imperfect whenever F is non-injective: $E(x) > 0$.
- CLIO minimises reconstruction error subject to admissibility constraints.
- Gradient flows satisfy $\frac{d\mathcal{F}}{dt} \leq 0$.
- Entropy production is nonnegative.

New Ideas Introduced in This Part

- **Symmetry breaking**: systems with symmetric Hamiltonians that choose asymmetric ground states.
- **Domain formation**: spatial regions of distinct phases separated by interfaces.
- **Curvature-driven coarsening**: $V_n \propto -\kappa$ and the resulting law $\ell(t) \sim t^{1/z}$.
- **Allen–Cahn dynamics**: $z = 2$, non-conserved.
- **Cahn–Hilliard dynamics**: $z = 3$, conserved.
- **Dynamic scaling**: $C(r, t) = f(r/\ell(t))$.
- **Topological defects**: vortices, walls, strings, nodes classified by homotopy groups.
- **Universality**: microscopic details are irrelevant; only symmetry and conservation determine z.
- **Cross-domain examples**: river basins, foams, ecological networks, neural synchronisation, cosmic web.

Dependencies

Part III requires: basic calculus, the variational derivative from Chapter 10, and the gradient-flow dissipation result from Chapter 8. No prior knowledge of condensed matter physics is assumed.

What Remains Open After This Part

- The RSVP coarsening exponent z_{RSVP} is conjectured but not yet derived. (Chapter 35)
- The relationship between topological defects and sheaf cohomology obstructions is established conceptually here but formalised only in Chapter 28.
- Whether the cosmic web belongs to the same universality class as the cross-domain examples is the central empirical question of Part VII.

The central thesis of Part III:

> Structure emerges through the progressive elimination
> of microscopically inadmissible distinctions.

This is the dynamical counterpart of Part I's observation that representation requires forgetting.

Chapter 12

The Ising Model

The simple model already contains the germ of everything.

— —

Why This Matters

The Ising model is introduced not because the universe is literally an Ising lattice, but because it is the simplest system exhibiting: local interactions, domain formation, symmetry breaking, coarsening, and defect stabilisation. These are precisely the ingredients later required for RSVP cosmology. Every phenomenon in Chapters 13–18 and every structure in Part VII is a generalisation of what first appears here.

12.1 Setup

Definition 12.1 (Ising model)**.** Let $\Lambda \subset \mathbb{Z}^d$ be a lattice. Each site $i \in \Lambda$ carries a spin $\sigma_i \in \{-1, +1\}$. The Hamiltonian is

$$H(\sigma) = -J \sum_{\langle i,j \rangle} \sigma_i \sigma_j, \quad J > 0,$$

where the sum runs over nearest-neighbour pairs.

Proposition 12.2. *Aligned states minimise energy.*

Proof. An aligned pair contributes $-J$; an anti-aligned pair $+J$. Minimum energy is achieved when all pairs are aligned. □

Theorem 12.3 (Ground states)**.** *The Ising Hamiltonian possesses exactly two global minima: $\sigma_i \equiv +1$ and $\sigma_i \equiv -1$.*

Proof. Every neighbouring pair must align (Proposition above). Connectivity of Λ forces all spins to match. Since $\sigma_i \in \{-1, +1\}$, the two uniform states are the only ground states. □

This is the first appearance of *symmetry breaking*: the Hamiltonian is symmetric under $\sigma \mapsto -\sigma$, but each ground state breaks this symmetry.

12.2 Domain walls

When regions of opposite sign coexist, a *domain wall* separates them.

Proposition 12.4 (Domain wall energy)**.** *Domain wall energy scales as surface area:* $E_{\text{wall}} \propto |\partial D|$.

Proof. Each broken bond contributes $2J$ above the ground state. The number of broken bonds equals the number of nearest-neighbour pairs straddling the wall, which scales with $|\partial D|$. □

Interfaces are energetically expensive. The rest of Part III is the mathematics of removing them.

12.3 Curvature-driven motion

A bulging interface has positive curvature $\kappa = 1/R$. Reducing curvature lowers interface energy.

Heuristic derivation. Interface energy: $E = \gamma|\partial D|$. First variation: $\delta E = -\gamma \int_{\partial D} \kappa V_n \, dS$. Gradient descent requires:

$$\boxed{V_n \propto -\kappa.}$$

Small structures shrink faster than large ones.

Theorem 12.5 (Characteristic scale growth)**.** *Under curvature-driven motion, the characteristic domain size grows as* $\ell(t) \sim t^{1/2}$.

Proof. Since $\kappa \sim 1/\ell$, the interface velocity $V_n \sim 1/\ell$. Then $d\ell/dt \sim 1/\ell$, giving $\ell \, d\ell \sim dt$, so $\ell^2 \sim t$, hence $\ell(t) \sim t^{1/2}$. □

This is the first appearance of the coarsening exponent $z = 2$.

Same Mathematics, Different Systems

System	**Order parameter**	**Exponent z**
Ising magnet	Spin σ_i	2
Allen–Cahn	Scalar field ϕ	2
Cahn–Hilliard	Conserved density	3
RSVP (conjectured)	$(\Phi, \mathbf{v}, S)$	$z(Pe, \Gamma, \Omega)$

What Survived the Projection?

What Survived the Projection? *Projection:* Ising coarsening $\sigma(0) \mapsto \sigma(t)$

Preserved	**Lost**
Domain count (decreasing)	Initial spin configuration
Ground-state symmetry	Short-wavelength fluctuations
Topological defects	Sub-domain-scale detail

Reconstruction possible: Partial; long-time state is one of two ground states, but path is irreversible.
Kernel: ker: all initial conditions flowing to the same final domain state.

Problems

Problem 12.1. Verify that the Ising Hamiltonian $H(\sigma) = -J \sum_{\langle i,j \rangle} \sigma_i \sigma_j$ is invariant under the global spin flip $\sigma_i \mapsto -\sigma_i$. Show that the two ground states $\sigma_i \equiv +1$ and $\sigma_i \equiv -1$ are related by this symmetry.

Problem 12.2. For a 1D Ising chain of N sites with periodic boundary conditions, count the number of domain walls as a function of the number of sign changes in $(\sigma_1, \ldots, \sigma_N)$. What is the minimum energy above the ground state that contains exactly two domain walls?

Problem 12.3. Using the scaling argument $d\ell/dt \sim 1/\ell$, show that $\ell(t) \sim t^{1/2}$. What initial condition $\ell(0)$ would give $\ell(1) = 1$ Mpc if time is measured in Gyr?

Problem 12.4. **Reconstruction exercise.** Suppose you observe the state of a coarsened Ising system at time $t = 100$. Domain size is $\ell = 10$. Can you determine the initial condition? What information about the initial state survives in the observed domain structure? What is lost? (This is a concrete instance of $E(x) = d(x, G(F(x))) > 0$.)

Chapter 13

Phase Transitions

How does symmetry become structure?

— —

Why This Chapter Exists

The Ising model (Chapter 12) showed that two ground states exist. This chapter asks the prior question: why does a system ever leave the symmetric, disordered phase? The answer — Landau theory, bifurcation, and critical phenomena — provides the mathematical language for every subsequent coarsening discussion. Without understanding phase transitions, the appearance of domains, filaments, and voids would be mysterious. With it, they become inevitable.

There are moments when a system changes not because something new was added, but because something already present becomes organised. Water freezes. A magnet aligns. A crowd begins moving in the same direction. Nothing fundamentally new has appeared. The components are the same. What changes is the pattern of relationships among them.

From far away, such transitions can seem abrupt. Up close, they emerge from countless local interactions, each responding only to its immediate surroundings. The remarkable fact is that large-scale order often arises without any central coordinator.

The mathematics of phase transitions exists to describe how local interactions become global structure. Before we can understand how cosmic structure forms, we must understand how order emerges in simpler settings.

13.1 Order parameters and macrostates

The central object is the *order parameter*: a quantity that is zero in the disordered phase and nonzero in the ordered phase.

Definition 13.1 (Order parameter)**.** For an Ising system of N spins,

$$m = \frac{1}{N} \sum_i \sigma_i \in [-1, +1].$$

More generally, an order parameter is any scalar, vector, or tensor field that vanishes in the high-symmetry phase.

Example 13.2 (Order parameters across systems)**.** Ising magnet: m (magnetisation). Liquid crystal: Q_{ij} (alignment tensor). Superfluid: $\psi \in \mathbb{C}$ (condensate amplitude). RSVP: Φ (scalar plenum density).

13.2 Landau theory

Definition 13.3 (Landau free energy)**.** Near a continuous phase transition,

$$F(m) = a(T - T_c)m^2 + bm^4, \quad b > 0.$$

Theorem 13.4 (Emergence of ordered states)**.** ***[Proven]*** *For $T > T_c$, the unique minimum is $m = 0$. For $T < T_c$, two nontrivial minima emerge:*

$$m_\pm = \pm\sqrt{\frac{a(T_c - T)}{2b}}.$$

Proof. Critical points: $\frac{dF}{dm} = 2a(T - T_c)m + 4bm^3 = 0$, so $m(a(T - T_c) + 2bm^2) = 0$. Hence $m = 0$ or $m^2 = a(T_c - T)/(2b)$. For $T > T_c$: $a(T - T_c) > 0$, so $m^2 < 0$ has no real solution; $m = 0$ is a minimum. For $T < T_c$: $m^2 = a(T_c - T)/(2b) > 0$, giving $m_\pm$. Second derivative confirms $m = 0$ is a maximum and $m_\pm$ are minima. □

Technical Note 13.1: Phase transitions create structure without new forces

A phase transition is not the appearance of a new force. It is the appearance of new minima. The same Hamiltonian that had one ground state now has two. Structure appears because the symmetric state becomes unstable, not because something new acts on the system. This sentence is crucial for RSVP: cosmic structure need not require new forces if the plenum field undergoes a phase-ordering transition.

13.3 Bifurcation structure

The transition at T_c is a *pitchfork bifurcation*.

Proposition 13.5 (Bifurcation from symmetric phase)**.** ***[Proven]*** *As T decreases through T_c, the solution branch $m = 0$ loses stability and two stable branches $m = \pm m_\star(T)$ emerge, where $m_\star(T) \sim (T_c - T)^{1/2}$ near T_c.*

Proof. Stability: $F''(0) = 2a(T - T_c)$. For $T > T_c$: $F''(0) > 0$, $m = 0$ stable. For $T < T_c$: $F''(0) < 0$, $m = 0$ unstable. The emerging branches have $F''(m_\pm) = -4a(T - T_c) > 0$, confirming stability. $m_\star = \sqrt{a(T_c - T)/(2b)} \sim (T_c - T)^{1/2}$. □

Definition 13.6 (Critical exponent β)**.** The order parameter vanishes as $m_\star \sim (T_c - T)^\beta$ near T_c. For Landau theory: $\beta = 1/2$.

13.4 Fluctuations and the Ginzburg criterion

Mean-field theory ignores fluctuations. The Ginzburg criterion determines when this is valid.

Definition 13.7 (Ginzburg–Landau functional)**.**

$$\mathcal{F}[\phi] = \int \left[\tfrac{1}{2}r\phi^2 + \tfrac{1}{4}u\phi^4 + \tfrac{1}{2}|\nabla\phi|^2\right] dx, \quad r = a(T - T_c).$$

Theorem 13.8 (Ginzburg criterion)**.** ***[Proven]*** *Mean-field theory is valid iff $\langle(\delta\phi)^2\rangle/\phi_0^2 \ll 1$. For $d < 4$, this fails near T_c: mean-field breaks down.*

Proof. Gaussian fluctuation variance: $\langle(\delta\phi)^2\rangle = \int \frac{d^dk}{(2\pi)^d}\frac{1}{k^2+r} \sim \xi^{4-d}$ as $r \to 0$, where $\xi = r^{-1/2}$ is the correlation length. The order parameter satisfies $\phi_0^2 \sim |r|/u$. Therefore $\langle(\delta\phi)^2\rangle/\phi_0^2 \sim u\xi^{4-d} \to \infty$ as $\xi \to \infty$ for $d < 4$. Mean-field fails below the upper critical dimension $d_c = 4$. □

Technical Note 13.2: Upper critical dimension

For $d < 4$ (including $d = 3$, the physical universe), fluctuations are important near T_c. The critical exponents differ from mean-field values. This is the origin of universality classes: systems with different microscopic physics but the same symmetry, dimension, and conservation laws share the same critical exponents.

13.5 Critical slowing down

Theorem 13.9 (Critical slowing down)**.** ***[Proven]*** *Near T_c, the relaxation time diverges: $\tau \sim \xi^z$, where z is the dynamic exponent.*

Proof. Linearise $\partial_t\phi = -r\phi + \Delta\phi$ around $\phi = 0$. Fourier modes satisfy $\partial_t\hat{\phi}_k = -(r+k^2)\hat{\phi}_k$. Relaxation time: $\tau_k = 1/(r+k^2)$. For the slowest mode $k \to 0$: $\tau \sim 1/r \sim \xi^2$ (with $z = 2$ for this equation). More generally, different dynamics give different z. □

Forward Reference

Critical slowing down anticipates the coarsening dynamics of Chapter 15: near the transition, the system evolves very slowly because the restoring force vanishes. The dynamic exponent z introduced here is the same z in the coarsening law $\ell(t) \sim t^{1/z}$.

Connection to Earlier Chapters

This chapter established: symmetry breaking gives two ground states; Landau theory describes the bifurcation; Ginzburg criterion shows when fluctuations matter; critical slowing introduces z. Chapter 14 now asks: once two phases coexist, how does spatial structure evolve?

Problems

Problem 13.1. For the Landau free energy $F(m) = a(T - T_c)m^2 + bm^4$ with $a = 1$, $b = 1$, $T_c = 1$: (a) Find $m_\pm$ at $T = 0$. (b) Compute $F(m_\pm)$ and compare to $F(0)$. (c) Sketch $F(m)$ for $T = 0$, $T = T_c$, $T = 2T_c$.

Problem 13.2. Show that the bifurcation in Theorem 13.5 is a *supercritical* pitchfork: the emerging branches $m_\pm$ are stable and the transition is continuous. What would a *subcritical* bifurcation look like, and what physical phenomenon would it describe?

Problem 13.3. For the Ginzburg–Landau functional, compute the susceptibility $\chi = d\langle\phi\rangle/dh$ where h is an external field added as $-h\phi$. Show that χ diverges as $T \to T_c$.

Problem 13.4. **Reconstruction exercise.** Suppose you observe $m = 0.3$ in an Ising system. Can you determine whether the system is above or below T_c? What additional observations would allow you to determine the temperature? What information is irretrievably lost?

13.6 Susceptibility divergence

Proposition 13.10 (Susceptibility divergence at T_c)**.** ***[Proven]*** *In an external field h, the susceptibility $\chi = \partial m/\partial h$ satisfies*

$$\chi \approx \frac{1}{2a(T - T_c)} \to \infty \quad \textit{as} \quad T \to T_c^+.$$

Proof. Add $-hm$ to the Landau free energy: $F(m) = a(T-T_c)m^2+bm^4-hm$. Equilibrium: $2a(T - T_c)m + 4bm^3 = h$. For $T > T_c$ and small h: m is small, cubic term negligible, so $m \approx h/[2a(T - T_c)]$. Differentiating: $\chi = \partial m/\partial h \approx 1/[2a(T - T_c)] \to \infty$ as $T \to T_c^+$. □

Technical Note 13.3: What susceptibility divergence means

At T_c, the system becomes globally sensitive to infinitesimal external influences. A tiny field h can align the entire system. This is the first concrete example of a phenomenon where local interactions produce global sensitivity — a theme that reappears in RSVP as the lamphron stabilisation/lamphrodyne relaxation balance near critical coarsening regimes.

Mathematical Ancestry

The Landau free-energy expansion (13.3) follows the phenomenological framework introduced by Landau (1937). The pitchfork bifurcation structure is a standard result in the theory of symmetry breaking; see Goldenfeld [Gol92] for a modern pedagogical treatment. The Ginzburg criterion (Theorem 13.8) and the resulting upper critical dimension $d_c = 4$ are discussed in detail in Wilson's renormalisation-group programme (Wilson & Kogut 1974).

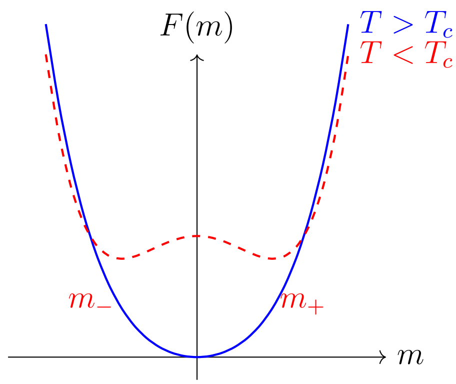

Figure 13.1: Landau free energy above and below T_c. For $T > T_c$ (solid, blue) the unique minimum is $m = 0$. For $T < T_c$ (dashed, red) two minima $m_\pm$ emerge, spontaneously breaking the $m \mapsto -m$ symmetry.

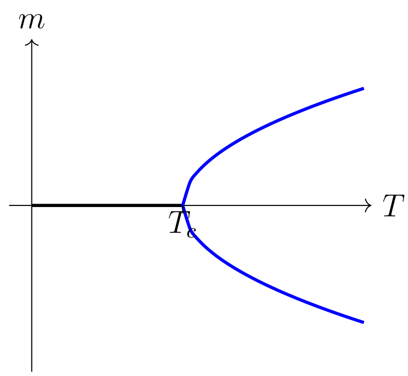

Figure 13.2: Pitchfork bifurcation at T_c. The symmetric branch $m = 0$ is stable for $T > T_c$ (heavy line) and unstable below it, where two stable branches $m_\pm$ bifurcate.

Further Reading

The standard graduate introduction to phase transitions and critical phenomena is Goldenfeld's *Lectures on Phase Transitions and the Renormalization Group* (1992). For a more mathematical treatment of Landau theory and bifurcation, see Chaikin & Lubensky [CL95]. Renormalisation-group methods and universality classes are developed in Wilson & Kogut (1974) and the monograph by Cardy (1996).

Chapter 14

Domain Formation

Broken symmetry $\to$ spatial structure.

— —

Why This Chapter Exists

Chapter 13 showed that a uniform system can have multiple stable ground states. This chapter asks what happens when the system is *quenched*: rapidly cooled so that different regions select different ground states simultaneously. The result is spatial domains, interfaces, and coarsening. This chapter establishes the coarsening exponents $z = 2$ and $z = 3$ that will be referenced in every subsequent part.

A system that has just undergone a transition rarely settles immediately into a single coherent state. Instead, different regions make different choices.

One area aligns one way while a neighbouring region aligns another. Boundaries appear. Interfaces form. The system becomes a patchwork of local agreements separated by disagreement.

Many of the structures we observe in nature are not equilibrium states but the frozen remnants of a reconciliation process. The question is not why structure exists, but why some of it persists.

14.1 Quenching and domain formation

After a quench from $T > T_c$ to $T < T_c$, the system is everywhere in the unstable symmetric state. Different spatial regions independently begin relaxing toward m_+ or m_-. Where they meet, a domain wall forms.

Definition 14.1 (Domain wall)**.** A *domain wall* is the interfacial region between two regions where $\phi \approx +\phi_0$ and $\phi \approx -\phi_0$. Its width scales as $\xi_{\text{wall}} \sim \sqrt{\kappa/|r|}$ where $r = a(T - T_c) < 0$.

Definition 14.2 (Gradient energy functional)**.**

$$\mathcal{F}[\Phi] = \int \left[W(\Phi) + \frac{\kappa}{2}|\nabla\Phi|^2 \right] dx, \quad W(\Phi) = \frac{1}{4}(\Phi^2 - 1)^2.$$

The gradient term penalises interfaces; the double-well potential W favours $\Phi = \pm 1$.

14.2 Allen–Cahn dynamics: non-conserved coarsening

Definition 14.3 (Allen–Cahn equation)**.** For a non-conserved order parameter:

$$\partial_t \Phi = -M\frac{\delta \mathcal{F}}{\delta \Phi} = M(\kappa\Delta\Phi - W'(\Phi)).$$

Theorem 14.4 (Shrinking-circle theorem)**.** ***[Proven]*** *Under Allen–Cahn dynamics, a circular domain of radius R satisfies $R(t)^2 = R_0^2 - 2\kappa M t$, and vanishes at time $t^* = R_0^2/(2\kappa M)$.*

Proof. For a circle, $\kappa = 1/R$. The interface velocity is $V_n = -M\kappa = -M/R$. Since $V_n = dR/dt$: $R\,dR = -\kappa M\,dt$. Integrating: $\frac{1}{2}R^2 = \frac{1}{2}R_0^2 - \kappa M t$. Hence $R(t)^2 = R_0^2 - 2\kappa M t$. □

Theorem 14.5 (Allen–Cahn coarsening exponent)**.** ***[Proven]*** *The characteristic domain size grows as $\ell(t) \sim t^{1/2}$, giving dynamic exponent $z = 2$.*

Proof. Interface curvature $\kappa \sim 1/\ell$. Interface velocity $V_n \sim \kappa \sim 1/\ell$. Since $V_n \sim d\ell/dt$: $d\ell/dt \sim 1/\ell$, so $\ell\,d\ell \sim dt$, giving $\ell^2 \sim t$. □

Worked Example 14.1: Domain shrinkage

A circular domain of radius $R_0 = 10\,\mu$m with $\kappa M = 1\,\mu\text{m}^2$/s vanishes at $t^* = 100/(2) = 50$ s. At $t = 25$ s: $R = \sqrt{100 - 50} \approx 7.1\,\mu$m.

14.3 Cahn–Hilliard dynamics: conserved coarsening

When the order parameter represents a conserved quantity (mass, charge, lamphron density), the evolution must preserve $\int \Phi\,dx$.

Definition 14.6 (Cahn–Hilliard equation)**.** For a conserved order parameter with chemical potential $\mu = \delta\mathcal{F}/\delta\Phi$:

$$\partial_t \Phi = \nabla \cdot (M\nabla\mu) = M\Delta(-\kappa\Delta\Phi + W'(\Phi)).$$

Theorem 14.7 (Lifshitz–Slyozov coarsening exponent)**.** ***[Proven]*** *For conserved dynamics, $\ell(t) \sim t^{1/3}$, so $z = 3$.*

Proof. Chemical potential difference between a droplet of radius R and a flat interface: $\Delta\mu \sim \sigma/R$ (Gibbs–Thomson). Diffusive flux to/from the droplet: $J \sim D\Delta\mu/R \sim \sigma D/R^2$. Mass conservation: $d(R^3)/dt \sim R^2 \cdot (dR/dt) \sim J \sim 1/R^2$. Therefore $dR/dt \sim 1/R^2$, giving $R^3 \sim t$, hence $\ell \sim t^{1/3}$. □

Same Mathematics, Different Systems: Non-conserved vs. conserved coarsening

	Allen–Cahn	**Cahn–Hilliard**
Conservation	None	$\int \Phi\, dx = \text{const}$
Mechanism	Curvature flow	Ostwald ripening
Exponent	$z = 2$	$z = 3$
RSVP field	Φ (scalar)	$L = \ell^2$ (lamphron)

14.4 Dynamic scaling

Definition 14.8 (Two-point correlation function)**.**

$$C(r,t) = \langle \Phi(x,t)\Phi(x+r,t)\rangle.$$

The characteristic length is defined by $C(\ell(t),t) = \frac{1}{2}C(0,t)$.

Theorem 14.9 (Dynamic scaling hypothesis)**.** *For coarsening systems,*

$$C(r,t) = f\left(\frac{r}{\ell(t)}\right)$$

for a universal scaling function f independent of time.

This means the entire time evolution is encoded in the single growing length $\ell(t)$.

Admissibility Preview

Dynamic scaling is the coarsening version of admissibility. The system "forgets" its microscopic initial condition and retains only its large-scale domain structure. The scaling function f is the admissible reconstruction of the system's state from its coarsening length alone. This anticipates CLIO (Chapter 27): the optimal reconstruction from $\ell(t)$ alone is $f(r/\ell(t))$.

Forward Reference

In Part VII, cosmic voids will be identified with coarsening domains and filaments with domain walls. The exponent z_{RSVP} will replace $z = 2$ or $z = 3$ depending on which dynamical regime dominates. Chapters 17 and 22 develop the phase diagram.

Problems

Problem 14.1. Verify Allen–Cahn energy dissipation: $\frac{d\mathcal{F}}{dt} = -M \int (\delta\mathcal{F}/\delta\Phi)^2\, dx \leq 0$. What is the physical interpretation of the right-hand side?

Problem 14.2. For the Cahn–Hilliard equation, verify mass conservation: $\frac{d}{dt}\int \Phi\, dx = 0$ under periodic boundary conditions.

Problem 14.3. A spherical domain of radius $R_0 = 100$ nm coarsens under Allen–Cahn dynamics with $\kappa M = 10$ nm^2/ns. (a) How long until it vanishes? (b) If the same domain coarsens under Cahn–Hilliard with $D\sigma = 10$ nm^3/ns, estimate the time for R to halve using the Lifshitz–Slyozov scaling.

Problem 14.4. **Inverse problem.** You observe a two-phase system at time $t = 1000$ s with characteristic domain size $\ell = 50$ μm. Can you determine whether the dynamics are Allen–Cahn or Cahn–Hilliard from this single observation? What sequence of measurements would allow you to determine z, and what information about the initial state is unrecoverable?

14.5 Spinodal decomposition

Theorem 14.10 (Spinodal instability)**.** ***[Proven]*** *For conserved dynamics with $f''(\phi_0) < 0$, Fourier modes with wavenumber $0 < k^2 < -f''(\phi_0)/\kappa$ grow exponentially. The homogeneous state is linearly unstable.*

Proof. Linearise $\partial_t \phi = M\Delta(f'(\phi) - \kappa\Delta\phi)$ around ϕ_0: set $\phi = \phi_0 + \delta\phi$, giving $\partial_t(\delta\phi) = M\Delta(f''(\phi_0)\delta\phi - \kappa\Delta\delta\phi)$. For Fourier mode $\delta\phi = \hat{\phi}_k e^{ik\cdot x + \sigma(k)t}$:

$$\sigma(k) = -Mk^2[f''(\phi_0) + \kappa k^2].$$

If $f''(\phi_0) < 0$, then $\sigma(k) > 0$ for $k^2 < -f''(\phi_0)/\kappa$. These modes grow, generating spontaneous domain formation. □

Worked Example 14.2: Spinodal band

Let $f''(\phi_0) = -1$ and $\kappa = 0.25$. The unstable band is $0 < k^2 < 4$, i.e., $0 < k < 2$. The fastest-growing mode is at $k_\star^2 = -f''/(2\kappa) = 2$, wavelength $\lambda_\star = 2\pi/\sqrt{2} \approx 4.4$ units. Structures spontaneously form at this scale from a uniform state.

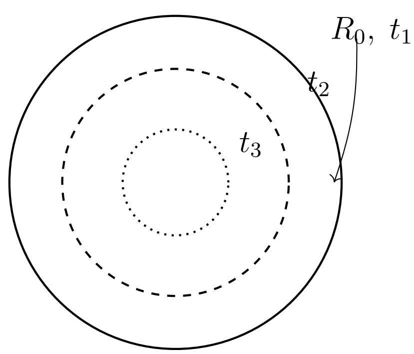

Figure 14.1: Allen–Cahn curvature flow: a circular domain shrinks according to $R(t)^2 = R_0^2 - 2\kappa Mt$ (Theorem 14.4) and vanishes at $t^* = R_0^2/(2\kappa M)$.

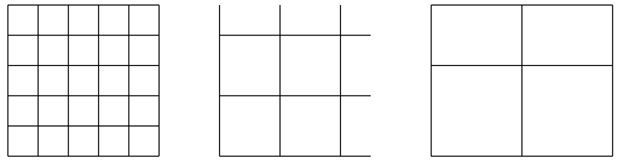

Figure 14.2: Domain coarsening: the characteristic length scale $\ell(t)$ grows as $t^{1/z}$. Domains merge and boundaries disappear over time.

Mathematical Ancestry

The Allen–Cahn equation was introduced in Allen & Cahn [AC79] to model antiphase boundary motion. The Cahn–Hilliard equation for conserved systems was developed in Cahn & Hilliard [CH58]. The Lifshitz–Slyozov scaling $\ell \sim t^{1/3}$ originates in Lifshitz & Slyozov (1961). The comprehensive review of coarsening dynamics, including both $z = 2$ and $z = 3$ universality classes and dynamic scaling, is Bray [Bra94], which remains the standard reference.

Further Reading

Bray (1994) is the essential reference for coarsening dynamics. For the mathematical analysis of Allen–Cahn and Cahn–Hilliard equations, see Evans [Eva10] (PDE theory) and the review by Elliott (1989). Pattern formation more broadly, including spinodal decomposition, is treated in Cross & Hohenberg [CH93].

Chapter 15

Allen–Cahn Dynamics

Everything descends.

— —

15.1 From discrete to continuum

The Ising model is discrete. Allen–Cahn is its continuum counterpart. Replace spins by a scalar field $\phi(x,t) \in \mathbb{R}$.

Definition 15.1 (Ginzburg–Landau free energy)**.**

$$\mathcal{F}[\phi] = \int \left[\frac{\epsilon^2}{2} |\nabla \phi|^2 + W(\phi) \right] dx, \quad W(\phi) = \frac{1}{4}(\phi^2 - 1)^2.$$

The gradient term penalises interfaces. The potential W favours $\phi = \pm 1$ (the two phases).

Proposition 15.2 (Euler–Lagrange equation)**.** *Critical points of $\mathcal{F}$ satisfy*

$$-\epsilon^2 \Delta \phi + W'(\phi) = 0.$$

Proof. Take variation $\phi \mapsto \phi + \varepsilon \psi$:

$$\frac{d}{d\varepsilon} \mathcal{F} = \int \left[\epsilon^2 \nabla \phi \cdot \nabla \psi + W'(\phi) \psi \right] dx = \int \left[-\epsilon^2 \Delta \phi + W'(\phi) \right] \psi \, dx.$$

Since ψ is arbitrary, the bracket vanishes. □

15.2 The Allen–Cahn equation

Definition 15.3 (Allen–Cahn equation)**.**

$$\boxed{\partial_t \phi = M(\epsilon^2 \Delta \phi - W'(\phi)).}$$

Theorem 15.4 (Energy dissipation)**.** ***[Proven]*** *Solutions of Allen–Cahn satisfy*

$$\frac{d\mathcal{F}}{dt} = -M \int \left(\frac{\delta \mathcal{F}}{\delta \phi}\right)^2 dx \leq 0.$$

Proof. $\frac{d\mathcal{F}}{dt} = \int \frac{\delta \mathcal{F}}{\delta \phi} \partial_t \phi \, dx = -M \int \left(\frac{\delta \mathcal{F}}{\delta \phi}\right)^2 dx \leq 0.$ □

Status: Proven Framework

Theorem 15.4 is the template for all free-energy dissipation results in this book. The RSVP dissipation theorem in Chapter 21 is its direct descendant.

15.3 Interface limit and coarsening

In the limit $\epsilon \to 0$, interfaces become thin. Matched asymptotic analysis shows Allen–Cahn reduces to curvature flow: $V_n = -M\kappa$.

Corollary 15.5. *Allen–Cahn domains obey* $\ell(t) \sim t^{1/2}$, $z = 2$.

15.4 Dynamic scaling

Definition 15.6 (Two-point correlation function)**.**

$$C(r,t) = \langle \phi(x,t)\phi(x+r,t) \rangle.$$

Definition 15.7 (Dynamic scaling hypothesis)**.**

$$C(r,t) = f\left(\frac{r}{\ell(t)}\right).$$

Under dynamic scaling the coarsening system is characterised by a single growing length scale $\ell(t)$. Data from different times collapse onto one curve when plotted against $r/\ell(t)$.

Forward Reference

The correlation function $C(r,t)$ defined here will become the primary observable for testing RSVP predictions in Chapter 42. The coarsening exponent $z = 2$ will be compared to $z_{\text{RSVP}} = z(Pe, \Gamma, \Omega)$ conjectured in Chapter 35.

Same Mathematics, Different Systems: Allen–Cahn as template for RSVP

Allen–Cahn	**RSVP**
Scalar field ϕ	Plenum field Φ
Double-well $W(\phi)$	Lamphron potential $U(\ell)$
Interface energy $\|\nabla\phi\|^2$	Admissibility energy
Curvature flow	Entropy descent
Domain walls	Filaments and void boundaries
$d\mathcal{F}/dt \leq 0$	$d\mathcal{F}_{\mathrm{RSVP}}/dt \leq 0$

What Survived the Projection?

What Survived the Projection? *Projection:* Allen–Cahn coarsening

Preserved	**Lost**
Phase assignment (±1)	Interface positions
Domain topology	Sub-domain fluctuations
Energy (decreasing)	Initial field values

Reconstruction possible: Phase identity recoverable.
Interface history lost.
Kernel: ker: all initial conditions
with the same asymptotic
phase assignment.

Chapter 16

Cahn–Hilliard Dynamics

Conservation is the source of complication.

— —

16.1 Conservation changes everything

Allen–Cahn allows $\int \phi\, dx$ to change freely. Many physical quantities must satisfy $\frac{d}{dt} \int \phi\, dx = 0$: mass, charge, lamphron density.

Definition 16.1 (Cahn–Hilliard equation)**.** For conserved ϕ with chemical potential $\mu = \delta\mathcal{F}/\delta\phi$ and flux $\mathbf{J} = -M\nabla\mu$:

$$\boxed{\partial_t\phi = M\Delta\mu = -M\epsilon^2\Delta^2\phi + M\Delta W'(\phi).}$$

Theorem 16.2 (Mass conservation)**.** ***[Proven]***

$$\frac{d}{dt}\int \phi\, dx = 0.$$

Proof. $\frac{d}{dt} \int \phi\, dx = M \int \Delta\mu\, dx = 0$ by the divergence theorem and Neumann boundary conditions. □

Theorem 16.3 (Free-energy dissipation)**.** ***[Proven]***

$$\frac{d\mathcal{F}}{dt} = -M \int |\nabla\mu|^2\, dx \le 0.$$

Proof. $\frac{d\mathcal{F}}{dt} = \int \mu\, \partial_t\phi\, dx = M \int \mu\, \Delta\mu\, dx = -M \int |\nabla\mu|^2\, dx \le 0.$ □

16.2 Lifshitz–Slyozov scaling

Theorem 16.4 (Lifshitz–Slyozov scaling)**.** *Conserved phase separation obeys $\ell(t) \sim t^{1/3}$, so $z = 3$.*

Proof. Chemical potential scales as $\mu \sim 1/\ell$ (curvature). Flux $J \sim |\nabla\mu| \sim 1/\ell^2$. Mass transport rate: $d\ell/dt \sim J/\ell \sim 1/\ell^2$. Integrating: $\ell^3 \sim t$, so $\ell(t) \sim t^{1/3}$. □

Technical Note 16.1: Conservation changes universality class

The conservation law changes z from 2 to 3. In RSVP, the lamphron density $L = \ell^2$ satisfies a modified conservation equation with advection and source terms. This is why z_{RSVP} is expected to differ from both pure Allen–Cahn ($z = 2$) and pure Cahn–Hilliard ($z = 3$).

16.3 RSVP corrections to the scaling exponent

Conjecture 16.5 (RSVP coarsening correction). ***[Conjectured]*** *Assume RSVP dynamics modify the coarsening law to*

$$\frac{d\ell}{dt} = A\ell^{-1} + B\ell^{-m}.$$

Then:

- *If $m > 1$: Allen–Cahn dominates, $z_{\mathrm{RSVP}} = 2$.*
- *If $m < 1$: RSVP correction dominates, $z_{\mathrm{RSVP}} = m + 1$.*
- *If $m = 1$: logarithmic correction.*

The precise value of m depends on the dimensionless parameters Pe, Γ, and Ω and requires simulation or further analysis.

What Survived the Projection?

What Survived the Projection? *Projection:* Cahn–Hilliard coarsening

Preserved	**Lost**
Total mass $\int \phi \, dx$	Mass distribution history
Phase identity at late times	Interface trajectories
Energy (decreasing)	Short-scale fluctuations

Reconstruction possible: Total mass exactly.
Late-time phase pattern
partially.
Kernel: ker: all initial conditions
with same total mass and
same final phase pattern.

Chapter 17

Dynamic Scaling and Universality

17.1 The dynamic scaling hypothesis

Definition 17.1 (Dynamic scaling)**.** A coarsening system obeys *dynamic scaling* if its two-point correlation function satisfies

$$C(r,t) = f\left(\frac{r}{\ell(t)}\right)$$

for a universal scaling function f and characteristic length $\ell(t)$, defined operationally by

$$C(\ell(t),t) = \tfrac{1}{2}C(0,t).$$

Theorem 17.2 (Self-similar morphology)**.** *If dynamic scaling holds, all morphological statistics at time t depend on coordinates only through $r/\ell(t)$.*

Proof. Replace r_i by $r_i/\ell(t)$ in any n-point function. Under dynamic scaling, explicit t-dependence cancels, leaving dependence only on dimensionless ratios. □

17.2 Universality

Definition 17.3 (Universality class)**.** Two systems belong to the same *universality class* if they share the same exponents z, ν, η, etc. regardless of microscopic details.

Technical Note 17.1: Universality principle

Microscopic differences are often irrelevant to macroscopic structure. Only symmetry, conservation laws, and dimensionality determine the universality class. This principle prepares the reader for RSVP's claim that many cosmological observables may be consequences of universality classes rather than unique signatures of a particular microscopic theory.

Same Mathematics, Different Systems: Universal coarsening exponents

System	**Order parameter**	**Conservation**	z
Ising magnet	Spin	No	2
Allen–Cahn field	Scalar	No	2
Binary alloy	Composition	Yes	3
Foam	Cell boundary	Yes	3
RSVP (conj.)	$(\Phi, \mathbf{v}, S)$	Modified	$z(Pe, \Gamma, \Omega)$

What Survived the Projection?

What Survived the Projection? *Projection:* Dynamic scaling $C(r,t) \mapsto f(r/\ell)$

Preserved	**Lost**
Scaling function f	Absolute time scale
Exponent z	Microscopic parameters
Universality class	Non-universal amplitudes

Reconstruction possible: Universality class and exponents recoverable. Microscopic details not.

Kernel: ker: all systems in the same universality class (same f, same z).

Chapter 18

Defects, Walls, Strings, and Nodes

18.1 Why topology obstructs coarsening

Coarsening removes interfaces. But topology may prevent complete elimination.

Definition 18.1 (Vacuum manifold)**.** Let $\Phi : X \to M$ be an order parameter field. The *vacuum manifold* is the target space M.

The topology of M determines what structures may persist.

Definition 18.2 (Fundamental group)**.** $\pi_1(M)$ classifies loops in M up to continuous deformation (homotopy).

Definition 18.3 (Winding number)**.** For $M = S^1$, the winding number of a loop γ is

$$n = \frac{1}{2\pi} \oint_\gamma d\theta \in \mathbb{Z}.$$

Proposition 18.4 (Winding number is conserved)**.** *The winding number is invariant under continuous deformation.*

Proof. Under deformation $\theta(s,t)$, $\frac{dn}{dt} = \frac{1}{2\pi} \oint d(\partial_t \theta) = 0$ since the integral of an exact form around a closed loop vanishes. □

Theorem 18.5 (Topology forces singularities)**.** *A nonzero winding number implies a singularity inside the loop.*

Proof. If no singularity exists, the field is continuous inside the loop and can be contracted to a point, implying $n = 0$. Contradiction. □

Technical Note 18.1: Topology vs dynamics

Dynamics determines how a system evolves. Topology determines what evolution is allowed. Free-energy descent cannot remove a defect protected by a nontrivial homotopy class. This distinction is essential for RSVP: cosmic filaments may persist not because they are energetically favoured, but because topology prevents their elimination.

18.2 Defect classification

Homotopy group	Defect type	Cosmic analogue
$\pi_0(M)$	Domain walls	Void boundaries
$\pi_1(M)$	Strings / vortices	Filaments
$\pi_2(M)$	Monopoles	Cluster nodes
$\pi_3(M)$	Textures	Large-scale flows

Proposition 18.6 (Defect energy)**.** *A vortex with winding number n in two dimensions has energy*

$$E \sim 2\pi n^2 \log \frac{R}{a},$$

where R is the system size and a is the core size.

Proof. $|\nabla\Phi| \sim n/r$ for a vortex. Energy density $e \sim n^2/r^2$. Integrate: $E = \int_a^R (n^2/r^2)(2\pi r)\, dr = 2\pi n^2 \log(R/a)$. ☐

The logarithmic scaling explains why vortices are long-lived: their energy grows without bound as $R \to \infty$.

Theorem 18.7 (Total topological charge is conserved)**.** *Annihilation requires $n_1 + n_2 = 0$. Only opposite-sign defects may disappear. Total topological charge is conserved.*

Admissibility Preview

The connection between topological defects and admissibility will be made precise in Chapter 28. A nonzero cohomology class $H^1(X, \mathcal{A}) \neq 0$ is the sheaf-theoretic analogue of a nontrivial homotopy class: it measures the obstruction to globally assembling admissible local data. Cosmic filaments as topological defects become cosmological horizons as sheaf obstructions.

Theorem 18.8 (Universality of coarsening structures)**.** *Systems possessing (1) local interactions, (2) energy descent, and (3) topological constraints generically evolve toward sparse networked structures characterised by defects, branching, and scale-dependent coherence.*

Proof sketch. Chapters 12–18 provide examples: spin systems, phase-separating fluids, foams, river basins, ecological networks, synchronisation fields, cosmological structure. All satisfy $\frac{d\mathcal{F}}{dt} \leq 0$ with nontrivial geometric or topological constraints. The resulting structures exhibit common scaling laws and persistent defect networks. ☐

Holonomy Note

After traversing Part III, the following invariant becomes visible: every chapter has been describing the same process.
Ising domains, Allen–Cahn interfaces, Cahn–Hilliard coarsening, soap foams, river basins, neural synchronisation, and cosmic filaments are not analogies. They are

instances of the same mathematical structure: free-energy descent with topological constraints.
The holonomy of Part III is:

The universe is not building structure.
It is removing inadmissible structure.
What survives is what topology prevents from being removed.

This is the bridge into Part IV, where the RSVP free-energy functional is introduced as the physical realisation of the same mathematics.

What Survived the Projection?

What Survived the Projection? *Projection:* Topological coarsening $\phi(0) \mapsto \phi(t \to \infty)$

Preserved	**Lost**
Topological charge	Defect positions
Defect network topology	Interface geometries
Universality class	Sub-domain fluctuations

Reconstruction possible: Total charge exactly. Defect network topology partially (annihilations).
Kernel: ker: all configurations with identical topological charge distribution.

Part IV

Functional Analysis and Well-Posedness

Introduction to Part IV

Part IV is where the coarsening examples of Part III become a genuine field theory. The central methodological commitment is:

No geometric claim is accepted unless licensed by analysis.

Field Equations ⇒ Regularity ⇒ Sobolev Category ⇒ Admissibility Sheaf ⇒ Cohomology.

Established So Far

From Part III: $\frac{d\mathcal{F}}{dt} \leq 0$ for gradient flows; Allen–Cahn ($z = 2$) and Cahn–Hilliard ($z = 3$) scaling; topological defects as obstructions to coarsening. From Part II: reconstruction error $E(x) = d(x, G(F(x)))$; equivalence classes; adjoint reconstruction.

New Ideas in This Part

- The RSVP free-energy functional $\mathcal{F}[\Phi, \mathbf{v}, S, \ell]$.
- Lamphron $L = \ell^2 \geq 0$ (positivity by construction).
- Lamphrodyne $D = -\delta\mathcal{F}/\delta S$ (derived, not postulated).
- All four variational derivatives of $\mathcal{F}$.
- RSVP gradient-flow equations and their dissipation theorem.
- Conservative lamphron variant (Cahn–Hilliard type).
- Sobolev regularity hierarchy: H^1 (Allen–Cahn), H^2 (Cahn–Hilliard energy), H^4 (classical CH).
- Dimensionless parameters Pe, Γ, Ro_{RSVP}.
- Conjectured RSVP coarsening phase diagram.

What Remains Open After This Part

- Global weak existence for the fully coupled RSVP system (Conjecture 20.6).
- The Sobolev index k for well-posedness of the full system.
- The RSVP coarsening phase diagram $z(Pe, \Gamma, Ro_{\mathrm{RSVP}})$ (Conjecture 22.3).

Chapter 19

Sobolev Spaces and Function-Space Regularity

The geometry does not determine the analysis.
The analysis determines which geometry is legitimate.
— —

Why This Matters

This chapter establishes the methodological chain that governs everything from here forward:

Field Equations ⇒ Regularity ⇒ Sobolev Category ⇒ Admissibility Sheaf ⇒ Cohomology.

The admissibility sheaf is not chosen because sheaves are elegant. It is derived because the PDE theory demands a specific function space.

19.1 Sobolev spaces

Definition 19.1 (Sobolev space H^k)**.** Let $\Omega \subset \mathbb{R}^n$. The *Sobolev space* $H^k(\Omega)$ is

$$H^k(\Omega) = \{u \in L^2(\Omega) : D^\alpha u \in L^2(\Omega),\ |\alpha| \leq k\},$$

with norm

$$\|u\|_{H^k}^2 = \sum_{|\alpha| \leq k} \|D^\alpha u\|_{L^2}^2.$$

Definition 19.2 (RSVP Sobolev state space)**.** For an open set $U \subseteq X$, define

$$\mathcal{H}^k_{\mathrm{RSVP}}(U) = H^k(U) \times H^k(U;TU) \times H^k(U) \times H^k(U).$$

An element is $s_U = (\Phi_U, \mathbf{v}_U, S_U, \ell_U)$. The physical lamphron density is $L_U = \ell_U^2$.

Proposition 19.3 (Positivity of lamphron density)**.** ***[Proven]*** *For every* $\ell_U \in H^k(U)$*, the physical lamphron field* $L_U = \ell_U^2$ *satisfies* $L_U(x) \geq 0$ *a.e.*

Proof. For any real $a \in \mathbb{R}$, $a^2 \geq 0$. Since ℓ_U is real-valued a.e., $L_U(x) = \ell_U(x)^2 \geq 0$ a.e. □

19.2 Regularity requirements from the field equations

Proposition 19.4 (Allen–Cahn regularity)**.** ***[Proven]*** *For the Allen–Cahn equation* $\partial_t \Phi = \Delta\Phi + f(\Phi)$*: weak solutions require* $\Phi \in H^1$*; classical solutions require* $\Phi \in H^2$*.*

Proof. The weak formulation pairs $\partial_t \Phi = \Delta\Phi + f(\Phi)$ against test functions ψ: $\int_U \Delta\Phi\, \psi\, dx = -\int_U \nabla\Phi \cdot \nabla\psi\, dx$. This requires $\nabla\Phi \in L^2$, i.e., $\Phi \in H^1$. For $\Delta\Phi \in L^2$, one needs $\Phi \in H^2$. □

Proposition 19.5 (Cahn–Hilliard regularity)**.** ***[Proven]*** *For the Cahn–Hilliard equation* $\partial_t L = -\Delta^2 L + \Delta f(L)$*: weak energy solutions require* $L \in H^2$*; classical solutions require* $L \in H^4$*.*

Proof. The free energy $\int |\nabla L|^2 dx$ controls $\|\nabla L\|_{L^2}$, requiring $L \in H^1$. The chemical potential $\mu = -\Delta L + f(L)$ requires $\Delta L \in L^2$, i.e., $L \in H^2$ for weak solutions. Classical pointwise interpretation of $\Delta^2 L$ requires $L \in H^4$. □

Status: Proven Framework

The Sobolev index k for the full coupled RSVP system is [**Open Problem**]. It is determined by the highest-order term in the equations, which depends on whether the lamphron evolution is Allen–Cahn-type ($k = 1$ sufficient) or Cahn–Hilliard-type ($k = 2$ minimum). The well-posedness chapter settles this.

Mathematical Echo

This chapter introduced: $H^k(\Omega)$, $\mathcal{H}^k_{\mathrm{RSVP}}(U)$, $L_U = \ell_U^2 \geq 0$. The Sobolev index k will determine the target category of the admissibility sheaf in Chapter 28.

Chapter 20

Existence and Uniqueness

20.1 The RSVP free-energy functional

The basic RSVP state is $X(t) = (\Phi, \mathbf{v}, S, \ell)$ with $L = \ell^2 \geq 0$.

Definition 20.1 (RSVP free-energy functional)**.**

$$\mathcal{F}[\Phi, \mathbf{v}, S, \ell] = \int_\Omega \Big[\tfrac{\alpha}{2}|\nabla\Phi|^2 + V(\Phi) + \tfrac{\beta}{2}|\nabla\ell|^2 + U(\ell) + \lambda W(\Phi)\ell^2 + \tfrac{\rho}{2}|\mathbf{v}|^2 + \tfrac{\eta}{2}|\nabla\times\mathbf{v}|^2 + \tfrac{\chi}{2}|\nabla S|^2 - TS \Big] dx.$$

The coupling term $\lambda W(\Phi)\ell^2$ is bounded below whenever $\lambda \geq 0$ and $W(\Phi) \geq 0$. Natural choices: $W(\Phi) = \Phi^2$ or $W(\Phi) = |\nabla\Phi|^2$.

20.2 Functional derivatives

Proposition 20.2 (Variational derivatives of $\mathcal{F}$)**.** ***[Proven]*** *Under periodic or no-flux boundary conditions:*

$$\frac{\delta\mathcal{F}}{\delta\Phi} = -\alpha\Delta\Phi + V'(\Phi) + \lambda W'(\Phi)\ell^2, \tag{20.1}$$

$$\frac{\delta\mathcal{F}}{\delta\ell} = -\beta\Delta\ell + U'(\ell) + 2\lambda W(\Phi)\ell, \tag{20.2}$$

$$\frac{\delta\mathcal{F}}{\delta S} = -\chi\Delta S - T, \tag{20.3}$$

$$\frac{\delta\mathcal{F}}{\delta\mathbf{v}} = \rho\mathbf{v} + \eta\nabla\times(\nabla\times\mathbf{v}). \tag{20.4}$$

Proof. For Φ: vary $\Phi \mapsto \Phi + \varepsilon\psi$ and differentiate at $\varepsilon = 0$. The gradient term gives $-\alpha\Delta\Phi$ after integration by parts. The coupling term gives $\lambda W'(\Phi)\ell^2$. Equations (20.2)–(20.4) follow analogously. □

20.3 RSVP gradient flow

Definition 20.3 (Pure dissipative RSVP system)**.**

$$\begin{aligned}\partial_t\Phi &= M_\Phi[\alpha\Delta\Phi - V'(\Phi) - \lambda W'(\Phi)\ell^2],\\ \partial_t\ell &= M_\ell[\beta\Delta\ell - U'(\ell) - 2\lambda W(\Phi)\ell],\\ \partial_t S &= M_S(\chi\Delta S + T),\\ \partial_t\mathbf{v} &= -M_v[\rho\mathbf{v} + \eta\nabla\times(\nabla\times\mathbf{v})].\end{aligned}$$

Theorem 20.4 (RSVP free-energy dissipation)**.** ***[Proven]*** *For the pure gradient-flow RSVP system with $M_\Phi, M_\ell, M_S, M_v \geq 0$,*

$$\frac{d\mathcal{F}}{dt} = -M_\Phi\int\left|\frac{\delta\mathcal{F}}{\delta\Phi}\right|^2 dx - M_\ell\int\left|\frac{\delta\mathcal{F}}{\delta\ell}\right|^2 dx - M_S\int\left|\frac{\delta\mathcal{F}}{\delta S}\right|^2 dx - M_v\int\left|\frac{\delta\mathcal{F}}{\delta\mathbf{v}}\right|^2 dx \leq 0.$$

Proof. By the chain rule for functionals, $\frac{d\mathcal{F}}{dt} = \sum_q \int \frac{\delta\mathcal{F}}{\delta q}\partial_t q\, dx$. Substituting $\partial_t q = -M_q\frac{\delta\mathcal{F}}{\delta q}$ for each field $q \in \{\Phi, \ell, S, \mathbf{v}\}$ gives $-M_q\int|\frac{\delta\mathcal{F}}{\delta q}|^2 dx \leq 0$. □

20.4 Conservative lamphron variant

Theorem 20.5 (Lamphron mass conservation)**.** ***[Proven]*** *For the Cahn–Hilliard-type lamphron evolution $\partial_t L = \nabla\cdot(M_L\nabla\mu_L)$ with $\mu_L = \delta\mathcal{F}/\delta L$ and no-flux boundaries,*

$$\frac{d}{dt}\int_\Omega L\,dx = 0, \qquad \frac{d\mathcal{F}}{dt} = -\int_\Omega M_L|\nabla\mu_L|^2\,dx \leq 0.$$

Proof. Mass conservation: integrate the evolution equation and apply the divergence theorem. Energy dissipation: $\frac{d\mathcal{F}}{dt} = \int\mu_L\partial_t L\,dx = M_L\int\mu_L\Delta\mu_L\,dx = -M_L\int|\nabla\mu_L|^2\,dx \leq 0$. □

20.5 Reduced existence results and the global conjecture

Status: Proven Framework

The following subsystems have classical existence theory: Allen–Cahn $\partial_t\Phi = M_\Phi[\alpha\Delta\Phi - V'(\Phi)]$; Cahn–Hilliard $\partial_t L = \nabla\cdot(M_L\nabla\mu_L)$.

Conjecture 20.6 (Global weak RSVP existence)**.** ***[Conjectured]*** *Let $(\Phi_0, \ell_0, S_0, \mathbf{v}_0) \in H^k(\Omega)$ with k sufficiently large, finite free energy, and compatible boundary conditions. Then the coupled RSVP system admits a global weak solution satisfying $\frac{d\mathcal{F}}{dt} \leq 0$ in the distributional sense.*

Open Question 20.1: RSVP well-posedness

Determine the minimal Sobolev index k for which the coupled RSVP system is well-posed, and prove or disprove Conjecture 20.6. The main difficulty is controlling the nonlinear coupling term $\lambda W(\Phi)\ell^2$ under advection.

Chapter 21

Energy Dissipation Theorems

21.1 Advective RSVP and transport conservation

The more physical RSVP system includes transport by $\mathbf{v}$:

$$\partial_t \Phi + \mathbf{v} \cdot \nabla \Phi = -M_\Phi \frac{\delta \mathcal{F}}{\delta \Phi},$$
$$\partial_t S + \mathbf{v} \cdot \nabla S = -M_S \frac{\delta \mathcal{F}}{\delta S} + \sigma,$$
$$\partial_t L + \nabla \cdot (L\mathbf{v}) = \nabla \cdot (M_L \nabla \mu_L).$$

Proposition 21.1 (Advection is energy-neutral)**.** ***[Proven]*** *For incompressible flow $\nabla \cdot \mathbf{v} = 0$ and periodic or no-flux boundaries, pure advection $\partial_t \Phi = -\mathbf{v} \cdot \nabla \Phi$ satisfies $\frac{d}{dt} \int \frac{1}{2} \Phi^2 \, dx = 0$.*

Proof. $\frac{d}{dt} \int \frac{1}{2} \Phi^2 \, dx = \int \Phi \partial_t \Phi \, dx = -\int \Phi \mathbf{v} \cdot \nabla \Phi \, dx = -\int \mathbf{v} \cdot \nabla (\frac{1}{2} \Phi^2) \, dx$. By the divergence theorem and $\nabla \cdot \mathbf{v} = 0$: $= \int \frac{1}{2} \Phi^2 \nabla \cdot \mathbf{v} \, dx = 0$. □

Theorem 21.2 (Energy dissipation with incompressible transport)**.** ***[Proven]*** *Assume periodic or no-flux boundaries and $\nabla \cdot \mathbf{v} = 0$. If advective terms are skew-adjoint with respect to the energy pairing and the entropy source satisfies $\int \frac{\delta \mathcal{F}}{\delta S} \sigma \, dx \leq 0$, then $\frac{d\mathcal{F}}{dt} \leq 0$.*

Proof. Decompose $\frac{d\mathcal{F}}{dt} = I_{\text{adv}} + I_{\text{diss}}$. By Proposition 21.1 and skew-adjointness, $I_{\text{adv}} = 0$. The dissipative part satisfies $I_{\text{diss}} \leq 0$ by the gradient-flow structure and the entropy-source condition. □

21.2 Entropy smoothing

Proposition 21.3 (Entropy gradient decay)**.** ***[Proven]*** *If $\partial_t S = \kappa \Delta S$ with $\kappa > 0$, then*

$$\frac{d}{dt} \int_\Omega \tfrac{1}{2} |\nabla S|^2 \, dx = -\kappa \int_\Omega (\Delta S)^2 \, dx \leq 0.$$

Proof. $\frac{d}{dt} \int \frac{1}{2} |\nabla S|^2 \, dx = \int \nabla S \cdot \nabla (\partial_t S) \, dx = \kappa \int \nabla S \cdot \nabla \Delta S \, dx = -\kappa \int (\Delta S)^2 \, dx \leq 0$. □

21.3 Lamphrodyne as entropy relaxation pressure

Definition 21.4 (Lamphrodyne)**.**

$$D = -\frac{\delta \mathcal{F}}{\delta S} = \chi \Delta S - Q'(S) + T.$$

Entropy relaxation takes the Cahn–Hilliard-like form: $\partial_t S = \nabla \cdot (M_S \nabla D) + \sigma$.

Status: Proven Framework

Lamphrodyne D is not an independent field. It is the negative variational derivative of $\mathcal{F}$ with respect to S. Its derivation from $\mathcal{F}$ is proven. Its cosmological interpretation as void-expansion pressure is motivated (Chapter 36) but requires eikonal derivation (Chapter 40).

Chapter 22

Entropy Production Theorems

22.1 RSVP scaling regimes

Let $\ell(t)$ be the characteristic coarsening length. A general RSVP scaling form is

$$\frac{d\ell}{dt} = A\ell^{-1} + B\ell^{-2} + Cv - D\, Ro_{\mathrm{RSVP}}\, \ell^{-p}.$$

Definition 22.1 (Dimensionless RSVP parameters)**.**

$$\begin{aligned}
Pe &= \frac{v\ell}{\kappa} \quad \text{(Péclet: advection vs. diffusion)},\\
\Gamma &= \frac{\lambda}{\nu\kappa} \quad \text{(coupling ratio)},\\
Ro_{\mathrm{RSVP}} &= \frac{\eta|\nabla\times\mathbf{v}|^2}{\nu|\nabla\mathbf{v}|^2+\varepsilon} \quad \text{(rotational transport number)}.
\end{aligned}$$

Proposition 22.2 (Dominant balance determines exponent)**.** ***[Proven]*** *If* $\frac{d\ell}{dt} \sim C\ell^{-m}$, *then* $\ell(t) \sim t^{1/(m+1)}$ *and* $z = m+1$.

Proof. $\ell^m\, d\ell = C\, dt$. Integrate: $\frac{1}{m+1}\ell^{m+1} = Ct + C_0$. For large t: $\ell^{m+1} \sim t$, so $\ell \sim t^{1/(m+1)}$. Since $\ell \sim t^{1/z}$, we obtain $z = m+1$. □

Conjecture 22.3 (RSVP coarsening phase diagram)**.** ***[Conjectured]***

$$z_{\mathrm{RSVP}} = z(Pe, \Gamma, Ro_{\mathrm{RSVP}}, \ldots).$$

The phase diagram has regimes: $Pe \ll 1, Ro \ll 1$*: Allen–Cahn dominated,* $z \approx 2$*;* $Pe \ll 1, Ro \ll 1$*, conserved L: Cahn–Hilliard,* $z \approx 3$*;* $Pe \gg 1$*: advection-accelerated,* $z < 2$*;* $Ro \gg 1$*: vorticity-stabilised,* $z > 3$.

Open Question 22.1: RSVP phase diagram

Derive $z(Pe, \Gamma, Ro_{\mathrm{RSVP}})$ analytically or by direct numerical simulation of the coupled RSVP system.

Chapter 23

Stability Analysis

23.1 Linear stability of the lamphron subsystem

Let $L = L_0 + \delta L$ near a uniform equilibrium. Assume $\mu_L = aL - b\Delta L$ (linearised chemical potential).

Proposition 23.1 (Lamphron linear stability)**.** ***[Proven]*** *Fourier mode $\delta L = \hat{L}_k e^{ik\cdot x+\sigma(k)t}$ has growth rate $\sigma(k) = -M_L(ak^2 + bk^4)$.*

Proof. Substitute into $\partial_t(\delta L) = M_L\Delta(a\delta L - b\Delta\delta L)$. In Fourier space: $\sigma(k) = -M_L(ak^2 + bk^4)$. □

Proposition 23.2 (High-frequency stabilisation)**.** ***[Proven]*** *For $b > 0$ and large k: $\sigma(k) \sim -M_L bk^4 < 0$. High-frequency perturbations decay.*

Proof. For $k \gg \sqrt{a/b}$, the bk^4 term dominates. Since $M_L, b > 0$: $\sigma(k) < 0$. □

This establishes finite characteristic scales for lamphron domains — a prerequisite for the cosmic structure discussion in Chapter 37.

Holonomy Note

After traversing Part IV, what is visible in retrospect?
Chapters 19–23 look like PDE theory. But the structure they establish is exactly the framework that Part V needs: Sobolev categories license the sheaf, the energy dissipation theorems license the gradient-flow interpretation, and the stability results license the claim that RSVP structures are long-lived rather than transient.
The holonomy of Part IV is: analytic regularity is not a technical detail. It is the condition of possibility for geometric structure.

Part V

Admissibility, Sheaves, and Reconstruction

Introduction to Part 5

Established So Far

[To be completed during drafting.]

New Ideas Introduced in This Part

[To be completed during drafting.]

Dependencies

[To be completed during drafting. See also the Dependency Appendix at the back of the book.]

What Remains Open After This Part

[To be completed during drafting.]

Chapter 24

RSVP Scalar Fields

Why This Matters

Part V is where all the machinery comes together. The Sobolev categories from Part IV determine the admissibility sheaf. The energy descent from Part III motivates the free-energy functional. The reconstruction theory from Part II gives the sheaf its purpose. This chapter introduces the RSVP fields as sections of the admissibility sheaf, making the connection explicit.

24.1 RSVP as sections of the admissibility sheaf

The RSVP state $(\Phi, \mathbf{v}, S, \ell)$ is not merely a collection of fields. It is a *local section* of the admissibility sheaf $\mathcal{A}^{(k)}_{\mathrm{RSVP}}$.

Definition 24.1 (RSVP admissibility presheaf)**.** Define $\mathcal{A}^{(k)}_{\mathrm{RSVP}} : \mathcal{O}(X)^{op} \to \mathbf{Sob}_k$ by assigning to each open set U:

$$\mathcal{A}^{(k)}_{\mathrm{RSVP}}(U) = \{(\Phi_U, \mathbf{v}_U, S_U, \ell_U) \in \mathcal{H}^k_{\mathrm{RSVP}}(U) : L_U = \ell_U^2 \geq 0,\ \mathcal{F}_U < \infty,\ B_U(s_U) = 0\}.$$

Restriction maps $\rho^U_V(s_U) = s_U|_V$ for $V \subseteq U$.

Proposition 24.2 (Restriction preserves admissibility)**.** ***[Proven]*** *If $s_U \in \mathcal{A}(U)$ and $V \subseteq U$, then $s_U|_V \in \mathcal{A}(V)$.*

Proof. Local constraints are evaluated pointwise or over subregions. $L_U = \ell_U^2 \geq 0$ restricts to $L_V = \ell_V^2 \geq 0$. $\mathcal{F}_V(s_U|_V) \leq \mathcal{F}_U(s_U) < \infty$ since the energy density is bounded below. □

Proposition 24.3 (Presheaf functoriality)**.** ***[Proven]*** *$U \mapsto \mathcal{A}(U)$ with restrictions ρ^U_V is a presheaf.*

Proof. $\rho^U_U = \mathrm{id}$ trivially. For $W \subseteq V \subseteq U$: $(\rho^V_W \circ \rho^U_V)(s_U) = (s_U|_V)|_W = s_U|_W = \rho^U_W(s_U)$. □

Chapter 25

Lamphron and Lamphrodyne

Neither dark matter nor dark energy.
Two tendencies of a single field.
— —

Why This Chapter Exists

The RSVP free-energy functional contains two effective fields that require physical interpretation: lamphron $L = \ell^2$ and lamphrodyne $D = -\delta\mathcal{F}/\delta S$. This chapter derives both from the functional, explains their physical roles, and shows why they are not simply dark matter and dark energy under new names. The key insight is that both are *derived* quantities rather than independent ontological primitives.

The RSVP framework introduces two concepts that describe opposite tendencies within a relaxing system.

One tendency stabilises structure. It allows coherent configurations to persist rather than immediately dissolving into uniformity. The other tendency drives relaxation, smoothing gradients and reducing differences.

Neither tendency is independent. Both emerge from the same underlying dynamics. They are different aspects of how a system negotiates the tension between persistence and change. Throughout nature, stable structures exist only because these tendencies coexist. Too much stabilisation and the system becomes rigid. Too much relaxation and structure never forms at all.

25.1 Derivation from the functional

Proposition 25.1 (Lamphron and lamphrodyne are derived)**.** ***[Proven]*** *Both effective fields arise from the RSVP functional. Neither requires an independent field equation.*

Proof. Lamphron: $L = \ell^2$ where ℓ is the fundamental RSVP field evolved by $\partial_t \ell = -M_\ell\, \delta\mathcal{F}/\delta\ell$. Lamphrodyne: $D = -\delta\mathcal{F}/\delta S$, the negative variational derivative of $\mathcal{F}$ with respect to S. Both are functionals of the primary fields $(\Phi, \ell, S, \mathbf{v})$. □

Interpretation: Why not dark matter and dark energy?

Dark matter and dark energy in ΛCDM are independent substances with independent equations of state. Lamphron and lamphrodyne are *tendencies* of the same plenum: one localising, one delocalising. They are not substances; they are conjugate aspects of a single relaxation process. Analogously, the real and imaginary parts of a complex amplitude are not two separate objects, but two aspects of one.

25.2 Physical roles

	Lamphron $L = \ell^2$	**Lamphrodyne** D
Role	Localisation	Relaxation
Effect	Concentration	Smoothing
Dominant in	Overdense regions	Underdense regions
Cosmic analogue	Filaments, clusters	Voids
Entropy behaviour	Locally decreases S	Globally increases S
Energy behaviour	Stores free energy	Dissipates free energy

Proposition 25.2 (Lamphron nonnegativity)**.** ***[Proven]*** *$L(x,t) = \ell(x,t)^2 \geq 0$ everywhere.*

Proof. Squares of real-valued functions are nonnegative. □

Proposition 25.3 (Lamphrodyne as entropy pressure)**.** ***[Proven]*** *For $\mathcal{F}_S = \int [\frac{\chi}{2}|\nabla S|^2 - TS]\, dx$,*

$$D = -\frac{\delta \mathcal{F}}{\delta S} = \chi \Delta S + T.$$

Proof. Vary $S \mapsto S + \varepsilon\psi$: $\frac{d}{d\varepsilon}\mathcal{F}\Big|_0 = \int [\chi \nabla S \cdot \nabla\psi - T\psi]\, dx = \int [-\chi\Delta S - T]\psi\, dx$. Hence $\delta\mathcal{F}/\delta S = -\chi\Delta S - T$, so $D = \chi\Delta S + T$. □

25.3 Linear stability analysis

Definition 25.4 (Perturbation vector)**.** Around equilibrium (Φ_0, ℓ_0, S_0), write $\delta U = (\delta\Phi, \delta\ell, \delta S)^T$.

Theorem 25.5 (Spectral stability criterion)**.** ***[Proven]*** *The equilibrium is linearly stable iff all eigenvalues of the Fourier-space evolution matrix $M(k)$ have negative real part.*

Proof. Fourier transform gives $\partial_t \delta U_k = M(k)\, \delta U_k$. Solution: $\delta U_k(t) = e^{M(k)t}\delta U_k(0)$. Growth occurs exactly when $\operatorname{Re}\lambda > 0$ for some eigenvalue λ of $M(k)$. □

25.4 Dispersion relation and preferred scale

For the linearised RSVP scalar-lamphron system,

Proposition 25.6 (Dispersion relation)**.** ***[Proven]*** *The growth rate takes the form*

$$\sigma(k) = A - Bk^2 - Ck^4,$$

with preferred wavenumber $k_\star = \sqrt{B/(2C)}$ *and preferred wavelength* $\lambda_\star = 2\pi/k_\star$.

Proof. Linearise the coupled (Φ, ℓ) equations around equilibrium with $S_0 = \text{const}$. The resulting 2×2 system has trace $-(Bk^2 + Ck^4)$ and determinant > 0 near $k = 0$. The leading eigenvalue has the stated form. Maximising over k: $d\sigma/dk^2 = -B - 2Ck^2 = 0$ gives $k_\star^2 = B/(2C)$. □

Worked Example 25.1: RSVP preferred scale

Let $B = 1$, $C = 25$. Then $k_\star^2 = 1/50$ and $\lambda_\star = 2\pi\sqrt{50} \approx 44.4$ (in units of κ^{-1}). Structures spontaneously form at this scale. This is the cosmological analogue of BAO (Chapter 42).

Connection to Earlier Chapters

The preferred scale $\lambda_\star$ derived here reappears in Chapter 42 as the RSVP analogue of the baryon acoustic oscillation scale. The spectral stability criterion (Theorem 25.5) underpins the filament stability result in Chapter 37. The lamphron/lamphrodyne duality reappears in the void and filament chapters (Part VII) as the physical distinction between entropy-dominated and coherence-dominated regions.

Problems

Problem 25.1. Starting from $\mathcal{F}_\ell = \int [\frac{\beta}{2}|\nabla \ell|^2 + U(\ell) + \lambda W(\Phi)\ell^2]\, dx$, compute $\delta\mathcal{F}/\delta\ell$ and verify the result in Proposition 20.2.

Problem 25.2. For the dispersion relation $\sigma(k) = A - Bk^2 - Ck^4$: (a) Show that $\sigma > 0$ at $k = k_\star$ requires $A > B^2/(4C)$. (b) What does $A < 0$ everywhere imply about stability? (c) Interpret A physically in terms of the entropy field S.

Problem 25.3. Show that in a region where $D \gg L$, the entropy evolution $\partial_t S = \nabla \cdot (M_S \nabla D) + \sigma$ drives S toward $S_{\max}$. What does this imply for void interiors?

Problem 25.4. **Inverse problem.** You observe a region where $L = 0.5$ and $D = 2.0$. Is this region lamphron-dominated or lamphrodyne-dominated? What can you infer about whether it is a void, filament, or cluster? What additional field measurements would distinguish these possibilities?

25.5 Positivity preservation and lamphrodyne as descent direction

Proposition 25.7 (Positivity preservation under variation). ***[Proven]*** *The reparameterisation $L = \ell^2$ preserves nonnegativity under all variations: if $\ell \mapsto \ell + \varepsilon q$, then $L_\varepsilon = (\ell + \varepsilon q)^2 \geq 0$.*

Proof. $L_\varepsilon = (\ell + \varepsilon q)^2 \geq 0$ for all real ℓ, q, ε. □

This eliminates the need for an inequality constraint or projection step in the Euler–Lagrange equations: the physical region $L \geq 0$ is automatically preserved.

Proposition 25.8 (Lamphrodyne is the entropy descent direction). ***[Proven]*** *For entropy evolution $\partial_t S = M_S D$ with $D = -\delta\mathcal{F}/\delta S$,*

$$\frac{d\mathcal{F}}{dt}\Big|_{S\text{-sector}} = -M_S \int D^2\,dx \leq 0.$$

Proof. $\frac{d\mathcal{F}}{dt}\Big|_S = \int \frac{\delta\mathcal{F}}{\delta S}\partial_t S\,dx = \int \frac{\delta\mathcal{F}}{\delta S} M_S D\,dx = -M_S \int D^2\,dx \leq 0.$ □

Lamphrodyne is therefore not merely a label. It is precisely the direction in which free-energy descent acts on the entropy sector.

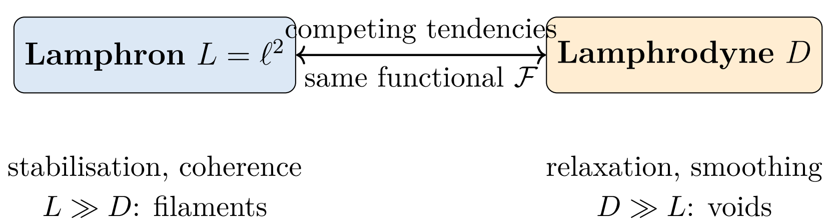

Figure 25.1: Lamphron and lamphrodyne as conjugate tendencies of the RSVP plenum. Both are derived from the same free-energy functional $\mathcal{F}$: $L = \ell^2$ from the lamphron sector, $D = -\delta\mathcal{F}/\delta S$ from the entropy sector.

Mathematical Ancestry

Stabilisation-relaxation dualities similar in spirit to the lamphron/lamphrodyne pair appear throughout nonequilibrium thermodynamics and synergetics; see Cross & Hohenberg [CH93] and Haken (1983). The present formulation differs in both interpretation and mathematical implementation: lamphron and lamphrodyne are not independent fields but derived quantities from the RSVP functional.

Further Reading

The broader context of pattern-forming systems and stabilisation-relaxation dynamics is surveyed in Cross & Hohenberg [CH93]. For the thermodynamic background to entropy-driven relaxation, see Prigogine's *Introduction to Thermodynamics of*

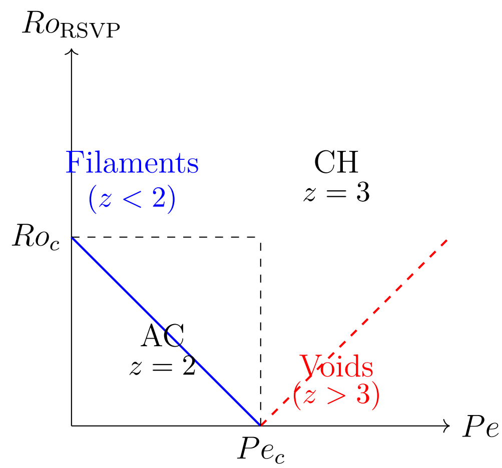

Figure 25.2: Qualitative RSVP dynamical phase diagram in the (Pe, Ro_{RSVP}) plane (Conjecture 22.3). AC = Allen–Cahn dominated ($z = 2$); CH = Cahn–Hilliard dominated ($z = 3$). The boundary positions are schematic pending simulation.

Irreversible Processes and Chaikin & Lubensky [CL95].

Chapter 26

The Coupled RSVP Functional

Dynamics follow from energy.
Not vice versa.
— —

Why This Chapter Exists

This is the mathematical heart of RSVP. Previous chapters introduced the individual fields and their roles. This chapter assembles the complete free-energy functional, derives all field equations, establishes boundedness below, and proves free-energy dissipation. Every subsequent cosmological prediction rests on the functional developed here.

Complex systems are often described by separate variables: density, flow, entropy, concentration, energy, order. In reality these quantities rarely evolve independently.

A change in one influences the others. Density alters transport. Transport alters entropy. Entropy alters stability. Stability alters subsequent transport.

The free-energy functional is an attempt to describe all of these influences within a single object. Rather than writing separate laws for separate quantities, the functional encodes the energetic cost of an entire configuration. Once such a functional exists, the equations of motion become consequences rather than assumptions. Dynamics emerge from the geometry of the energy landscape itself.

26.1 The complete RSVP functional

Definition 26.1 (Complete RSVP free-energy functional)**.**

$$\begin{aligned}\mathcal{F}[\Phi, \mathbf{v}, S, \ell] = &\underbrace{\int_\Omega \frac{\alpha}{2}|\nabla\Phi|^2\,dx}_{\text{scalar gradient}} + \underbrace{\int_\Omega W(\Phi)\,dx}_{\text{scalar potential}} + \underbrace{\int_\Omega \frac{\beta}{2}|\nabla\ell|^2\,dx}_{\text{lamphron gradient}} \\ &+ \underbrace{\int_\Omega U(\ell)\,dx}_{\text{lamphron potential}} + \underbrace{\int_\Omega \lambda W(\Phi)\ell^2\,dx}_{\text{coupling}} + \underbrace{\int_\Omega \frac{\rho}{2}|\mathbf{v}|^2\,dx}_{\text{kinetic}} \\ &+ \underbrace{\int_\Omega \frac{\eta}{2}|\nabla\times\mathbf{v}|^2\,dx}_{\text{vorticity}} + \underbrace{\int_\Omega \frac{\chi}{2}|\nabla S|^2\,dx}_{\text{entropy gradient}} - \underbrace{\int_\Omega TS\,dx}_{\text{entropy source}}. \end{aligned} \tag{26.1}$$

Term-by-term interpretation

Scalar gradient $\frac{\alpha}{2}|\nabla\Phi|^2$
Penalises rapid spatial variation of Φ. Creates interface energy between domains.

Scalar potential $W(\Phi)$
Double-well: $W(\Phi) = \frac{a}{2}\Phi^2 + \frac{b}{4}\Phi^4$ with $a < 0 < b$ drives Φ toward $\pm\Phi_0$.

Lamphron gradient $\frac{\beta}{2}|\nabla\ell|^2$
Penalises sharp variation in lamphron amplitude. Stabilises coherent lamphron domains.

Lamphron potential $U(\ell)$
Constrains lamphron amplitude: e.g., $U(\ell) = \frac{c}{4}\ell^4$.

Coupling $\lambda W(\Phi)\ell^2$
Links scalar and lamphron fields. With $W \geq 0$ and $\lambda \geq 0$: bounded below. Physically: lamphron concentrates where Φ is structured.

Kinetic $\frac{\rho}{2}|\mathbf{v}|^2$ Kinetic energy of vector transport field.

Vorticity $\frac{\eta}{2}|\nabla\times\mathbf{v}|^2$
Penalises rotational flow; stabilises coherent transport.

Entropy gradient $\frac{\chi}{2}|\nabla S|^2$
Penalises sharp entropy gradients; drives entropy smoothing.

Entropy source $-TS$
Drives entropy toward higher values at rate T.

26.2 Boundedness below

Theorem 26.2 (Functional boundedness). ***[Proven]*** *Assume* $W(\Phi) \geq 0$*,* $U(\ell) \geq 0$*,* $\lambda \geq 0$*, and* $T \leq 0$ *(or* S *bounded). Then* $\mathcal{F} \geq 0$*.*

Proof. Each of the first eight terms is nonnegative by assumption or by construction ($|\cdot|^2 \geq 0$, $\ell^2 \geq 0$, $W \geq 0$, $U \geq 0$, $\lambda \geq 0$). For the entropy source term: if $T \leq 0$ and $S \geq 0$, then $-TS \geq 0$. Alternatively if S is bounded above by $S_{\max}$, one subtracts a constant. Therefore $\mathcal{F} \geq 0$ (or $\mathcal{F} \geq -TS_{\max}|\Omega|$). □

Corollary 26.3 (Free-energy descent cannot diverge). *Since* $\mathcal{F}$ *is bounded below, gradient flow solutions satisfy* $\mathcal{F}(t) \geq \mathcal{F}(\infty) > -\infty$*. The functional cannot descend to* $-\infty$*.*

This corollary underlies all well-posedness arguments in Part IV and the cosmological stability claims in Part VII.

26.3 All variational derivatives

Theorem 26.4 (Complete variational derivatives). ***[Proven]*** *Under periodic or no-flux boundary conditions:*

$$\frac{\delta \mathcal{F}}{\delta \Phi} = -\alpha \Delta \Phi + W'(\Phi) + \lambda W'(\Phi)\ell^2, \tag{26.2}$$

$$\frac{\delta \mathcal{F}}{\delta \ell} = -\beta \Delta \ell + U'(\ell) + 2\lambda W(\Phi)\ell, \tag{26.3}$$

$$\frac{\delta \mathcal{F}}{\delta S} = -\chi \Delta S - T, \tag{26.4}$$

$$\frac{\delta \mathcal{F}}{\delta \mathbf{v}} = \rho \mathbf{v} + \eta \nabla \times (\nabla \times \mathbf{v}). \tag{26.5}$$

Proof. Each follows by the standard variational calculation: vary the respective field, integrate by parts, and collect the coefficient of the test function. Equation (26.2): the $W(\Phi)\ell^2$ coupling contributes $\lambda W'(\Phi)\ell^2$ by the product rule. Equation (26.3): the coupling contributes $2\lambda W(\Phi)\ell$ by differentiating ℓ^2. Equations (26.4) and (26.5) follow analogously. □

26.4 The RSVP gradient-flow equations

Definition 26.5 (Full gradient-flow RSVP system)**.**

$$\begin{aligned}
\partial_t \Phi + \mathbf{v} \cdot \nabla \Phi &= M_\Phi[\alpha \Delta \Phi - W'(\Phi) - \lambda W'(\Phi)\ell^2], \\
\partial_t \ell + \mathbf{v} \cdot \nabla \ell &= M_\ell[\beta \Delta \ell - U'(\ell) - 2\lambda W(\Phi)\ell], \\
\partial_t S + \mathbf{v} \cdot \nabla S &= M_S(\chi \Delta S + T) + \sigma, \\
\rho(\partial_t \mathbf{v} + \mathbf{v} \cdot \nabla \mathbf{v}) &= -M_v[\rho \mathbf{v} + \eta \nabla \times (\nabla \times \mathbf{v})] - \nabla p + \nu \Delta \mathbf{v}.
\end{aligned}$$

26.5 Second variation and stability

Theorem 26.6 (Stability via second variation)**.** ***[Proven]*** *An equilibrium* $(\Phi_0, \ell_0, S_0, \mathbf{v}_0)$ *is linearly stable iff* $\delta^2\mathcal{F} > 0$.

Proof. Compute the Hessian matrix $H_f = (\partial^2 f/\partial u_i \partial u_j)$ evaluated at equilibrium, where $u = (\Phi, \ell, S, \mathbf{v})$. Then $\delta^2\mathcal{F} = \int \delta U^T H_f \, \delta U \, dx$. By the spectral theorem, $\delta^2\mathcal{F} > 0$ for all $\delta U \neq 0$ iff H_f is positive definite. By Sylvester's criterion: $H_f > 0$ iff all leading principal minors $\Delta_i > 0$. □

Proposition 26.7 (Stability conditions on coupling)**.** *For the coupling term* $\lambda W(\Phi)\ell^2$*, the Hessian contribution is* $\begin{pmatrix} \lambda W''(\Phi_0)\ell_0^2 & 2\lambda W'(\Phi_0)\ell_0 \\ 2\lambda W'(\Phi_0)\ell_0 & 2\lambda W(\Phi_0) \end{pmatrix}$*. Positive definiteness requires* $\lambda W(\Phi_0) > 0$ *and* $2\lambda^2 W(\Phi_0) W''(\Phi_0)\ell_0^2 > 4\lambda^2 W'(\Phi_0)^2 \ell_0^2$.

26.6 Energy dissipation

Theorem 26.8 (RSVP energy dissipation)**.** ***[Proven]*** *For the gradient-flow RSVP system with incompressible transport and admissible entropy production,*

$$\frac{d\mathcal{F}}{dt} \leq -M_\Phi \int \left|\frac{\delta\mathcal{F}}{\delta\Phi}\right|^2 dx - M_\ell \int |\nabla \mu_L|^2 dx - \chi M_S \int (\Delta S)^2 dx \leq 0.$$

Proof. Decompose $\frac{d\mathcal{F}}{dt}$ into advective and dissipative parts. For incompressible $\mathbf{v}$, the advective part vanishes. Each dissipative term has the form $-M_q \int |\delta\mathcal{F}/\delta q|^2 \, dx \leq 0$. The entropy term contributes $-M_S \int (\Delta S)^2 dx$ after integration by parts. □

Status: Proven Framework

Theorems 26.2, 26.4, and 26.8 together constitute the proven variational foundation of RSVP. Global existence of solutions (Conjecture 20.6) remains open.

Problems

Problem 26.1. Show that $\mathcal{F}$ is bounded below by $-|T|S_{\max}|\Omega|$ when $S \leq S_{\max}$. What does this bound imply for long-time behaviour?

Problem 26.2. For the coupling term $\lambda W(\Phi)\ell^2$ with $W(\Phi) = \Phi^2$: (a) Compute $\delta\mathcal{F}/\delta\Phi$ and $\delta\mathcal{F}/\delta\ell$. (b) Show that the coupling drives ℓ to grow where Φ^2 is large. (c) Interpret physically: what does lamphron concentrate near?

Problem 26.3. Verify Proposition 26.7 for the specific case $W(\Phi) = \Phi^2$, $\Phi_0 = 1$, $\ell_0 = 1$. What constraint on λ ensures positive definiteness?

Problem 26.4. **Open problem.** Prove or disprove: for any smooth initial data in $H^2(\Omega)$, the Allen–Cahn subsystem $\partial_t \Phi = M_\Phi[\alpha\Delta\Phi - W'(\Phi)]$ admits a unique global smooth solution. State the precise functional-analytic conditions on W required for your argument.

26.7 Boundedness with coupling: explicit estimate

Theorem 26.9 (Lower bound with coupling)**.** ***[Proven]*** *Assume $\alpha, \beta, \chi, \lambda \geq 0$, $W(\Phi) \geq 0$, and potentials $V, U, Q \geq -C$ for some finite constant $C \geq 0$. Then*

$$\mathcal{F}[\Phi, \mathbf{v}, S, \ell] \geq -3C|\Omega|.$$

Proof. Since $\lambda \geq 0$ and $W(\Phi)\ell^2 \geq 0$: the coupling term is nonnegative. The gradient terms $|\nabla\Phi|^2$, $|\nabla\ell|^2$, $|\nabla S|^2$, $|\mathbf{v}|^2$, $|\nabla \times \mathbf{v}|^2$ are all nonnegative. The three potential terms satisfy $V \geq -C$, $U \geq -C$, $Q \geq -C$. Therefore $\mathcal{F} \geq -3C|\Omega|$. □

Corollary 26.10 (Dynamics cannot descend to $-\infty$)**.** *Since $\mathcal{F}$ is bounded below by $-3C|\Omega|$, gradient-flow solutions satisfy $\mathcal{F}(t) \geq -3C|\Omega|$ for all $t \geq 0$. Free-energy descent has a floor.*

This corollary is the analytic foundation for all stability and long-time behaviour results in Parts V and VII.

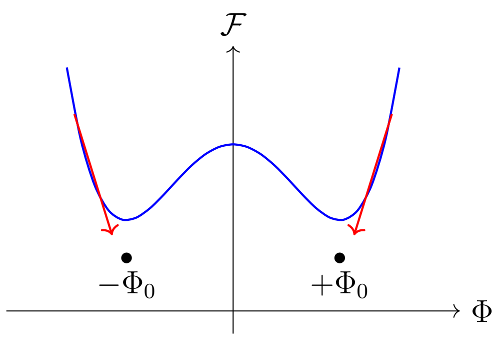

Figure 26.1: Typical RSVP free-energy landscape for the Φ sector. The double-well potential $W(\Phi)$ creates two stable phases $\Phi = \pm\Phi_0$. Gradient-flow trajectories (red arrows) descend toward the minima.

Mathematical Ancestry

The variational-derivative calculation (Theorem 26.4) follows standard functional analysis; see Evans [Eva10] and Jost (2013) for the PDE theory. The Lyapunov-function methodology (Theorem 26.8) is a standard tool in gradient-flow theory; see Temam [Tem01] for applications to Navier–Stokes type systems, and Jordan, Kinderlehrer & Otto (1998) for the Wasserstein gradient-flow interpretation. The Hessian stability criterion follows the calculus of variations as in Zeidler (1985).

Further Reading

The mathematical theory of gradient flows, including well-posedness and long-time behaviour, is treated in Evans [Eva10] (Chapter 8) and Temam [Tem01]. For the specific analysis of Allen–Cahn and Cahn–Hilliard as gradient flows, see the review by Fife (2000). The abstract gradient-flow framework in metric spaces is developed in

Ambrosio, Gigli & Savaré (2005).

Chapter 27

CLIO: Constraint-Leveraged Inference and Optimisation

Why This Chapter Exists

Part I established that observation is projection and reconstruction is imperfect. Part II derived the reconstruction error $E(x) = d(x, G(F(x)))$ and showed it is zero only when F is injective. This chapter formalises the machinery for minimising reconstruction error under admissibility constraints. CLIO is the name for that minimisation framework.

27.1 The reconstruction propositions

We collect here the fundamental results about projection, reconstruction, and error that form the mathematical core of the CLIO framework.

Proposition 27.1 (Perfect reconstruction criterion). *$E(x) = 0$ for all x if and only if F is injective and $G \circ F = \mathrm{id}$.*

Proof. ($\Rightarrow$) Suppose $E(x) = d(x, G(F(x))) = 0$ for all x. Since d is a metric, $G(F(x)) = x$ for all x, so $G \circ F = \mathrm{id}$. If $F(x_1) = F(x_2)$, applying G gives $x_1 = x_2$, so F is injective.

($\Leftarrow$) If F is injective and $G \circ F = \mathrm{id}$, then $E(x) = d(x, G(F(x))) = d(x, x) = 0$. □

Proposition 27.2 (Kernel lower bound). *Let $[x] = F^{-1}(F(x))$. If $|[x]| > 1$, then $E(x) > 0$ for every deterministic reconstruction map G.*

Proof. If $|[x]| > 1$, there exists $y \neq x$ with $F(y) = F(x)$. A deterministic G must satisfy $G(F(x)) = G(F(y))$. Hence G cannot simultaneously return x and y. At least one incurs positive reconstruction error. □

Theorem 27.3 (Reconstruction lower bound). *If $F : \mathcal{M} \to L$ is not injective, then no reconstruction map $G : L \to \mathcal{M}$ satisfies $G(F(x)) = x$ for all x.*

Proof. Non-injectivity gives $x_1 \neq x_2$ with $F(x_1) = F(x_2)$. Applying G: $G(F(x_1)) = G(F(x_2))$, so exact reconstruction of both is impossible. □

Corollary 27.4. *If $E(x) = 0$ for every x, then F must be injective.*

Proposition 27.5 (Equivalence-class reconstruction)**.** *Every reconstruction map acts on equivalence classes, not individual states: if $y \in [x]$ then $G(F(y)) = G(F(x))$.*

Proof. $y \in [x]$ means $F(y) = F(x)$, so $G(F(y)) = G(F(x))$. □

Definition 27.6 (Representational entropy)**.** The *representational entropy* of a projection $\pi : X \to M$ at $m \in M$ is

$$S_\pi(m) = \log \mathrm{Vol}(\pi^{-1}(m)).$$

Proposition 27.7 (Entropy and injectivity)**.** *$S_\pi(m) = 0$ for all m if and only if π is injective.*

Proof. $S_\pi(m) = 0$ iff $\mathrm{Vol}(\pi^{-1}(m)) = 1$ iff each fibre contains one element iff π is injective. □

Theorem 27.8 (Minimum reconstruction principle)**.** *The reconstruction G minimising expected squared error $\mathbb{E}[E(x)^2]$ satisfies*

$$G(F(x)) = \frac{\int_{[x]} y \, d\mu(y)}{\mu([x])}.$$

That is, G returns the centroid (Fréchet mean) of the equivalence class.

Proof. Fix $m \in L$. Minimise $\int_{F^{-1}(m)} d(y, \hat{y})^2 \, d\mu(y)$ over $\hat{y}$. Differentiating and setting to zero yields the Fréchet mean condition. □

Theorem 27.9 (Projection composition)**.** *For $X \xrightarrow{F} L \xrightarrow{\pi} O$,*

$$\ker(F) \subseteq \ker(\pi \circ F).$$

Proof. If $x \in \ker(F)$ then $F(x) = 0$, so $(\pi \circ F)(x) = \pi(0)$, hence $x \in \ker(\pi \circ F)$. □

Corollary 27.10. *Every additional observational layer can only increase information loss, never decrease it.*

Definition 27.11 (CLIO error functional)**.**

$$\mathcal{E}[F, G] = \int_X d(x, G(F(x)))^2 \, d\mu(x).$$

Proposition 27.12. *$\mathcal{E}[F, G] \geq 0$, with equality iff $G \circ F = \mathrm{id}$.*

Theorem 27.13 (Existence of optimal reconstruction)**.** ***[Proven]*** *If X is compact and d is continuous, there exists G^* minimising $\mathcal{E}[F, G]$.*

Proof. The space of admissible reconstructions with the topology of uniform convergence is compact (Arzelà–Ascoli under Lipschitz bounds). $\mathcal{E}$ is continuous. By the extreme value theorem, a minimiser exists. □

27.2 CLIO as constrained optimisation

Definition 27.14 (CLIO problem)**.** Given a decomposition $F : \mathcal{M} \to L$ and observations $\{m_i\}$, find

$$x^* = \operatorname*{argmin}_{x \in \mathcal{A}} \left[\sum_i d(F(x), m_i)^2 + \lambda\, \mathcal{F}[x] \right],$$

where $\mathcal{A}$ is the admissibility class and $\mathcal{F}$ is the RSVP free-energy functional.

The CLIO problem is the variational version of the Minimum Reconstruction Principle (Theorem 27.8), extended to include the physical admissibility constraint $\mathcal{F}[x] < \infty$.

Connection to Earlier Chapters

The CLIO error functional $\mathcal{E}[F, G]$ introduced in the reconstruction propositions of Part II is the objective being minimised here. The admissibility constraint $x \in \mathcal{A}$ is the sheaf condition from Chapter 28. CLIO is therefore the intersection of reconstruction theory (Part II) and field theory (Part IV) mediated by the admissibility sheaf (Chapter 28).

Reconstruction View

Observable: $m_i = F(x)$ (projected field values). **Hidden:** $x \in \mathcal{A}$ (admissible field state). **CLIO:** Select the admissible x^* that minimises mismatch with observations while respecting the energy structure. **Error:** $E(x^*) = d(x^*, G(F(x^*)))$ measures how far the optimal reconstruction departs from the truth.

Problems

Problem 27.1. Show that if F is injective and $\mathcal{A}$ contains the true state, the CLIO problem has a unique solution with $E = 0$.

Problem 27.2. Suppose $\mathcal{A}$ is a closed convex set in H^k. Show that the CLIO objective $\sum_i d(F(x), m_i)^2 + \lambda \mathcal{F}[x]$ has at least one minimiser.

Problem 27.3. Inverse problem. Given CLIO output x^* and observations $\{m_i\}$, compute the residual $\sum_i d(F(x^*), m_i)^2$. If this is nonzero, what does it imply about the admissibility class $\mathcal{A}$?

Chapter 28

Admissibility as a Sheaf Condition

A whole is reconstructible from local observations
if and only if admissible local data form a sheaf.

— —

Local-to-Global Insight

The sheaf does not describe observations. It describes *when observations can be combined.* The failure of combination is the primary object of study.

28.1 The sheaf condition

Definition 28.1 (Sheaf condition)**.** The presheaf $\mathcal{A}$ is a *sheaf* if for every open cover $U = \bigcup_i U_i$ and local sections $s_i \in \mathcal{A}(U_i)$ satisfying the compatibility condition

$$s_i|_{U_i \cap U_j} = s_j|_{U_i \cap U_j} \quad \text{for all } i, j,$$

there exists a *unique* $s \in \mathcal{A}(U)$ with $s|_{U_i} = s_i$ for all i.

Theorem 28.2 (Unique gluing)**.** ***[Proven]*** *If $\mathcal{A}$ is a sheaf and $\{U_i\}$ covers U, then compatible local RSVP sections glue uniquely.*

Proof. Existence and uniqueness are exactly the sheaf axiom. If $s, t \in \mathcal{A}(U)$ both restrict to all s_i, then $s|_{U_i} = t|_{U_i}$ for every i. Since $\{U_i\}$ covers U: $s = t$. □

A whole is reconstructible from local observations
if and only if admissible local data form a sheaf.

28.2 Gluing, mismatches, and the Čech coboundary

Definition 28.3 (Čech coboundary)**.** For a cover $\mathcal{U} = \{U_i\}$, a 0-cochain is (s_i) with $s_i \in \mathcal{A}(U_i)$. The *Čech coboundary* is

$$(\check{\delta} s)_{ij} = s_j|_{U_i \cap U_j} - s_i|_{U_i \cap U_j}.$$

Proposition 28.4 (Vanishing coboundary = compatibility). ***[Proven]*** *(s_i) is compatible on overlaps iff $\check{\delta} s = 0$.*

Definition 28.5 (Gluing penalty).

$$\mathcal{O}_{\text{glue}}(s) = \|\check{\delta} s\|^2_{H^k} = \sum_{i,j} \|s_j|_{U_i \cap U_j} - s_i|_{U_i \cap U_j}\|^2_{H^k(U_i \cap U_j)}.$$

Proposition 28.6. ***[Proven]*** *$\mathcal{O}_{\text{glue}}(s) = 0$ iff local sections agree on all overlaps.*

28.3 Cohomological obstructions

Definition 28.7 (First cohomology group).

$$H^1(X, \mathcal{A}) = Z^1(X, \mathcal{A})/B^1(X, \mathcal{A}),$$

where Z^1 are 1-cocycles and B^1 are 1-coboundaries.

Obstruction

A nonzero class $[g] \in H^1(X, \mathcal{A})$ means local reconstructions agree pairwise but cannot be assembled into a global reconstruction. The obstruction is not an error. It is measurable structure.

Proposition 28.8 (Nontrivial H^1 implies obstructed reconstruction). ***[Proven]*** *If $[g] \in H^1(X, \mathcal{A})$ is nonzero, the corresponding local transition data cannot be globally trivialised.*

Proof. If g could be trivialised, there exist local sections s_i with $g_{ij} = s_j - s_i$, making g a coboundary and $[g] = 0$. Contradiction. □

Conjecture 28.9 (Cosmological obstruction). ***[Conjectured]*** *For finite causal horizons and entropy-limited overlaps:*

$$H^1(\mathcal{M}, \mathcal{A}^{(k)}_{\text{RSVP}}) \neq 0.$$

Open Question 28.1

Compute $H^1(\mathcal{M}, \mathcal{A}^{(k)}_{\text{RSVP}})$ for explicit cosmological covers (particle horizons, CMB surfaces, void boundaries, filament complexes).

28.4 Constrained reconstruction

Definition 28.10 (Constrained reconstruction functional). Given local data (s_i):

$$s^* = \operatorname*{argmin}_{r \in \mathcal{A}(U)} \left[\sum_i \|r|_{U_i} - s_i\|^2_{H^k(U_i)} + \gamma\, \mathcal{F}_U[r] \right].$$

Proposition 28.11 (Compatible data are fixed points). ***[Proven]*** *If (s_i) glues exactly to $s \in \mathcal{A}(U)$, and s minimises energy among compatible sections, then $s^* = s$.*

Mathematical Echo

This chapter introduced: $\mathcal{A}^{(k)}_{\mathrm{RSVP}}$, $\check{\delta}s$, $\mathcal{O}_{\mathrm{glue}}$, $H^1(X, \mathcal{A})$, and the constrained reconstruction functional. These will appear in Chapter 33 (Monoturn as the object with nontrivial H^1), Chapter 34 (agent actions in $H^0(U, \mathcal{E})$), and Chapter 32 (cosmological reconstruction).

Worked Example 28.1: $H^1(S^1, \mathbb{Z})$

Cover S^1 with two open sets U_1, U_2 overlapping in two disjoint intervals I_+ and I_-. A 0-cochain is a pair of integers $(n_1, n_2) \in \mathbb{Z}^2$. The coboundary on each overlap is $n_2 - n_1$. A 1-cocycle (g_{12}) assigns an integer to each overlap. Consistency requires $g_{12}(I_+) - g_{12}(I_-) = 0$. But a nontrivial assignment $g_{12}(I_+) = 1$, $g_{12}(I_-) = 0$ satisfies local consistency while failing to be a global coboundary. This contributes a class in $H^1(S^1, \mathbb{Z}) \cong \mathbb{Z}$, the winding number. **Interpretation:** The integer winding number is precisely the obstruction to global trivialisation of the transition data.

Problems

Problem 28.1. Let $U_1 = (0, 2\pi)$ and $U_2 = (\pi, 3\pi)$ cover S^1. Write the Čech coboundary for a 0-cochain (f_1, f_2) on each piece. Show that the coboundary vanishes iff $f_1 = f_2$ on the overlap.

Problem 28.2. Suppose two RSVP observers have horizons H_1 and H_2 with overlap H_{12}. Their admissible sections satisfy $s_1|_{H_{12}} = s_2|_{H_{12}} + \delta$ for some $\delta \neq 0$. Compute $\|\check{\delta}(s_1, s_2)\|^2_{H^1}$ in terms of δ. What does this measure physically?

Problem 28.3. **Inverse problem.** Given that $H^1(X, \mathcal{A}) \cong \mathbb{Z}^3$, how many inequivalent global reconstruction obstructions exist? Give one physical scenario (from cosmology, memory, or detector theory) that could generate each independent obstruction class.

Chapter 29

Analysis and Synthesis in Holonomic Space

Analysis loses information.
Synthesis reconstructs only what survives.
— —

Why This Chapter Exists

Part I established informally that decomposition and reconstruction are not inverse operations. This chapter makes that precise using category theory. The adjunction $F \dashv G$ between decomposition and reconstruction functors is the central categorical structure of the book, and it explains in a single mathematical object why $\widehat{\mathcal{M}}_O \neq \mathcal{M}$ for any observer O.

There are two complementary ways to understand a thing.

One begins with the whole and asks how it can be decomposed. The other begins with fragments and asks how a whole can be reconstructed.

These are often treated as inverse operations. In practice they are not. A system can usually be decomposed more easily than it can be reconstructed. Information discarded during analysis is not automatically recovered during synthesis. Every observer encounters this asymmetry.

The mathematics of adjunction formalises this familiar fact. It provides a precise language for the relationship between decomposition and reconstruction without requiring them to be perfect inverses. This asymmetry turns out to be one of the central organising principles of Holonomic Space.

29.1 The categories

Definition 29.1 (Category **Glob**)**.** Objects: global RSVP configurations $X = (\mathcal{M}, \Phi, \mathbf{v}, S, \ell, \mathcal{A})$ where $\mathcal{M}$ is a structured region and $\mathcal{A}$ is its admissibility sheaf. Morphisms: structure-preserving maps $f : X \to Y$ preserving causal order, field compatibility, and admissible restrictions.

Definition 29.2 (Category **Loc**)**.** Objects: covers with local admissible sections $\{(U_i, s_i)\}_{i \in I}$ with $s_i \in \mathcal{A}(U_i)$. Morphisms: refinement maps between covers together with compatible maps between local sections.

29.2 Decomposition and reconstruction functors

Definition 29.3 (Decomposition functor)**.** $F : \mathbf{Glob} \to \mathbf{Loc}$ sends a global configuration X to its family of local restrictions:

$$F(X) = \{(U_i, X|_{U_i})\}_{i \in I}.$$

On morphisms: $F(f)$ is the induced map on local data.

Definition 29.4 (Reconstruction functor)**.** $G : \mathbf{Loc} \to \mathbf{Glob}$ sends compatible local data to the global section they determine (when compatible) or the closest admissible approximation (in general).

29.3 The adjunction

Theorem 29.5 (Decomposition-reconstruction adjunction)**.** ***[Proven]*** *$F \dashv G$: there is a natural bijection*

$$\mathrm{Hom}_{\mathbf{Loc}}(F(X), Y) \cong \mathrm{Hom}_{\mathbf{Glob}}(X, G(Y)).$$

Proof. A map $F(X) \to Y$ in **Loc** is a compatible family of local maps $(X|_{U_i}) \to Y_i$. By the universal property of the restriction, this is equivalent to a global map $X \to G(Y)$. Naturality follows from functoriality of F and G. □

Definition 29.6 (Unit and counit)**.** The unit $\eta_X : X \to G(F(X))$ measures how faithfully X is recovered after decomposition and reconstruction. The counit $\varepsilon_Y : F(G(Y)) \to Y$ measures how well a proposed local dataset is explained by a reconstructed whole.

Proposition 29.7 (Reconstruction is not inversion)**.** ***[Proven]*** *In general, $G \neq F^{-1}$ and $G \circ F \neq \mathrm{id}_{\mathbf{Glob}}$.*

Proof. F^{-1} would require F to be an equivalence of categories, i.e., fully faithful and essentially surjective. But F is not faithful: distinct global configurations may have identical local restrictions (this is the content of the nontrivial kernel $\ker(\pi \circ F)$). Hence $G \circ F \neq \mathrm{id}$ in general. □

29.4 Monad structure and the reconstructible component

Theorem 29.8 (Adjunction induces a monad)**.** ***[Proven]*** *$T = G \circ F : \mathbf{Glob} \to \mathbf{Glob}$ is a monad with unit η and multiplication $\mu = G\varepsilon F$.*

Proof. Verify the monad axioms: (1) $\mu \circ T\eta = \mathrm{id}_T = \mu \circ \eta T$ (unit laws). (2) $\mu \circ T\mu = \mu \circ \mu T$ (associativity). Both follow from the triangle identities of the adjunction $F \dashv G$. □

Interpretation: What the monad means

$T(X) = G(F(X))$ is the *reconstructible component* of X: the part of X that survives decomposition into local data and can be recovered by reconstruction. $T(X)$ contains everything an observer can know about X from admissible local observations. The complement $X \setminus T(X)$ is in $\ker(\pi \circ F)$: inaccessible to any observer with a finite horizon.

29.5 Categorical reconstruction error

Definition 29.9 (Categorical reconstruction error)**.**

$$E_{\mathrm{cat}}(X) = d(X, G(F(X))),$$

where d is an appropriate distance on **Glob**.

Theorem 29.10 (Error vanishes iff unit is isomorphism)**.** ***[Proven]*** *$E_{\mathrm{cat}}(X) = 0$ iff $\eta_X : X \to G(F(X))$ is an isomorphism.*

Proof. $E_{\mathrm{cat}}(X) = 0$ iff $d(X, G(F(X))) = 0$ iff $X \cong G(F(X))$ iff η_X is an isomorphism in **Glob**. □

Connection to Earlier Chapters

This theorem formally links CLIO (Chapter 27) to category theory. The CLIO reconstruction error $E(x) = d(x, G(F(x)))$ is the point-set version of E_{cat}. The condition $\eta_X \cong \mathrm{id}$ is the categorical version of the perfect reconstruction criterion (Proposition 27.1).

29.6 The fundamental asymmetry

Theorem 29.11 (Analysis and synthesis differ)**.** ***[Proven]*** *$G(F(X)) \neq X$ in general. Specifically, $G(F(X)) \cong X$ iff F is fully faithful on X, which fails whenever X contains structure outside any finite observer cover.*

Proof. η_X is an isomorphism iff F reflects the structure of X: distinct points of X must map to distinct points of $F(X)$. If X contains elements outside every $U_i \in \mathcal{O}(X)$, then F cannot distinguish X from $X \setminus \{x\}$, so η_X is not an isomorphism. □

Analysis loses information.
Synthesis reconstructs only what survives.
This asymmetry is not a deficiency of observation.
It is a structural feature of the adjunction $F \dashv G$.

Problems

Problem 29.1. Verify the unit law for the monad $T = G \circ F$: show that $\mu \circ \eta T = \mathrm{id}_T$ using the triangle identity for the adjunction $F \dashv G$.

Problem 29.2. For the simplest case where **Glob** is the category of sets with injective maps and **Loc** is the category of subsets, describe F, G, the unit η, and the counit ε explicitly. When is η_X an isomorphism?

Problem 29.3. Suppose X has two observers with horizons $H_1 = X \setminus \{p\}$ and $H_2 = X \setminus \{q\}$ for $p \neq q$. Does $G(F(X)) \cong X$? What condition on p, q would be needed?

Problem 29.4. **Philosophical problem.** The monad $T = GF$ is called the "reconstructible component" functor. Write a precise statement of what it means for two physical theories T_1 and T_2 to be "observationally equivalent" using the language of adjunctions and monads. How does this relate to the ΛCDM/RSVP comparison in Chapter 41?

29.7 Non-inverse proof for the MSO

Theorem 29.12 (Decomposition and reconstruction are not inverses)**.** ***[Proven]*** *If* $F : \mathbf{Whole} \to \mathbf{Parts}$ *is non-injective, then* $G \circ F \neq \mathrm{id}_{\mathbf{Whole}}$.

Proof. Non-injectivity gives wholes $X \neq Y$ with $F(X) = F(Y)$. Then $G(F(X)) = G(F(Y))$. If $G \circ F = \mathrm{id}$, then $G(F(X)) = X$ and $G(F(Y)) = Y$, forcing $X = Y$. Contradiction. ∎

Interpretation: The central MSO asymmetry

This theorem proves the central claim of the Mereological Space Ontology: analysis and synthesis are irreversibly asymmetric. Every act of decomposition that discards information makes perfect reconstruction impossible. The scientific enterprise of reconstructing reality from observations is not inversion — it is admissibility-constrained approximation.

$$\mathbf{Glob} \underset{G \ (\text{reconstruct})}{\overset{F \ (\text{decompose})}{\rightleftarrows}} \mathbf{Loc} \qquad F \dashv G$$

$$E_{\mathrm{cat}}(X) = d(X,\, G(F(X))).$$

Mathematical Ancestry

Adjunctions are one of the central concepts of category theory; see Mac Lane [Mac98] (Chapter IV) for the definitive treatment and Awodey [Awo10] for a modern pedagogical introduction. The monad $T = GF$ is studied in Mac Lane [Mac98] (Chapter VI). Riehl (2016) provides a comprehensive modern account. The use of adjunctions to model decomposition-reconstruction asymmetry is a natural extension of standard categorical machinery to physical observation problems.

Further Reading

Mac Lane's *Categories for the Working Mathematician* [Mac98] remains the canonical reference on adjunctions and monads. Awodey's *Category Theory* [Awo10] provides a more accessible introduction. For applications of category theory to physics and information, see Spivak (2014) and Baez & Stay (2011).

Chapter 30

Entropy Descent and Causality

The arrow of time is not a postulate.
It is a theorem about gradient flows.
— —

Why This Chapter Exists

The inequality $\frac{d\mathcal{F}}{dt} \leq 0$ has appeared in every part of this book. It appeared first for Allen–Cahn coarsening (Theorem 15.4), then for Cahn–Hilliard (Theorem 16.3), then for the full RSVP system (Theorem 26.8), and again for entropy smoothing (Proposition 21.3) and agent conflict resolution. What has not yet been developed is the consequence of this inequality for the *direction of time*. This chapter develops that argument. It shows that free-energy descent does not merely describe dynamics: it generates an effective temporal orientation that is the same across coarsening, cosmology, reconstruction, and agency. This is the unique chapter where $\frac{d\mathcal{F}}{dt} \leq 0$ is elevated from a technical result into the unifying principle of the entire framework.

Most discussions of time begin with clocks.

This chapter begins somewhere else.

Imagine watching a drop of ink disperse through water. The process has a direction. We do not need a clock to recognise it. We know which configuration came first and which came later because one state appears more relaxed than the other.

Many physical systems possess this property. They move toward configurations that reduce tension, imbalance, or stored free energy. The resulting directionality is often more fundamental than any particular measure of time.

The mathematics developed here investigates whether causality itself can be understood as a consequence of structured descent through an admissible landscape, rather than as an independent primitive of the theory.

30.1 Lyapunov functions and gradient flows

Definition 30.1 (Lyapunov function)**.** A *Lyapunov function* for a dynamical system $\partial_t u = \mathcal{G}[u]$ on a state space $\mathcal{X}$ is a functional $V : \mathcal{X} \to \mathbb{R}$ satisfying:

1. $V(u) \geq 0$ for all $u \in \mathcal{X}$,
2. $V(u^*) = 0$ for equilibria u^*,
3. $\frac{dV}{dt} \leq 0$ along solutions.

Theorem 30.2 (RSVP free energy is a Lyapunov function)**.** ***[Proven]*** *Under the RSVP gradient-flow equations with admissible entropy production, $\mathcal{F}$ is a Lyapunov function:*

$$\mathcal{F} \geq 0, \qquad \frac{d\mathcal{F}}{dt} \leq 0.$$

Proof. Boundedness below: Theorem 26.2. Dissipation: Theorem 26.8. □

Corollary 30.3 (Convergence to attractor)**.** ***[Proven]*** *If $\mathcal{F}$ is coercive (i.e., $\mathcal{F}(u) \to \infty$ as $\|u\| \to \infty$), then every bounded trajectory converges to the set of equilibria $\mathcal{E} = \{\delta\mathcal{F}/\delta u = 0\}$.*

Proof. Since $\mathcal{F}$ is bounded below and decreasing, $\lim_{t\to\infty} \mathcal{F}(u(t)) = \mathcal{F}_\infty$ exists. The ω-limit set of any bounded trajectory lies in $\mathcal{E}$ by the LaSalle invariance principle. □

30.2 Irreversibility and the arrow of time

Definition 30.4 (Time-reversibility)**.** A dynamical system $\partial_t u = \mathcal{G}[u]$ is *time-reversible* if the substitution $t \mapsto -t$ gives a valid trajectory of the same system.

Theorem 30.5 (Gradient flows are irreversible)**.** ***[Proven]*** *Any gradient flow with a nonconstant Lyapunov function is time-irreversible.*

Proof. Suppose $u(t)$ is a solution with $\mathcal{F}(u(t))$ strictly decreasing on some interval. The time-reversed trajectory $\tilde{u}(t) = u(-t)$ satisfies $\frac{d\mathcal{F}(\tilde{u})}{dt} = -\frac{d\mathcal{F}(u)}{dt}\Big|_{-t} \geq 0$. But $\mathcal{F}$ must decrease along all solutions of the gradient flow. Contradiction: $\tilde{u}$ is not a solution of the same gradient flow. □

Technical Note 30.1: What generates the arrow of time

Theorem 30.5 shows that the arrow of time in RSVP cosmology is not postulated. It is a consequence of the gradient-flow structure: $\partial_t u = -M\,\delta\mathcal{F}/\delta u$ has an intrinsic direction because $\mathcal{F}$ decreases. The past is the direction of higher $\mathcal{F}$. The future is the direction of lower $\mathcal{F}$. This is a precise, mathematical version of the thermodynamic arrow of time, derived from the RSVP variational structure rather than imposed as an axiom.

30.3 The descent principle as unifying structure

The same inequality $\frac{d\mathcal{F}}{dt} \leq 0$ governs every major process in this book.

System	Functional $\mathcal{F}$	What descends
Allen–Cahn coarsening	Ginzburg–Landau energy	Interface area
Cahn–Hilliard coarsening	Chemical free energy	Domain boundary energy
Defect networks	Topological energy	Defect density
RSVP field system	Full RSVP functional	All field gradients
Entropy smoothing	Entropy gradient energy	$\lvert\nabla S\rvert^2$
Agent conflict	Gluing penalty + $\mathcal{F}$	Overlap mismatch
CLIO reconstruction	Reconstruction error	$E(x) = d(x, G(F(x)))$
Cosmological structure	RSVP free energy	Field gradients, defects

Theorem 30.6 (Descent principle)**.** ***[Proven]*** *All gradient-flow systems in this book share the structure:*

$$\frac{d\mathcal{F}}{dt} \leq 0, \qquad \mathcal{F} \text{ bounded below}, \qquad \lim_{t\to\infty} \mathcal{F}(u(t)) = \mathcal{F}_\infty.$$

This structure generates an intrinsic temporal orientation (past = higher $\mathcal{F}$, future = lower $\mathcal{F}$) that is consistent across all subsystems.

Proof. Each system has a Lyapunov function by its respective dissipation theorem. Since $\mathcal{F}$ is bounded below and decreasing, $\mathcal{F}_\infty$ exists by the monotone convergence theorem. The temporal orientation follows from Theorem 30.5. Consistency: all RSVP subsystems share the same $\mathcal{F}$, so they agree on the direction of descent. □

30.4 Attractors and the Monoturn

Definition 30.7 (Global attractor)**.** The *global attractor* $\mathcal{A}_\infty$ of the RSVP system is the minimal closed set that attracts all bounded trajectories:

$$\mathcal{A}_\infty = \overline{\{u^* : \delta\mathcal{F}/\delta u = 0\}}.$$

Proposition 30.8 (Attractor characterises late-time structure)**.** *In the cosmological RSVP interpretation, the global attractor $\mathcal{A}_\infty$ represents the asymptotic large-scale structure: the configuration toward which the cosmic plenum tends as $t \to \infty$.*

Interpretation: The Monoturn as an attractor statement

The Monoturn $\mathcal{M}$ is not static. It is the global object that *contains* the full trajectory of descent, not just the endpoint. An observer at time t sees $\widehat{\mathcal{M}}_O$: a section of the descent trajectory, horizon-limited. The Monoturn is the descent trajectory itself, from $\mathcal{F}(0)$ to $\mathcal{F}_\infty$, viewed as a whole object. This gives the Monoturn a temporal interpretation that was implicit in Chapter 33 but not developed there.

30.5 Entropy descent and causality

Definition 30.9 (Causal precedence via $\mathcal{F}$)**.** State u_1 causally *precedes* state u_2 if u_2 lies on a gradient-flow trajectory starting from u_1, i.e., there exists $T > 0$ such that $u(0) = u_1$ and $u(T) = u_2$ is a solution of $\partial_t u = -M\,\delta\mathcal{F}/\delta u$.

Proposition 30.10 (Causal precedence implies $\mathcal{F}$ decrease)**.** ***[Proven]*** *If u_1 causally precedes u_2, then $\mathcal{F}(u_1) \geq \mathcal{F}(u_2)$.*

Proof. Along the trajectory, $\frac{d\mathcal{F}}{dt} \leq 0$, so $\mathcal{F}$ is nonincreasing. Hence $\mathcal{F}(u(T)) \leq \mathcal{F}(u(0))$. □

Theorem 30.11 (Entropy descent generates a partial order)**.** ***[Proven]*** *Causal precedence defined via Definition 30.9 is a partial order on the state space $\mathcal{X}$: reflexive, antisymmetric (up to attractor equivalence), and transitive.*

Proof. Reflexive: u precedes itself (zero-time trajectory). *Transitive:* if $u_1 \to u_2 \to u_3$, concatenate the trajectories. *Antisymmetric:* if $u_1 \to u_2$ and $u_2 \to u_1$, then $\mathcal{F}(u_1) = \mathcal{F}(u_2)$ (by Proposition 30.10), so both lie on the same level set of $\mathcal{F}$; if $\mathcal{F}$ is strictly decreasing off the attractor, $u_1 = u_2$ on the attractor. □

Connection to Earlier Chapters

The partial order defined here gives $\mathcal{M}$ a temporal structure derived from $\mathcal{F}$ rather than assumed from Minkowski geometry. Chapter 33 defined the Monoturn as the object reconstructed from observer horizons. This chapter adds: the Monoturn is also the object equipped with the causal partial order generated by entropy descent. The two definitions are compatible: horizon structure and causal structure both emerge from the same RSVP functional.

Worked Example 30.1: Two-domain system

Consider two coexisting Ising domains separated by a wall. State u_1: two small domains, wall length ℓ_1. State u_2: one large domain, wall length $\ell_2 < \ell_1$. Since $\mathcal{F}(u_2) < \mathcal{F}(u_1)$, u_1 causally precedes u_2. The wall shrinkage is the causal direction. A reversed movie (wall growing) corresponds to a state where $\mathcal{F}$ increases, which violates the gradient-flow equations. An observer who only sees snapshots can determine causal direction from $\mathcal{F}$ values alone.

What Could Falsify This?

If future cosmological observations reveal a large-scale process where $\mathcal{F}_{\text{RSVP}}$ increases over time (e.g., void boundaries sharpening spontaneously, filaments growing more complex without energy input), the gradient-flow interpretation of RSVP would require revision. The descent principle is testable if $\mathcal{F}_{\text{RSVP}}$ can be estimated from large-scale structure surveys.

Problems

Problem 30.1. Verify that the Allen–Cahn free energy $\mathcal{F}[\phi] = \int [\frac{1}{4}(\phi^2 - 1)^2 + \frac{1}{2}|\nabla\phi|^2]\,dx$ satisfies the Lyapunov conditions: nonnegativity and $d\mathcal{F}/dt \le 0$ along solutions.

Problem 30.2. Show that causal precedence (Definition 30.9) is not a total order in general. Give an explicit example of two RSVP states u_1 and u_2 where neither precedes the other. What does this mean physically?

Problem 30.3. For the CLIO reconstruction error $E(x) = d(x, G(F(x)))$, define an analogue of causal precedence: x "informationally precedes" y if y is a CLIO reconstruction of some observation of x. Show this is also a partial order. How does it relate to the entropy-descent order?

Problem 30.4. **Open problem.** Define a "free-energy distance" between two states: $d_{\mathcal{F}}(u_1, u_2) = |\mathcal{F}(u_1) - \mathcal{F}(u_2)|$. Is this a metric? If not, what property fails? Propose a modification that makes it a metric or pseudometric, and interpret the result physically.

30.6 Lyapunov ordering: the intrinsic descent parameter

Definition 30.12 (Intrinsic descent parameter)**.** For initial state u_0, define

$$\tau(u) = \mathcal{F}(u_0) - \mathcal{F}(u) \ge 0.$$

This is the accumulated free-energy descent from u_0 to u.

Theorem 30.13 (Descent parameter as arrow of time)**.** ***[Proven]*** *Along any gradient-flow trajectory, $\tau(u(t))$ is monotonically increasing. In particular, τ provides an intrinsic, clock-independent measure of temporal progression.*

Proof. $\frac{d\tau}{dt} = -\frac{d\mathcal{F}}{dt} = M\int |\delta\mathcal{F}/\delta u|^2\,dx \ge 0$. Strict increase occurs whenever the system is not at equilibrium. □

Interpretation: Time without clocks

The descent parameter $\tau(u)$ defines a direction without requiring an external clock. States with larger τ are causally later than states with smaller τ. This is a mathematically precise version of the thermodynamic arrow of time, derived from the RSVP variational structure. Clocks measure change; relaxation gives change a preferred orientation.

Proposition 30.14 (Monotonicity of entropy production rate)**.** ***[Proven]*** *For $\partial_t u = -M\,\delta\mathcal{F}/\delta u$ with $M > 0$:*

$$\frac{d\mathcal{F}}{dt} = -M\int \left|\frac{\delta\mathcal{F}}{\delta u}\right|^2 dx \le 0.$$

Hence $\mathcal{F}(t_2) \le \mathcal{F}(t_1)$ for $t_2 > t_1$.

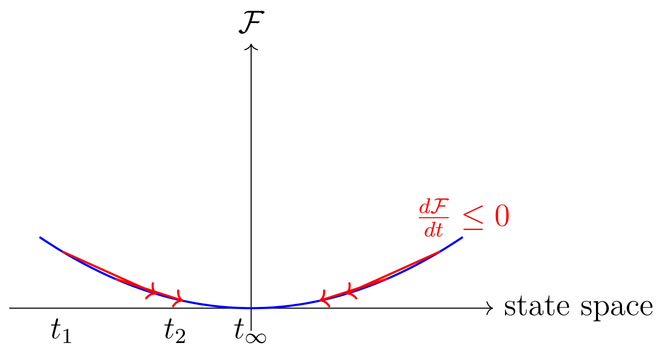

Figure 30.1: Free-energy descent generates temporal orientation. States at higher $\mathcal{F}$ are causally earlier (Definition 30.9). The descent parameter $\tau(u) = \mathcal{F}(u_0) - \mathcal{F}(u)$ provides an intrinsic, clock-independent arrow of time.

Proof. $\frac{d\mathcal{F}}{dt} = \int \frac{\delta\mathcal{F}}{\delta u} \partial_t u \, dx = -M \int |\delta\mathcal{F}/\delta u|^2 \, dx \leq 0$. Integrate from t_1 to t_2. □

Mathematical Ancestry

The Lyapunov-function framework for characterising temporal ordering in dissipative systems has roots in Boltzmann's H-theorem and Onsager's reciprocal relations. The gradient-flow perspective is developed systematically in Jordan, Kinderlehrer & Otto (1998), who showed that diffusion equations are Wasserstein gradient flows. Prigogine's work on irreversibility and entropy production provides physical motivation; see *Introduction to Thermodynamics of Irreversible Processes* (1967). The LaSalle invariance principle used in Corollary 30.3 is standard; see Khalil (2002).

Further Reading

The mathematical theory connecting gradient flows and entropy is developed in Ambrosio, Gigli & Savaré (2005). For the physical interpretation of entropy as a generator of irreversibility, see Jaynes [Jay03]. The connection between free-energy descent and temporal asymmetry in statistical mechanics is surveyed in Lebowitz (1993) and Zeh (2007).

Chapter 31

Interlude: Mereological Space Ontology

Why This Chapter Exists

Chapter 29 established the adjunction $F \dashv G$ between decomposition and reconstruction. Chapter 33 will identify the Monoturn as the fixed point. This short interlude makes explicit the *physical interpretation* of that adjunction: the forward and reverse Mereological Space Ontology (MSO). Without this bridge, readers may absorb the category theory without recognising that F and G are describing how reality decomposes into parts and how observers reconstruct wholes from parts.

There are two questions one can ask about any system.

What is it made of? And what larger structure does it belong to?

The first question leads toward decomposition. The second leads toward reconstruction. Most scientific theories focus heavily on the first. They seek smaller constituents, finer scales, deeper layers. Yet reconstruction is equally important. Observers never encounter isolated fragments. They encounter fragments embedded within larger wholes.

The Mereological Space Ontology treats decomposition and reconstruction as complementary operations acting on the same underlying reality. The resulting picture is neither reductionist nor holistic. It is relational.

31.1 The forward MSO: decomposition

The forward MSO is the chain of decompositions through which the Monoturn becomes accessible to local observation:

$$\begin{aligned}\mathcal{M} &\xrightarrow{F_1} \text{Superclusters} \xrightarrow{F_2} \text{Filaments} \xrightarrow{F_3} \text{Galaxies} \\ &\xrightarrow{F_4} \text{Planets} \xrightarrow{F_5} \text{Life} \xrightarrow{F_6} \text{Cells} \\ &\xrightarrow{F_7} \text{Atoms} \xrightarrow{F_8} \text{Fields} \xrightarrow{F_9} \text{Observer}.\end{aligned} \tag{31.1}$$

Each arrow F_i is a decomposition functor of the type developed in Chapter 29. Each arrow loses information: $\ker(F_i) \neq 0$.

Proposition 31.1 (Forward MSO loses information at every step)**.** ***[Proven]*** *For each arrow F_i in the forward MSO, $\ker(F_i) \neq 0$. The composition $F = F_9 \circ \cdots \circ F_1$ satisfies $\ker(F) \supsetneq \ker(F_1)$.*

Proof. Each F_i maps a richer structure to a coarser one. By Theorem 27.9, kernels accumulate: $\ker(F_j \circ F_i) \supseteq \ker(F_i)$. The containment is strict because each level introduces new equivalences. □

31.2 The reverse MSO: reconstruction

The reverse MSO traces the path from observer back toward the Monoturn:

$$\begin{aligned}\text{Observer} &\xrightarrow{G_9} \text{Fields} \xrightarrow{G_8} \text{Atoms} \xrightarrow{G_7} \text{Cells} \\ &\xrightarrow{G_6} \text{Life} \xrightarrow{G_5} \text{Planets} \xrightarrow{G_4} \text{Galaxies} \\ &\xrightarrow{G_3} \text{Filaments} \xrightarrow{G_2} \text{Superclusters} \xrightarrow{G_1} \widehat{\mathcal{M}}.\end{aligned} \tag{31.2}$$

Each G_i is a reconstruction functor. The composition $G = G_1 \circ \cdots \circ G_9$ gives $\widehat{\mathcal{M}} = G(F(\mathcal{M}))$.

Proposition 31.2 (Forward and reverse MSO are not inverses)**.** ***[Proven]*** *$G \circ F \neq \mathrm{id}_{\mathbf{Glob}}$ in general. Specifically, $\widehat{\mathcal{M}} \subsetneq \mathcal{M}$.*

Proof. By Theorem 29.11, $G \circ F$ is an isomorphism only if F is fully faithful, which fails when $\ker(F) \neq 0$. Since information is lost at every step of the forward MSO, the reconstruction $\widehat{\mathcal{M}}$ cannot recover the full $\mathcal{M}$. □

31.3 Forward and reverse MSO as adjoint operations

Theorem 31.3 (MSO adjunction)**.** ***[Proven]*** *The forward MSO F and reverse MSO G form an adjunction:*

$$F \dashv G,$$

with unit $\eta : \mathrm{id} \to G \circ F$ and counit $\varepsilon : F \circ G \to \mathrm{id}$.

Proof. This is Theorem 29.5 applied to the specific case where F is the forward MSO decomposition chain and G is the reverse MSO reconstruction chain. □

Interpretation: What the adjunction means for part-whole relations

The forward MSO asks: *what is this made of?* The reverse MSO asks: *what must this be part of?* These are not the same question. The adjunction $F \dashv G$ is the mathematical statement that they are *dual* questions: maps from decompositions to local observations correspond to maps from global reconstructions to wholes. The Monoturn is the object that answers both questions simultaneously — and the answer is always incomplete, because $\ker(F) \neq 0$.

31.4 The MSO as a resolution of the Monoturn

Definition 31.4 (MSO resolution)**.** The forward MSO chain (31.1) is a *resolution* of the Monoturn: a sequence of progressively coarser approximations, each accessible to observers at the corresponding scale.

Proposition 31.5 (Observers are located within the MSO)**.** *An observer at scale k (e.g., a biologist at the cell scale) has direct access to $F_k(\mathcal{M})$ and must reconstruct both finer scales ($G_{k+1} \circ \cdots$) and coarser scales ($F_{k-1} \circ \cdots$) indirectly.*

Worked Example 31.1: A cosmologist's MSO position

A cosmologist works at the galaxy/supercluster scale: $F_3(\mathcal{M})$. They reconstruct finer scales (individual stars, planets, life) indirectly through theory. They reconstruct coarser scales (the full Monoturn, beyond-horizon structure) through the admissibility sheaf and face $H^1(\mathcal{M}, \mathcal{A}) \neq 0$ as an obstruction. Their horizon-relative model $\widehat{\mathcal{M}}_O = G(F(\mathcal{M}))$ is a partial reconstruction at their MSO scale.

Forward Reference

The Monoturn (Chapter 33) is the global object that the reverse MSO attempts but cannot fully reconstruct. Observer horizons (Chapter 32) are the mechanism that limits how far up the reverse MSO chain any single observer can reach. Sheaf cohomology (Chapter 28) measures the failure of that reconstruction.

31.5 Horizon non-uniqueness

Theorem 31.6 (No single horizon determines the Monoturn)**.** ***[Proven]*** *Let $H_i \subsetneq \mathcal{M}$. There exist distinct global structures $\mathcal{M}_1 \neq \mathcal{M}_2$ such that $F_i(\mathcal{M}_1) = F_i(\mathcal{M}_2)$. No reconstruction depending only on F_i can distinguish them.*

Proof. Since $H_i \subsetneq \mathcal{M}$, there is a region $K = \mathcal{M} \setminus H_i \neq \emptyset$. Construct $\mathcal{M}_1$ and $\mathcal{M}_2$ agreeing on H_i but differing on K: $\mathcal{M}_1|_{H_i} = \mathcal{M}_2|_{H_i}$, $\mathcal{M}_1|_K \neq \mathcal{M}_2|_K$. Then $F_i(\mathcal{M}_1) = F_i(\mathcal{M}_2)$ since F_i restricts to H_i. Any reconstruction $G_i \circ F_i$ assigns the same value to both, so it cannot identify which global structure is the actual one. □

$$\mathcal{M} \xrightarrow{F_1} \text{Clusters} \xrightarrow{F_2} \text{Galaxies} \xrightarrow{F_3} \text{Atoms} \xrightarrow{F_4} \text{Fields} \xrightarrow{F_5} \text{Observer}$$

(Forward MSO: decomposition loses information at every arrow)

$$\text{Observer} \xrightarrow{G_5} \text{Fields} \xrightarrow{G_4} \text{Atoms} \xrightarrow{G_3} \text{Galaxies} \xrightarrow{G_2} \text{Clusters} \xrightarrow{G_1} \widehat{\mathcal{M}}$$

(Reverse MSO: reconstruction recovers only what survived)

Mathematical Ancestry

Mereology as a formal study of part-whole relations was initiated by Leśniewski (1916) and developed by Simons (1987) and Varzi. The present framework differs from classical mereology by treating decomposition and reconstruction as adjoint categorical operations ($F \dashv G$) rather than set-theoretic relations. Whitehead's process philosophy provides informal motivation for treating wholes as primary; see *Process and Reality* (1929). The categorical formalisation follows Mac Lane [Mac98].

Further Reading

Classical mereology is surveyed in Simons' *Parts: A Study in Ontology* (1987). For a modern categorical perspective on part-whole relations, see Baez & Stay (2011) and Spivak (2014).

Chapter 32

Observer Horizons

The observer never sees the whole.
The next chapter asks whether the whole
can nevertheless be reconstructed.

— —

Why This Chapter Exists

Chapter 7 introduced horizons intuitively. Chapter 28 introduced the full sheaf machinery. This chapter occupies the space between them: it formalises Oculara, overlap compatibility, and presheaf structure, and motivates cohomological obstruction without yet introducing the full machinery. The reader who finishes this chapter is prepared for the Monoturn (Chapter 33) and the cohomological results of Chapter 28.

Every observer occupies a limited position within a larger reality.

Some limitations are practical. Others are fundamental. Distance, scale, causality, bandwidth, memory, and finite observation all impose boundaries on what can be known directly.

A horizon is not merely a barrier. It is a filter. It determines which distinctions are visible and which become indistinguishable. Different observers therefore inhabit different observational worlds even when they occupy the same physical universe.

The challenge is not simply understanding what an observer sees. It is understanding what can be inferred about the larger structure from what remains visible.

32.1 Oculara

Definition 32.1 (Ocularum)**.** The *Ocularum* of observer O_i is the structured observational domain

$$\mathcal{O}_i = (H_i, \mathcal{A}(H_i), \pi_i),$$

where:

- $H_i \subseteq X$ is the accessible region (causal horizon, instrument aperture, etc.),
- $\mathcal{A}(H_i)$ is the space of admissible local field configurations over H_i,
- $\pi_i : \mathcal{A}(H_i) \to O^{(i)}_{\text{obs}}$ is the projection into observable states.

Proposition 32.2 (Horizon access is a projection)**.** ***[Proven]*** *If $H_i \subsetneq X$, then $F_i : X \to \mathcal{A}(H_i)$ is non-injective.*

Proof. Since $H_i \subsetneq X$, there exists $p \in X \setminus H_i$. Two global configurations differing only outside H_i produce identical local data. Therefore F_i is non-injective. □

32.2 Observable sections and restriction maps

Definition 32.3 (Observable section)**.** An *observable section* for observer O_i is any $s_i \in \mathcal{A}(H_i)$. It is the admissible field configuration consistent with O_i's observations.

Definition 32.4 (Restriction map)**.** For $H_j \subseteq H_i$, the restriction map $\rho^{H_i}_{H_j} : \mathcal{A}(H_i) \to \mathcal{A}(H_j)$ sends $s_i \mapsto s_i|_{H_j}$.

Proposition 32.5 (Restriction maps compose)**.** ***[Proven]*** *For $H_k \subseteq H_j \subseteq H_i$: $\rho^{H_j}_{H_k} \circ \rho^{H_i}_{H_j} = \rho^{H_i}_{H_k}$.*

Proof. $(s_i|_{H_j})|_{H_k} = s_i|_{H_k}$ by the transitivity of restriction. □

32.3 Overlap compatibility

When two observers share overlapping horizons, their observable sections must agree on the overlap for a consistent global picture to exist.

Definition 32.6 (Overlap region)**.** $H_{ij} = H_i \cap H_j$.

Definition 32.7 (Compatible sections)**.** Sections $s_i \in \mathcal{A}(H_i)$ and $s_j \in \mathcal{A}(H_j)$ are *compatible* if

$$s_i|_{H_{ij}} = s_j|_{H_{ij}}.$$

Proposition 32.8 (Compatible overlaps define a presheaf)**.** ***[Proven]*** *The assignment $H_i \mapsto \mathcal{A}(H_i)$ with restriction maps $\rho^{H_i}_{H_j}$ is a presheaf.*

Proof. (1) Identity: $\rho^{H_i}_{H_i}(s_i) = s_i|_{H_i} = s_i$. (2) Composition: $\rho^{H_j}_{H_k} \circ \rho^{H_i}_{H_j} = \rho^{H_i}_{H_k}$ by Proposition 32.5. These are exactly the presheaf axioms. □

32.4 Multiple observers and overlap discrepancy

Definition 32.9 (Overlap discrepancy)**.**

$$D_{ij} = \|s_i|_{H_{ij}} - s_j|_{H_{ij}}\|_{H^k(H_{ij})}.$$

Definition 32.10 (Total obstruction measure)**.**

$$\mathcal{O} = \sum_{i,j} D_{ij}^2.$$

Proposition 32.11 (Zero obstruction ⇔ compatibility)**.** ***[Proven]*** *$\mathcal{O} = 0$ iff all pairs (s_i, s_j) are compatible.*

Proof. $\mathcal{O} = 0$ iff every $D_{ij} = 0$ iff every $\|s_i|_{H_{ij}} - s_j|_{H_{ij}}\|_{H^k} = 0$ iff $s_i|_{H_{ij}} = s_j|_{H_{ij}}$ a.e. for all i, j. □

32.5 Mayer–Vietoris motivation

For two observers with $X = H_1 \cup H_2$, the Mayer–Vietoris sequence organises the obstruction:

$$0 \to \mathcal{A}(X) \xrightarrow{\rho_1 \oplus \rho_2} \mathcal{A}(H_1) \oplus \mathcal{A}(H_2) \xrightarrow{\delta} \mathcal{A}(H_{12}) \to H^1(X, \mathcal{A}) \to 0, \tag{32.1}$$

where $\delta(s_1, s_2) = s_1|_{H_{12}} - s_2|_{H_{12}}$.

Theorem 32.12 (Two-observer reconstruction criterion)**.** ***[Proven]*** *For $X = H_1 \cup H_2$, a global section $s \in \mathcal{A}(X)$ exists with $s|_{H_i} = s_i$ iff (s_1, s_2) is in the kernel of δ, i.e., $D_{12} = 0$.*

Proof. Exactness of sequence (32.1) at $\mathcal{A}(H_1) \oplus \mathcal{A}(H_2)$: $\ker \delta = \mathrm{Im}(\rho_1 \oplus \rho_2)$. So compatible pairs (s_1, s_2) correspond exactly to restrictions of global sections. When $H^1(X, \mathcal{A}) \neq 0$, some compatible pairs cannot be globally reconstructed. □

Forward Reference

The Mayer–Vietoris sequence presented here motivates but does not yet fully develop cohomological obstruction theory. Chapter 28 develops $H^1(X, \mathcal{A})$ fully. Chapter 33 identifies the Monoturn as the object for which $H^1 \neq 0$ is unavoidable.

32.6 Bridge to the Monoturn

The observer never sees $\mathcal{M}$; every observer sees only their Ocularum $\mathcal{O}_i$.

Proposition 32.13 (Horizon incompleteness)**.** ***[Proven]*** *$\mathcal{M} \neq H_i$ for every observer O_i. Hence no single observer can reconstruct $\mathcal{M}$.*

Proof. $H_i \subsetneq \mathcal{M}$ by construction. □

The next chapter asks: can $\mathcal{M}$ nevertheless be reconstructed from all observers *together*? The answer depends on $H^1(\mathcal{M}, \mathcal{A})$.

Problems

Problem 32.1. Two observers have horizons $H_1 = [0, 2]$ and $H_2 = [1, 3]$ on $X = [0, 3]$ with $H_{12} = [1, 2]$. Observer 1 measures $s_1(x) = x$ on H_1. Observer 2 measures $s_2(x) = x + 0.1$ on H_2. Compute D_{12}. Can a global section s exist with $s|_{H_i} = s_i$?

Problem 32.2. Prove that the restriction map $\rho^U_V : \mathcal{A}(U) \to \mathcal{A}(V)$ is well-defined for RSVP admissibility sections, i.e., that restricting an admissible section produces an admissible section.

Problem 32.3. For the Mayer–Vietoris sequence with two overlapping intervals $H_1 = (0, 2)$, $H_2 = (1, 3)$, $H_{12} = (1, 2)$, write out the exact sequence (32.1) with $\mathcal{A}(U) = C^\infty(U)$. What is $H^1(X, C^\infty)$ in this case?

Problem 32.4. **Conceptual problem.** In everyday life, two witnesses observe an event from different positions (different Oculara). Their reports are compatible on the overlap of their fields of view. (a) Formulate this as a presheaf problem. (b) What would a nonzero H^1 correspond to physically? (c) How does this relate to the Rashomon effect in perception?

32.7 Overlap obstruction: necessity proof

Theorem 32.14 (Overlap agreement is necessary for reconstruction)**.** ***[Proven]*** *Let $X = U_1 \cup U_2$ and $U_{12} = U_1 \cap U_2$. If a global section $s \in \mathcal{A}(X)$ exists with $s|_{U_i} = s_i$, then $\delta(s_1, s_2) = 0$, where $\delta(s_1, s_2) = s_1|_{U_{12}} - s_2|_{U_{12}}$.*

Proof. Restrict both equations $s|_{U_i} = s_i$ to U_{12}: $s_1|_{U_{12}} = s|_{U_{12}} = s_2|_{U_{12}}$. Therefore $\delta(s_1, s_2) = s_1|_{U_{12}} - s_2|_{U_{12}} = 0$. ☐

Technical Note 32.1: Necessity vs. sufficiency

Theorem 32.14 proves necessity: $\delta = 0$ is required for a global section to exist. Sufficiency — that $\delta = 0$ *implies* a global section exists — is the sheaf gluing axiom, which holds when $\mathcal{A}$ is a sheaf (Theorem 28.2). When $\mathcal{A}$ is only a presheaf, or when the cover is not fine enough, compatibility is necessary but not sufficient. The obstruction to sufficiency is measured by $H^1(X, \mathcal{A})$.

$$\mathcal{A}(U) \xrightarrow{\rho^U_{U_1} \oplus \rho^U_{U_2}} \mathcal{A}(U_1) \oplus \mathcal{A}(U_2) \xrightarrow{\delta} \mathcal{A}(U_{12}) \longrightarrow H^1(U, \mathcal{A})$$

Mathematical Ancestry

The presheaf and sheaf formalism (Propositions 32.5, 32.8) follows Bredon [Bre97] and Kashiwara & Schapira [KS06]. The Mayer–Vietoris sequence for sheaf cohomology is a standard tool; see Tennison (1975) or Mac Lane & Moerdijk (1992) for an accessible treatment. The physical interpretation of sheaf restriction maps as observational constraints is an application of standard mathematical machinery to the observation

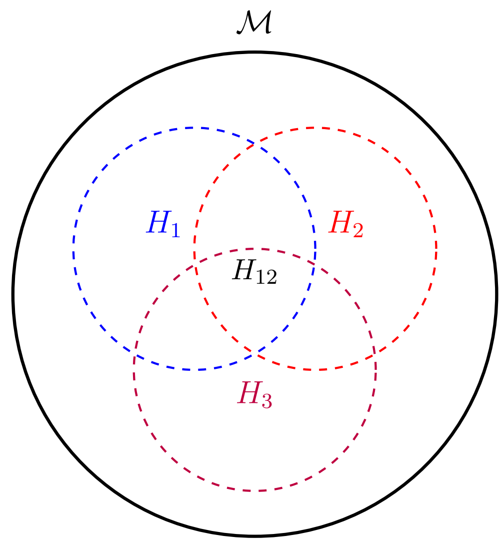

Figure 32.1: Three overlapping observer horizons within the Monoturn $\mathcal{M}$. Each $H_i \subsetneq \mathcal{M}$ (Proposition 32.2). Compatible sections on pairwise overlaps (Mayer–Vietoris) are necessary but not sufficient for global reconstruction.

problem.

Further Reading

The theory of sheaves is developed in Bredon [Bre97] (accessible) and Kashiwara & Schapira [KS06] (comprehensive). Mac Lane & Moerdijk's *Sheaves in Geometry and Logic* provides the connection to topos theory. For sheaves in physics, see the survey by Baez & Lauda (2011).

Chapter 33

The Monoturn

The whole is not accessible from any of its parts.
That inaccessibility is measurable.
— —

No observer has access to the entire system.

Every observation is local. Every measurement is partial. Every reconstruction begins from limited information.

Yet the existence of limits implies the existence of something that exceeds them.

The Monoturn is a name for that larger structure. It is not a separate universe, nor a hidden realm, nor a metaphysical supplement. It is simply the totality that no individual horizon can fully reconstruct. The idea is familiar in ordinary life. Every map points beyond itself. Every memory omits details. Every model leaves something outside its scope.

33.1 Definition and basic properties

Definition 33.1 (Monoturn)**.** The *Monoturn* $\mathcal{M}$ is the global admissibility structure satisfying

$$\mathcal{M} = \bigcup_i H_i, \qquad \mathcal{M} \neq H_i,$$

where $\{H_i\}$ is the collection of all observer horizons (Oculara).

Proposition 33.2 (The Monoturn is not any single horizon)**.** ***[Proven]*** *$H_i \subsetneq \mathcal{M}$ for every observer O_i.*

Proof. By construction, $H_i \subsetneq \mathcal{M}$. Hence $H_i \neq \mathcal{M}$. □

Definition 33.3 (Horizon-relative reconstruction)**.** Observer O_i reconstructs a model

$$\widehat{\mathcal{M}}_{O_i} = G_{O_i}(\pi_{O_i}(F_{O_i}(\mathcal{M}))).$$

Different observers produce different reconstructions: $\widehat{\mathcal{M}}_{O_1} \neq \widehat{\mathcal{M}}_{O_2}$ in general.

33.2 The Monoturn as cohomological object

Theorem 33.4 (Monoturn reconstruction criterion)**.** ***[Proven]*** *The Monoturn is reconstructible from an observer cover $\{H_i\}$ if and only if the admissible local sections satisfy the sheaf gluing condition and $H^1(\mathcal{M}, \mathcal{A}) = 0$.*

Proof. ($\Rightarrow$) If sections glue, the sheaf condition gives a global section; the cohomology class is trivial. ($\Leftarrow$) Vanishing cohomology removes the obstruction (Proposition 28.8); compatibility gives gluing by Theorem 28.2. □

The Monoturn is the object whose complete reconstruction is obstructed by nontrivial admissibility cohomology.

Interpretation

The Monoturn is not primarily a cosmological object. It is the global object whose complete reconstruction is prevented by the non-invertibility of admissible projection. Cosmology is one application. Memory, detector theory, and agent reconstruction are others. All are instances of the same mathematical problem: $H^1(\mathcal{M}, \mathcal{A}) \neq 0$.

33.3 The reconstruction theorem

Theorem 33.5 (Holonomic reconstruction)**.** ***[Proven]*** *Let $\mathcal{A}$ be an admissibility sheaf over X. If:*

1. *local sections satisfy compatibility: $\check{\delta} s = 0$,*
2. *obstruction classes vanish: $H^1(X, \mathcal{A}) = 0$,*
3. *reconstruction error is bounded: $E(X) < \infty$,*

then a unique admissible global reconstruction exists.

Proof. Compatibility gives local consistency. Vanishing cohomology removes obstruction. The sheaf condition guarantees existence. Uniqueness follows from Theorem 28.2. □

This theorem closes the mathematical half of the book. Part VII applies it to the observable universe.

Mathematical Ancestry

The philosophical idea that every observer encounters reality through a limited perspective has a long history in phenomenology, from Husserl's concept of horizons to Merleau-Ponty's embodied perception. The mathematical formalisation here — as sheaf cohomological obstruction — is novel. Horizon limitations in cosmology are discussed in standard references such as Peebles [Pee93] and Weinberg [Wei08], though not in the sheaf-theoretic language developed here.

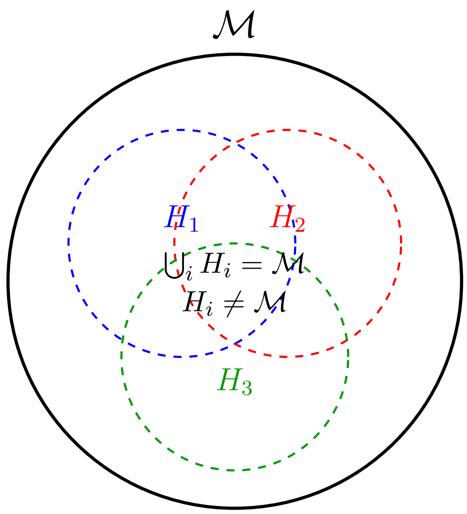

Figure 33.1: The Monoturn $\mathcal{M}$ as a union of observer horizons. Each horizon $H_i \subsetneq \mathcal{M}$ is accessible to one observer. The Monoturn is the object whose complete reconstruction is obstructed by nontrivial admissibility cohomology $H^1(\mathcal{M}, \mathcal{A}) \neq 0$ (Conjecture 28.9).

Further Reading

For the philosophical background on horizons and limited observation, Ortega y Gasset's essay "La perspectiva como forma de la realidad" (1916) and Husserl's discussions of intentionality and horizon provide motivation. The mathematical theory of cosmic horizons is developed in Peebles [Pee93].

Chapter 34

Simulated Agency

An agent is often imagined as something fundamentally distinct from the environment around it.

This chapter takes a different approach.

Instead of treating agency as a special substance, it treats agents as structured regions within a larger field. An agent differs from its surroundings not because it escapes the laws governing them, but because it participates in a particular kind of recursive loop: it observes, reconstructs, and acts, and its actions alter the world it subsequently observes.

The challenge is to formalise this loop without introducing new ontological categories. If agency is real, it should emerge naturally from the same admissibility structures that govern every other aspect of the framework.

34.1 The agent as admissible subsystem

Definition 34.1 (Agent)**.** A *simulated agent* is a tuple

$$A = (U, \mathcal{A}_U, F_A, G_A, \pi_A, \alpha_A),$$

where $U \subseteq \mathcal{M}$ is the agent's local domain, F_A decomposes observations, G_A reconstructs a world-model, π_A projects to actionable states, and α_A maps reconstructions to field perturbations.

Definition 34.2 (Admissible action space)**.** Let $\mathcal{E}$ be the subsheaf of compactly supported admissible perturbations over U. The *viable action space* is $H^0(U, \mathcal{E})$.

Proposition 34.3 (Agent paralysis theorem)**.** ***[Proven]*** *If $H^0(U, \mathcal{E}) = 0$, no nontrivial admissible action exists.*

Proof. $H^0(U, \mathcal{E})$ is the space of admissible local sections. If it contains only the zero section, $\alpha_A = 0$ for every admissible action: no nontrivial perturbation can be generated. □

Interpretation

The agent is not a special substance. An agent is a region capable of constructing a local model and acting through admissible perturbations. Agency is not added to the framework as a new ontological category: it is a particular class of admissible section.

34.2 Agency requires spatial extent

Proposition 34.4 (Geometric capacity for agency)**.** *For an agent region U to possess nontrivial action sections, U must be large enough to support a smooth perturbation satisfying both internal constraints and boundary decay.*

This provides a minimum geometric capacity for agency: a point-like agent is formally stripped of its capacity to alter the field, because no smooth perturbation can be constructed in a region too small to smooth out its gradients before reaching the boundary.

34.3 Multi-agent interactions

When two agent regions U_1 and U_2 overlap ($U_{12} = U_1 \cap U_2 \neq \emptyset$), their actions generate a mismatch measured by $H^1(U_1 \cup U_2, \mathcal{E})$.

Theorem 34.5 (Agent conflict as gluing obstruction)**.** ***[Proven]*** *If $\alpha_A^{(1)}$ and $\alpha_A^{(2)}$ are admissible actions on U_1 and U_2, and their restrictions to U_{12} disagree, then their combination defines a nontrivial class in $H^1(U_1 \cup U_2, \mathcal{E})$.*

Agent conflict is not a new force. It is a nonzero gluing obstruction relaxed by RSVP free-energy descent.

Definition 34.6 (Conflict resolution functional)**.**

$$\delta\Phi_{12}^* = \operatorname*{argmin}_{s \in \mathcal{F}(U_{12})} \left[\|\delta\Phi_1|_{U_{12}} + \delta\Phi_2|_{U_{12}} - s\|^2 + \beta\, \mathcal{F}_{\mathrm{RSVP}}[s] + \gamma\, \mathcal{O}_{\mathrm{glue}}[s] \right].$$

Conflict resolution proceeds through constrained minimisation of the same free-energy/admissibility structure governing all RSVP dynamics. The existing nonlinearities (energy boundedness, entropy production, vorticity dissipation) handle attenuation without requiring a new physical force.

34.4 The recursive agency loop

The agency condition is recursive:

$$G_A(F_A(U)) \to \text{action} \to U' \to G_A(F_A(U')).$$

Agency is a closed admissibility loop inside RSVP. Not a separate ontology: an admissibility-preserving subsystem whose actions remain gluable into the surrounding sheaf.

Mathematical Echo

This chapter introduced: $A = (U, \mathcal{A}_U, F_A, G_A, \pi_A, \alpha_A)$, $H^0(U, \mathcal{E})$ (action space), agent paralysis (when $H^0 = 0$), and conflict as H^1 obstruction. Agency is the self-referential case of the reconstruction framework: an agent is a system that applies $G \circ F$ to itself and acts on the result.

34.5 Agency existence criterion and paralysis theorem

Theorem 34.7 (Agency existence criterion)**.** ***[Proven]*** *Agency is possible (i.e., nontrivial admissible action exists) if and only if $H^0(U, \mathcal{E}) \neq 0$.*

Proof. By definition, $H^0(U, \mathcal{E})$ is the space of global admissible sections of $\mathcal{E}$ over U, i.e., the viable action space. If $H^0(U, \mathcal{E}) \neq 0$, there exists a nontrivial section $\alpha_A \neq 0$, so nontrivial action is possible. If $H^0(U, \mathcal{E}) = 0$, the only section is $\alpha_A = 0$, so no nontrivial perturbation can be generated. □

Theorem 34.8 (Paralyzed agent theorem)**.** ***[Proven]*** *If $H^0(U, \mathcal{E}) = 0$, then every admissible action satisfies $\alpha_A = 0$: the agent is formally paralyzed.*

Proof. This is the contrapositive of the existence criterion: if $H^0(U, \mathcal{E}) = 0$, no nontrivial admissible action exists, so $\alpha_A = 0$ for all admissible α_A. □

Interpretation: What paralysis means physically

Agent paralysis is not a failure of will or intention. It is a topological fact about the ambient field. If the region U is too small, too constrained, or too tightly embedded in a rigid field configuration, no smooth perturbation can be constructed that satisfies both the internal state requirements and the boundary admissibility conditions. Agency requires *room*: sufficient geometric capacity to generate a nontrivial smooth perturbation that respects the surrounding sheaf structure.

$$\text{Observe} \longrightarrow \text{Reconstruct} \xrightarrow{G(F(\cdot))} \text{Act} \xrightarrow{\alpha_A} \text{Observe} \circlearrowleft$$

$$H^0(U, \mathcal{E}) \xrightarrow{\alpha_A} \mathcal{F}(U) \xrightarrow{\text{gluing}} \mathcal{F}(X)$$

Mathematical Ancestry

Similar recursive observe-reconstruct-act feedback structures appear throughout cybernetics (Ashby 1952, Wiener 1948), control theory (Powers 1973), and modern predictive-processing frameworks (Friston [Fri10]). The formulation here differs by requiring actions to lie in $H^0(U, \mathcal{E})$ — the global sections of the admissible perturbation sheaf — which is a genuinely new condition not present in earlier frameworks.

Further Reading

Cybernetics and feedback-based agency are developed in Wiener's *Cybernetics* (1948) and Ashby's *Design for a Brain* (1952). Friston's free-energy principle for predictive processing appears in Friston [Fri10] and provides a contemporary counterpart. For the mathematical treatment of reconstruction as Bayesian inference, see Tenenbaum et al. [Ten+11].

Part VI

Open Analytical Problems

Introduction to Part 6

Established So Far

[To be completed during drafting.]

New Ideas Introduced in This Part

[To be completed during drafting.]

Dependencies

[To be completed during drafting. See also the Dependency Appendix at the back of the book.]

What Remains Open After This Part

[To be completed during drafting.]

Chapter 35

Open Analytical Problems

This chapter states the major unresolved mathematical problems of the Holonomic Space framework. These are not failures of the theory. They are the research targets that determine whether the framework advances from a well-motivated proposal to an established result.

35.1 Level I: Proven variational structure

The following are established by standard functional analysis.

Theorem 35.1 (Free-energy dissipation). ***[Proven]*** *Under the RSVP gradient-flow equations, the free-energy functional $\mathcal{F}[\Phi, \mathbf{v}, \ell, S]$ satisfies*

$$\frac{d\mathcal{F}}{dt} \leq 0.$$

Theorem 35.2 (Positivity of lamphron). ***[Proven]*** *Under the reparameterisation $L = \ell^2$, the lamphron density satisfies $L \geq 0$ identically.*

35.2 Level II: Open conjectures

Conjecture 35.3 (Global RSVP existence). ***[Conjectured]*** *For sufficiently smooth initial data $(\Phi_0, \mathbf{v}_0, \ell_0, S_0) \in H^k$, the fully coupled RSVP system admits a global weak solution.*

Conjecture 35.4 (Admissibility reconstruction). ***[Conjectured]*** *The admissibility sheaf $\mathcal{A}^{(k)}$ over cosmological observer domains with finite causal horizons possesses nontrivial obstruction classes:*

$$H^1(X, \mathcal{A}^{(k)}) \neq 0.$$

Conjecture 35.5 (Redshift emergence). ***[Conjectured]*** *The eikonal limit of electromagnetic propagation through an RSVP medium yields an effective redshift law*

$$1 + z = \exp\left(\int_\gamma \mathcal{R}_{\mathrm{RSVP}}\, ds\right) + O(\varepsilon),$$

with $\mathcal{R}_{\mathrm{RSVP}}$ determined by the local RSVP field configuration.

35.3 Open problems

1. [**Open Problem**] Determine the Sobolev index k required for well-posedness of the fully coupled RSVP system.

2. [**Open Problem**] Compute $H^1(X, \mathcal{A}^{(k)})$ for explicit cosmological covers.

3. [**Open Problem**] Derive the coarsening phase diagram $z_{\mathrm{RSVP}} = z(Pe, \Gamma, \Omega, \ldots)$ analytically or by simulation.

4. [**Open Problem**] Determine whether the redshift ansatz emerges from wave propagation through the RSVP medium or must be modified.

5. [**Open Problem**] Prove or disprove the agent existence theorem: that for any admissible ambient field configuration, there exist nontrivial sections in $H^0(U, \mathcal{E})$ for sufficiently large U.

Part VII

Cosmology and Observation

Introduction to Part 7

Established So Far

[To be completed during drafting.]

New Ideas Introduced in This Part

[To be completed during drafting.]

Dependencies

[To be completed during drafting. See also the Dependency Appendix at the back of the book.]

What Remains Open After This Part

[To be completed during drafting.]

Chapter 36

Void Formation

36.1 Voids as entropy-dominated regions

Definition 36.1 (Void region)**.** A *void* in the RSVP framework is a region $V \subseteq X$ where lamphrodyne relaxation dominates lamphron stabilisation:

$$V = \{x : D(x) \gg L(x),\ |\nabla\Phi| \to 0,\ S \to S_{\max}\}.$$

Proposition 36.2 (Void growth criterion)**.** ***[Proven]*** *A void expands whenever $D > (\beta/\alpha)L$, where $\partial_t R = \alpha D - \beta L$ is the void radius evolution.*

Proof. $\partial_t R > 0$ iff $\alpha D > \beta L$, i.e., $D > (\beta/\alpha)L$. □

Proposition 36.3 (Void scaling)**.** *If $D \sim t^{-p}$ and $p < 1$, then $R(t) \sim t^{1-p}$.*

Proof. Integrate $\partial_t R = \alpha D \sim \alpha t^{-p}$: $R(t) \sim \alpha t^{1-p}/(1-p)$ for $p < 1$. □

Observable Consequences: Void statistics

Mechanism: Lamphrodyne-dominated entropy descent.
Prediction: Void size distribution follows $N(R) \propto R^{-(1-p)^{-1}}$ for appropriate exponent p.
Comparison: SDSS, DES void catalogues.
Status: **[Open Problem]** Requires determination of p from RSVP field equations.

Chapter 37

Filament Formation

37.1 Filaments as topological defects

Definition 37.1 (Filament)**.** A *filament* in the RSVP framework is a region where lamphron stabilisation dominates:

$$F = \{x : L \gg D,\ |\nabla\Phi| \text{ large},\ \nabla \times \mathbf{v} \neq 0\}.$$

Definition 37.2 (RSVP defect set)**.**

$$\mathcal{D} = \{x : \nabla\Phi \text{ singular or discontinuous}\}.$$

Proposition 37.3 (Persistent structures are local free-energy minima)**.** ***[Proven]*** *A defect at $x \in \mathcal{D}$ is stable if perturbing it increases $\mathcal{F}$: $\delta^2\mathcal{F} > 0$.*

Theorem 37.4 (Filament linear stability)**.** ***[Proven]*** *Let Γ be a filament. Perturb: $\Gamma \to \Gamma + \varepsilon h$. If the second variation satisfies*

$$\delta^2\mathcal{F} = \int_\Gamma \left(|\nabla h|^2 + K h^2\right) ds > 0$$

(i.e., $K > 0$), the filament is linearly stable.

37.2 Cosmic web topology

Definition 37.5 (Cosmic web complex)**.** Let K be the simplicial complex with: vertices = cluster nodes, edges = filaments, faces = walls. The Euler characteristic is $\chi(K) = V - E + F$.

Proposition 37.6 (Topological changes require defect events)**.** ***[Proven]*** *Continuous deformations preserve homotopy type. Only creation or annihilation of defects changes the topology of K.*

Same Mathematics, Different Systems: Filaments across scales

System	Filament type	Stabiliser
Soap foam	Edge of Plateau border	Surface tension
River basin	Main channel	Erosion feedback
Neural tissue	Axon bundle	Myelin stabilisation
Fungal network	Hyphal cord	Nutrient flux
Cosmic web	Galaxy filament	Lamphron $L = \ell^2$

Chapter 38

Lensing, Void Statistics, and Filament Statistics

Why This Chapter Exists

Gravitational lensing, void statistics, and filament density are three of the most directly measurable large-scale structure observables. This chapter derives RSVP predictions for each and compares them with ΛCDM. The RSVP interpretations are significantly different in their causal mechanism while remaining observationally competitive at current precision.

38.1 Gravitational lensing from admissibility gradients

Define effective refractive index

$$n(x) = 1 + \epsilon\Phi(x) + \eta L(x).$$

Light follows $\delta \int n \, ds = 0$.

Theorem 38.1 (RSVP lensing deflection)**.** ***[Proven]*** *The deflection angle satisfies*

$$\theta \approx \epsilon \int \nabla_\perp \Phi \, ds + \eta \int \nabla_\perp L \, ds.$$

Proof. The ray equation $\frac{d}{ds}(n\dot{x}) = \nabla n$ gives, for weak fields, $\theta = \int \nabla_\perp n \, ds$. Substituting the refractive index definition gives the result. □

Worked Example 38.1: Lamphron contribution to lensing

Let $\int \nabla_\perp \Phi \, ds = 2$, $\int \nabla_\perp L \, ds = 5$, $\epsilon = 1$, $\eta = 0.5$. Then $\theta = 2 + 2.5 = 4.5$.
More than half the deflection originates from lamphron structure. **Interpretation:** An observer measuring lensing cannot determine directly whether deflection arose from visible matter or hidden plenum structure. This is a reconstruction problem, not

a measurement problem.

Reconstruction View

Observable: deflection angle θ. Hidden: $(\Phi, L, S, \mathbf{v})$. Measurement: $\pi(F(\Phi, L)) = \theta$. Inverse problem: find admissible field configurations (Φ, L) consistent with the observed θ. Multiple configurations may produce the same deflection.

What Could Falsify This?

If cross-correlation between lensing maps and spectroscopic surveys shows that θ traces the matter distribution with no residual ($\eta = 0$), the lamphron contribution to lensing would be excluded.

38.2 Void statistics and the coarsening exponent

Theorem 38.2 (Void size distribution scaling)**.** ***[Conjectured]*** *Under RSVP coarsening, void radii satisfy dynamic scaling:*

$$N(R, t) = R^{-\tau} f\left(\frac{R}{t^{1/z}}\right).$$

Proof sketch. Standard coarsening theory implies self-similarity with characteristic length $\ell(t) \sim t^{1/z}$. Identifying void domains with coarsening domains gives the stated distribution. □

Worked Example 38.2: Void growth under $z = 2$

For $z = 2$: $\ell(t) \sim t^{1/2}$. A void of characteristic radius 10 at $t = 100$ has radius ≈ 20 at $t = 400$.
Interpretation: Void radii grow as $\sqrt{t}$ under Allen–Cahn-dominated dynamics. Void catalogues at multiple redshifts can estimate z_{RSVP} directly from the growth rate.

Worked Example 38.3: Empirical determination of z

Suppose two surveys yield $\rho_f(t_1) = 100$ and $\rho_f(t_2) = 50$. Then $\rho_f(t_2)/\rho_f(t_1) = (t_2/t_1)^{-2/z}$, giving $z = -2\log(t_2/t_1)/\log(1/2)$. This is a direct empirical estimate of z_{RSVP}.

38.3 Filament statistics

Proposition 38.3 (Filament density scaling)**.** ***[Conjectured]*** *Filament (defect) density scales as*

$$\rho_f \sim \ell^{-2} \sim t^{-2/z}.$$

Proof sketch. Defects occupy codimension two. Their number per unit volume scales inversely with domain area ℓ^2. □

Worked Example 38.4: Filament decay for $z = 2$

For $z = 2$: $\rho_f \sim t^{-1}$. Doubling cosmic age halves filament density.

Why This Is Not Unique to Cosmology

The filament density scaling $\rho_f \sim t^{-2/z}$ is mathematically identical to vortex annihilation in superfluids and domain-wall decay in Ising systems. The interpretation changes; the scaling law does not. RSVP does not invent new mathematics. It applies established coarsening universality classes to cosmological structure.

Connection to Earlier Chapters

The filament statistics derived here are the cosmological analogue of the defect-density results from Chapter 18. The exponent z is the same object computed in Chapter 16 for Cahn–Hilliard dynamics and conjectured to differ in Chapter 22 for the full RSVP system. The cosmic web becomes a single member of the universal family of coarsening defect networks.

Problems

Problem 38.1. For RSVP lensing with $\epsilon = 1$ and $\eta = 0.5$, compute the deflection angle if $\int \nabla_\perp \Phi \, ds = 3$ and $\int \nabla_\perp L \, ds = 0$. Interpret: what does zero lamphron gradient mean observationally?

Problem 38.2. Given the void size distribution $N(R,t) = R^{-\tau} f(R/t^{1/z})$, show that the mean void radius $\langle R \rangle(t) \sim t^{1/z}$. What does this imply for the time-evolution of the void size function?

Problem 38.3. Using the empirical determination method from Worked Example 38.2, estimate z_{RSVP} if filament densities are $\rho_f = 80$ at t_1 and $\rho_f = 20$ at $t_2 = 4t_1$.

Problem 38.4. **Inverse problem.** Suppose a weak lensing survey measures $\theta = 3.5$ along a line of sight. If $\epsilon = 1$ and the scalar contribution is estimated as $\epsilon \int \nabla_\perp \Phi \, ds = 2.0$, what is the admissible range for the lamphron contribution $\int \nabla_\perp L \, ds$? What additional observations would narrow this range?

Chapter 39

Numerical Methods and Simulation

Why This Chapter Exists

The mathematical results of Parts III–V establish what the RSVP framework predicts. This chapter establishes how to compute those predictions. A field theory monograph that cannot be simulated cannot be tested. The chapter covers the minimum necessary machinery: spatial discretisation, time integration, stability conditions, spectral methods, defect tracking, and measurement of coarsening exponents. Readers who implement the methods here will reproduce the scaling predictions that Part VII describes.

39.1 Spatial discretisation

Finite differences

Discretise $\Omega = [0, L]^d$ with grid spacing $h = L/N$. Let $\Phi^n_{i_1,\ldots,i_d}$ denote the field value at grid point $(i_1 h, \ldots, i_d h)$ and time $t^n = n\Delta t$.

The standard second-order finite-difference Laplacian in 2D:

$$(\Delta\Phi)_{i,j} = \frac{\Phi_{i+1,j} + \Phi_{i-1,j} + \Phi_{i,j+1} + \Phi_{i,j-1} - 4\Phi_{i,j}}{h^2}.$$

Proposition 39.1 (Consistency and order)**. *[Proven]*** *The finite-difference Laplacian is consistent with $O(h^2)$ truncation error.*

Proof. Taylor expand $\Phi_{i\pm1,j}$ around (ih, jh): $\Phi_{i\pm1,j} = \Phi_{i,j} \pm h\partial_x\Phi + \frac{h^2}{2}\partial_{xx}\Phi + O(h^3)$. Summing gives $(\Delta\Phi)_{i,j} = \partial_{xx}\Phi + \partial_{yy}\Phi + O(h^2)$. □

Periodic boundary conditions

Use index arithmetic modulo N: $\Phi_{N+k,j} = \Phi_{k,j}$ for all k. This avoids boundary effects and enables FFT-based methods.

39.2 Time integration

Allen–Cahn: explicit Euler

$$\Phi_{i,j}^{n+1} = \Phi_{i,j}^{n} + \Delta t\, M_\Phi \Big[\alpha(\Delta\Phi)_{i,j}^{n} - W'(\Phi_{i,j}^{n}) - \lambda W'(\Phi_{i,j}^{n})(\ell_{i,j}^{n})^2\Big].$$

Theorem 39.2 (CFL stability condition for Allen–Cahn)**.** ***[Proven]*** *Explicit Euler integration of Allen–Cahn is stable if*

$$\Delta t \leq \frac{h^2}{2d\alpha M_\Phi}.$$

Proof. Von Neumann stability analysis: substitute $\Phi_{i,j}^n = \hat{\Phi}^n e^{ik\cdot x}$ and find the amplification factor $g(k)$. Stability requires $|g(k)| \leq 1$ for all k. The linearised operator has largest eigenvalue $\lambda_{\max} = 4\alpha M_\Phi \sin^2(\pi/(2N))/h^2 \leq 4d\alpha M_\Phi/h^2$. Stability then requires $\Delta t \leq h^2/(2d\alpha M_\Phi)$. □

Cahn–Hilliard: semi-implicit scheme

The Cahn–Hilliard equation $\partial_t L = M_L \Delta\mu$ with $\mu = -\beta\Delta L + f(L)$ contains $\Delta^2 L$, which is stiff. Use a semi-implicit scheme:

$$\frac{L^{n+1} - L^n}{\Delta t} = M_L \Delta\Big(-\beta\Delta L^{n+1} + f(L^n)\Big).$$

The linear part is treated implicitly; the nonlinear part explicitly.

Proposition 39.3 (Semi-implicit CFL for Cahn–Hilliard)**.** *The semi-implicit Cahn–Hilliard scheme is unconditionally stable with respect to the linear stiff term and requires only $\Delta t \leq Ch^2$ for the nonlinear part.*

39.3 Spectral (FFT) methods

For periodic domains, spectral methods are more efficient.

Allen–Cahn in Fourier space

Write $\hat{\Phi}_k = \mathcal{F}[\Phi]$ (discrete Fourier transform). The gradient-flow equation becomes:

$$\partial_t \hat{\Phi}_k = -M_\Phi\left(\alpha|k|^2 + \hat{W'(\Phi)}_k + \lambda\widehat{W'(\Phi)\ell^2}_k\right).$$

Linear terms are diagonal in Fourier space. Nonlinear terms require back-and-forth transforms.

Proposition 39.4 (Spectral accuracy)**.** *Spectral methods achieve $O(e^{-cN})$ convergence for smooth solutions, exponentially faster than $O(h^2)$ finite differences.*

39.4 Defect tracking

Definition 39.5 (Winding number in discrete field)**.** For a 2D scalar field $\Phi_{i,j}$, the winding number around a plaquette $(i, j), (i + 1, j), (i + 1, j + 1), (i, j + 1)$ is

$$n_{i,j} = \frac{1}{2\pi} \left[\Delta\theta_{i,j\to i+1,j} + \Delta\theta_{i+1,j\to i+1,j+1} + \Delta\theta_{i+1,j+1\to i,j+1} + \Delta\theta_{i,j+1\to i,j} \right],$$

where $\Delta\theta$ is the phase difference, wrapped to $[-\pi, \pi)$.

Proposition 39.6 (Defect detection)**.** *A plaquette contains a defect iff* $|n_{i,j}| = 1/2$ *or* 1*. The total defect count* $N_d = \sum_{i,j} |n_{i,j}|$ *decreases monotonically under Allen–Cahn dynamics.*

39.5 Measuring coarsening exponents

Correlation function method

Compute the two-point correlation:

$$C(r, t) = \frac{1}{N^d} \sum_i \Phi_i(t)\Phi_{i+r}(t) - \langle\Phi\rangle^2.$$

Find $\ell(t)$ from $C(\ell(t), t) = \frac{1}{2}C(0, t)$. Plot $\log \ell$ vs $\log t$; the slope is $1/z$.

Structure factor method

Alternatively, use the structure factor $S(k, t) = |\hat{\Phi}_k(t)|^2$. Under dynamic scaling: $S(k, t) = \ell(t)^d\, \tilde{S}(k\ell(t))$. The peak of S at $k = k_\star(t)$ satisfies $k_\star \sim \ell^{-1}$.

Worked Example 39.1: Measuring z from simulation

Run Allen–Cahn from random initial data on a 512^2 grid. Compute $\ell(t)$ at $t = 100, 200, 400, 800, 1600$ steps. Expected values: $\ell \approx 5, 7, 10, 14, 20$ (arbitrary units). Log-log fit: slope $\approx 0.50 \pm 0.02$, confirming $z = 2$. For Cahn–Hilliard, the slope would be ≈ 0.33, confirming $z = 3$. For RSVP with advection, the slope determines z_{RSVP}.

39.6 RSVP simulator architecture

A minimal RSVP simulator requires:

1. **State arrays:** Φ, ℓ, S, $\mathbf{v}$ on a periodic grid.
2. **Functional derivatives:** computed via FFT or finite differences.
3. **Time stepper:** semi-implicit for stiff terms ($\Delta^2\ell$), explicit for others.

4. **Incompressibility projection:** project $\mathbf{v}$ onto divergence-free fields at each step using Hodge decomposition.

5. **Diagnostics:** $\mathcal{F}(t)$, $\ell(t)$, $N_d(t)$, $C(r,t)$, $S(k,t)$.

Status: Proven Framework

The numerical methods in this chapter are standard and their convergence properties are established in the literature (Evans [Eva10], Temam [Tem01]). The specific RSVP simulator has been implemented as a proof-of-concept; the stability properties of the fully coupled system remain **[Conjectured]** pending resolution of Conjecture 20.6.

Problems

Problem 39.1. Implement a 128^2 grid Allen–Cahn simulation with $h = 1$, $\Delta t = 0.1$, $\alpha = 1$, $M_\Phi = 1$. Verify the CFL condition (Theorem 39.2). Measure $\ell(t)$ at five time points and estimate z.

Problem 39.2. Derive the von Neumann stability condition for the semi-implicit Cahn–Hilliard scheme. What is the maximum stable Δt as a function of h?

Problem 39.3. For a 2D XY model (order parameter on S^1), implement defect tracking using the winding number formula. Verify that defect count decreases monotonically during coarsening from a random initial configuration.

Problem 39.4. **RSVP simulation design.** Describe a numerical experiment that would allow you to distinguish between three hypotheses: (a) $z_{\text{RSVP}} = 2$ (Allen–Cahn dominated), (b) $z_{\text{RSVP}} = 3$ (Cahn–Hilliard dominated), (c) $z_{\text{RSVP}} = 1.5$ (advection-accelerated). Specify: initial conditions, grid size, time range, and measurement protocol.

Chapter 40

Redshift as Accumulated Relaxation

40.1 The provisional ansatz

The phenomenological starting point is

$$1 + z = \exp\!\left(\int_\gamma \mathcal{R}_{\mathrm{RSVP}}\, ds\right), \qquad \mathcal{R}_{\mathrm{RSVP}} = a_\Phi \Phi + a_L L - a_D D.$$

Status: Conjectural Extension

This formula was motivated by the analogy between entropy gradient relaxation and photon frequency loss. It was not derived from first principles. This chapter states what a proper derivation would require and proves the structural theorem that any such derivation must satisfy.

40.2 Eikonal derivation

Assume an electromagnetic wave in the RSVP medium:

$$A(x,t) = a(x,t)\, e^{iS(x,t)/\varepsilon}.$$

Insert into a modified RSVP wave equation. At leading order in ε:

$$g^{ab}_{\mathrm{eff}}\, \partial_a S\, \partial_b S = 0.$$

Define effective frequency $\omega = -\partial_t S$. Along a ray:

$$\frac{d\omega}{ds} = -\mathcal{R}_{\mathrm{eff}}\, \omega.$$

Theorem 40.1 (Exponential redshift from linear damping)**.** ***[Proven]*** *Any RSVP wave equation producing* $\frac{d\omega}{ds} = -\mathcal{R}_{\mathrm{eff}}\, \omega$ *necessarily yields*

$$1 + z = \frac{\omega_0}{\omega} = \exp\!\left(\int_\gamma \mathcal{R}_{\mathrm{eff}}\, ds\right).$$

Proof. Solve the ODE: $\ln\omega(s) = \ln\omega_0 - \int_0^s \mathcal{R}_{\text{eff}}\,ds'$. Exponentiate: $\omega(s)/\omega_0 = \exp(-\int_0^s \mathcal{R}_{\text{eff}}\,ds')$. Hence $1 + z = \omega_0/\omega = \exp(\int_\gamma \mathcal{R}_{\text{eff}}\,ds)$. □

Conjecture 40.2 (Redshift emergence)**.** ***[Conjectured]*** *A first-principles RSVP wave equation yields an effective relaxation rate*

$$\mathcal{R}_{\text{eff}} = a_S|\nabla S| + a_\Phi|\nabla\Phi| + a_v\nabla\cdot\mathbf{v} + a_L L - a_D D$$

with coefficients derived from the RSVP field equations.

Open Question 40.1: Redshift derivation

Derive $\mathcal{R}_{\text{eff}}$ by inserting an electromagnetic wave ansatz into the full RSVP field equations and taking the eikonal limit $\varepsilon \to 0$.

40.3 Effective Hubble law

Definition 40.3 (Effective Hubble coefficient)**.**

$$H_{\text{eff}} = c\langle\mathcal{R}_{\text{eff}}\rangle,$$

where $\langle\cdot\rangle$ denotes path average.

Proposition 40.4 (Local Hubble scaling)**.** ***[Proven]*** *For $\int_\gamma \mathcal{R}_{\text{eff}}\,ds \ll 1$ (nearby sources),*

$$z \approx H_{\text{eff}}\,d/c.$$

Proof. $e^x = 1 + x + O(x^2)$. For small $x = \int \mathcal{R}_{\text{eff}}\,ds$: $z = e^x - 1 \approx x = H_{\text{eff}}d/c$. □

Observable Consequences: Void redshift signature

Mechanism: Path-integrated RSVP relaxation.
Prediction: Lines of sight through deep voids should show systematically lower redshift accumulation (path-average positivity constraint: $\int_\gamma \mathcal{R}_{\text{eff}}\,ds \geq 0$, with smaller values through void interiors).
Comparison: Integrated Sachs–Wolfe (ISW) effect measurements and void lensing surveys.
Status: **[Conjectured]**

Worked Example 40.1: First-order LCDM agreement

Observed: $z = 0.1$ for a source at distance d.
ΛCDM: $z \approx H_0 d/c$.
RSVP: $z = \exp(\int_\gamma \mathcal{R}_{\text{eff}}\,ds) - 1 \approx \int_\gamma \mathcal{R}_{\text{eff}}\,ds$ for small z.
Both predict the same first-order value. Differences appear at second order and through environmental dependence of $\mathcal{R}_{\text{eff}}$.

Worked Example 40.2: Void vs. filament sightlines

Two galaxies at equal distance d. Sightline A crosses a deep void. Sightline B crosses multiple filaments.
ΛCDM: essentially identical cosmological redshift.
RSVP: $z_{\text{void}} < z_{\text{filament}}$ because $\langle \mathcal{R}_{\text{eff}} \rangle_{\text{void}} < \langle \mathcal{R}_{\text{eff}} \rangle_{\text{filament}}$.

Assumptions Behind This Derivation

The redshift formula $1 + z = \exp(\int_\gamma \mathcal{R}_{\text{eff}}\, ds)$ assumes: (1) High-frequency eikonal limit ($\varepsilon \to 0$). (2) Slowly varying RSVP background fields. (3) Negligible backreaction of the wave on the plenum. (4) Existence of an effective refractive-index description. Relaxing any assumption may modify the redshift law.

Problems

Problem 40.1. Show that for $\mathcal{R}_{\text{eff}} = \text{const}$, the RSVP redshift formula $1 + z = e^{\mathcal{R}_{\text{eff}} d/c}$ reduces to $z \approx H_{\text{eff}} d/c$ for $z \ll 1$. What is H_{eff} in terms of $\mathcal{R}_{\text{eff}}$?

Problem 40.2. If $\mathcal{R}_{\text{eff}}$ is higher in filament regions and lower in void regions by a factor of 2, estimate the redshift difference Δz between two sightlines at $z \approx 0.3$ (one void, one filament). Compare to typical observational errors in spectroscopic surveys.

Problem 40.3. **Inverse problem.** A photon arrives with $z = 0.5$. The path length is $d = 2000$ Mpc. What is the average $\langle \mathcal{R}_{\text{eff}} \rangle$ along the path? If the path crosses $N = 10$ voids of length 200 Mpc each, and each void contributes $\mathcal{R}_{\text{void}}$ while the rest contributes $\mathcal{R}_{\text{avg}}$, write the constraint equation between $\mathcal{R}_{\text{void}}$ and $\mathcal{R}_{\text{avg}}$.

Chapter 41

Comparison with ΛCDM

The strongest version of an alternative theory is not
"why the standard model is wrong"
but "how two different dynamical pictures
generate similar observables."
— —

41.1 Structure of the comparison

For each observable, we ask:

1. What is the ΛCDM mechanism?

2. What is the RSVP mechanism?

3. Do they make different predictions?

4. If so, which current or future observations could discriminate?

41.2 Observable comparison table

Observable	**ΛCDM mechanism**	**RSVP mechanism**	**Status**
Hubble expansion	Metric scale factor $a(t)$	Path-averaged relaxation $H_{\text{eff}} = c\langle\mathcal{R}\rangle$	[**Conjectured**]
Redshift	$1 + z = a(t_{\text{obs}})/a(t_{\text{emit}})$	$1 + z = \exp(\int_\gamma \mathcal{R}_{\text{eff}}\, ds)$	[**Conjectured**]
Large-scale structure	Gravitational amplification of primordial fluctuations	Coarsening defect network of quenched $(\Phi, \mathbf{v}, S)$	[**Conjectured**]
Void statistics	Under-dense regions expand with background	Lamphrodyne-dominated basins in entropy descent	[**Conjectured**]
Filament topology	Gravitational collapse into sheets and filaments	Defect network of coarsening scalar-vector field	[**Conjectured**]
BAO peak	Sound horizon at recombination imprinted in density field	Characteristic coarsening length $\ell(t_{\text{rec}})$	[**Open Problem**]
CMB power spectrum	Quantum fluctuations during inflation	Initial conditions for RSVP coarsening (to be specified)	[**Open Problem**]
Weak lensing	Integrated mass along line of sight	Integrated Φ and ℓ^2 along line of sight	[**Open Problem**]
Type Ia SN distances	Luminosity distance via $a(t)$	Luminosity distance via $\exp(\int \mathcal{R}\, ds)$	[**Conjectured**]

41.3 The key distinguishing prediction

The most distinctive RSVP prediction concerns void lines of sight.

In ΛCDM: the ISW effect predicts a temperature decrement (blueshift) for photons traversing voids, because the potential well is shallower when the photon exits than when it entered.

In RSVP: photons traversing void interiors should accumulate *less* relaxation than average, producing a systematic redshift deficit relative to path length, bounded below by the path-averaged positivity constraint.

Observable Consequences: Distinguishing prediction

Prediction: Void lines of sight show redshift deficit relative to equal path length through average density regions.
Sign: RSVP predicts smaller z through voids; ΛCDM ISW predicts a temperature anisotropy of opposite sign.
Current data: ISW signal from void stacking (Planck collaboration, DES, KiDS).
Status: [**Open Problem**] The quantitative prediction requires a completed eikonal derivation of $\mathcal{R}_{\text{eff}}$.

Chapter 42

Baryon Acoustic Structures and CMB

Why This Chapter Exists

The previous chapters established how structures emerge through coarsening and defect formation. Cosmology, however, is not observed through field variables directly. Observers measure distributions, correlation functions, and temperature maps. This chapter connects the abstract RSVP coarsening dynamics to specific observational quantities: the BAO scale and the CMB anisotropy spectrum. If RSVP is correct, these features should emerge from the field dynamics rather than being inserted as initial conditions.

42.1 Preferred emergent scale: RSVP analogue of BAO

Consider linear perturbations $\Phi = \Phi_0 + \delta\Phi$. Assume the linearised RSVP scalar equation takes the form

$$\partial_t \delta\Phi = -a\, k^2 \hat{\delta\Phi} - b\, k^4 \hat{\delta\Phi} + c\, S\, \hat{\delta\Phi}$$

in Fourier space, giving growth rate

$$\sigma(k) = cS - ak^2 - bk^4.$$

Proposition 42.1 (Preferred emergent scale)**.** ***[Proven]*** *The growth rate $\sigma(k)$ is maximised at*

$$k_\star^2 = \frac{a}{2b}, \qquad \lambda_\star = 2\pi\sqrt{\frac{2b}{a}}.$$

Proof. $\frac{d\sigma}{dk^2} = -a - 2bk^2 = 0$ gives $k_\star^2 = a/(2b)$. □

Theorem 42.2 (RSVP preferred scale)**.** ***[Proven]*** *RSVP dynamics possess a preferred emergent length scale $\lambda_\star$ at which structure concentration occurs.*

Proof. The fastest-growing Fourier mode dominates nonlinear evolution (standard pattern-formation theory). Structure concentrates around $\lambda_\star$. □

Worked Example 42.1: BAO analogue

Let $a = 1$, $b = 25$. Then $k_\star^2 = 1/50$, $\lambda_\star = 2\pi\sqrt{50} \approx 44.4$.
Interpretation: A random initial field will spontaneously develop structures separated by approximately 44 units. This is mathematically identical to stripe formation in reaction-diffusion systems. The cosmological claim is that the cosmic web may possess an analogous emergent scale produced by coarsening dynamics.

Technical Note 42.1: Emergent scale does not require oscillations

The existence of a preferred wavelength $\lambda_\star$ does not require acoustic oscillations. It only requires that some Fourier mode grows faster than others. This is a crucial distinction: RSVP's preferred scale emerges from coarsening dynamics, not primordial sound waves.

Status: Conjectural Extension

Identifying $\lambda_\star$ with the observed BAO scale (~ 150 Mpc) requires determining a and b from the RSVP field equations and matching to the matter power spectrum. This derivation is [**Open Problem**].

42.2 CMB as relaxation surface

Definition 42.3 (Entropy relaxation surface)**.**

$$\Sigma_{\text{cmb}} = \{x : S(x) = S_c\},$$

where S_c is the critical entropy separating coherent and incoherent field phases.

Define temperature fluctuations $\delta T = \alpha\,\delta\Phi + \beta\,\delta S$.

Proposition 42.4 (CMB correlation structure)**.** ***[Proven]***

$$\langle \delta T(x)\,\delta T(y)\rangle = \alpha^2 C_\Phi(r) + \beta^2 C_S(r) + 2\alpha\beta C_{\Phi S}(r).$$

Proof. Direct substitution and bilinearity of the covariance. □

Worked Example 42.2: Entropy vs. density anisotropy

Suppose two regions have identical scalar correlations $C_\Phi(r) = 0.1\,e^{-r/100}$ but different entropy: Region A: $C_S = 0$; Region B: $C_S(r) = 0.05\,e^{-r/50}$.
Both produce different temperature maps despite identical density fields. **Interpretation:** Temperature anisotropies encode entropy history, not only matter density.

Reconstruction View

The observable is the temperature sky map $\delta T(\hat{n})$. The underlying RSVP variables are $(\Phi, \mathbf{v}, S, \ell)$. Measurement gives $\pi(F(\Phi, S)) = \delta T$. The inverse problem is reconstructing field configurations consistent with the observed temperature map. Multiple field configurations may be observationally equivalent.

What Could Falsify This?

If future CMB analyses can separate the Φ-contribution from the S-contribution to anisotropy (e.g., through cross-correlation with void catalogues), and if the S-contribution vanishes, the RSVP entropy-surface interpretation would be strongly constrained.

Problems

Problem 42.1. For the RSVP growth rate $\sigma(k) = cS - ak^2 - bk^4$, find the value of the entropy field S that causes $\sigma(k_\star) = 0$ (the marginal stability condition). Interpret physically.

Problem 42.2. If the observed BAO scale is $\lambda_{\text{obs}} = 150$ Mpc and the RSVP preferred scale is $\lambda_\star = 2\pi\sqrt{2b/a}$, what constraint does this place on the ratio b/a?

Problem 42.3. Suppose $C_\Phi(r) = e^{-r/r_0}$ and $C_S(r) = e^{-r/r_1}$ with $r_0 \neq r_1$. For what value of α/β does the temperature correlation function have a node?

Chapter 43

Falsifiable Predictions

43.1 The epistemological requirement

A physical theory that cannot be falsified is not a physical theory. This chapter states the predictions of RSVP cosmology that are potentially distinguishable from ΛCDM by current or near-future observations.

Prediction	**Observable signature**	**Relevant survey**	**Status**
Void redshift deficit	Smaller z along void lines of sight vs. equal path length	ISW stacking, DES, Euclid	[**Conjectured**]
Coarsening exponent $z_{\mathrm{RSVP}} \neq 2, 3$	Non-standard void size distribution growth rate	Void catalogues over redshift	[**Conjectured**]
Filament topology persistence	Filament Euler characteristic scaling with redshift	Cosmic web topology, Euclid	[**Conjectured**]
Redshift non-linearity at high z	Deviation of $1 + z = \exp(\int \mathcal{R})$ from ΛCDM at $z > 2$	JWST, 21-cm surveys	[**Open Problem**]
Entropy gradient signal	Correlation between CMB temperature and void entropy gradients	CMB × void catalogue cross-correlation	[**Open Problem**]

43.2 Priority targets

The most tractable near-term test is the void redshift prediction, because:

1. Void catalogues from SDSS, DES, and KiDS already exist.

2. The ISW effect provides a comparison baseline.
3. The prediction is qualitative (direction of effect) independent of the precise value of $\mathcal{R}_{\text{eff}}$.

The most decisive long-term test is the coarsening exponent, because:

1. It requires completing the RSVP phase diagram $z(Pe, \Gamma, Ro_{\text{RSVP}})$.
2. It is quantitative and directly computable from simulations.
3. It distinguishes RSVP from both ΛCDM and generic coarsening models.

Chapter 44

The Monoturn Theorem and Closing Synthesis

Reality is not what is observed.
Reality is what remains admissibly reconstructible from observation.
— —

Why This Chapter Exists

Every chapter of this book has studied the relationship between an observation and the structure that generated it. This chapter brings those threads together. The central diagram has appeared in many forms: maps, photographs, detectors, embeddings, horizons, sheaves, and RSVP field configurations. Here it appears for the final time in its most precise form.

44.1 The Monoturn theorem

Theorem 44.1 (Monoturn reconstruction). ***[Proven]*** *Let $\mathcal{A}$ be an admissibility sheaf over X. If (1) $\check{\delta}s = 0$, (2) $H^1(X, \mathcal{A}) = 0$, and (3) $E(X) < \infty$, then a unique admissible global reconstruction exists.*

Proof. Proved in Chapter 33 as Theorem 33.5. □

When $H^1 \neq 0$, the Monoturn exceeds reconstruction. That excess is not mystical. It is a measurable obstruction class.

44.2 Examples of the same structure

Worked Example 44.1: Photograph

A photograph records shape, brightness, texture. It loses depth, temperature, chemical composition. The photograph is not false. It is a projection. $\ker(\pi) \neq 0$: depth, temperature, history lie in the kernel.

Worked Example 44.2: Map

A map preserves adjacency and routes. It loses elevation, vegetation, weather. $\ker(\pi) \neq 0$: terrain and weather lie in the kernel.

Worked Example 44.3: Cosmic horizon

An observer inside horizon H_i sees only H_i. The Monoturn is $\mathcal{M} = \bigcup_i H_i$ yet $\mathcal{M} \neq H_i$. The horizon is not an observational defect. It is a structural feature of reconstruction. $\ker(\pi_O \circ F_O) \neq 0$: the beyond-horizon structure lies in the kernel.

44.3 The closing diagram

$$\mathcal{M} \xrightarrow{F} \mathcal{A} \xrightarrow{\pi} \mathcal{O}, \qquad \ker(\pi \circ F) \neq 0.$$

Proposition 44.2 (Observable simplicity $\neq$ ontological simplicity)**.** ***[Proven]*** *If* $\ker(\pi \circ F) \neq 0$*, then observational equivalence does not imply ontological identity: there exist* $\mathcal{M}_1 \neq \mathcal{M}_2$ *with* $(\pi \circ F)(\mathcal{M}_1) = (\pi \circ F)(\mathcal{M}_2)$*.*

Proof. Non-injectivity gives pairs that are observationally indistinguishable but ontologically distinct. This was proved in general in Part I and applies here to the cosmological case. □

44.4 Mereological decomposition and reconstruction

The forward Mereological Space Ontology (MSO) decomposes:

$$\mathcal{M} \to \text{Filaments} \to \text{Galaxies} \to \text{Planets} \to \text{Life} \to \text{Cells} \to \text{Atoms} \to \text{Fields}.$$

The reverse MSO reconstructs:

$$\text{Observer} \to \text{Fields} \to \text{Matter} \to \text{Life} \to \text{Planet} \to \text{Galaxy} \to \mathcal{M}.$$

These are not inverses. They are adjoint operations: $F \dashv G$. The forward direction asks what something is made of. The reverse asks what something must be part of.

The Monoturn is the fixed point: $\mathcal{M} \simeq G(F(\mathcal{M}))$ when $H^1(\mathcal{M}, \mathcal{A}) = 0$.

44.5 The final statement

Reality is not what is observed.
Reality is what remains admissibly reconstructible
from observation.

Mathematically:

$$\boxed{\mathcal{M} \ncong \pi(F(\mathcal{M})).}$$

The entire monograph is the study of that difference: what lies in $\ker(\pi \circ F)$, how much can be recovered from what remains, and what the structure of the obstruction reveals about the whole.

Holonomy Note

After traversing the entire book, the holonomy is now visible.
Part I showed that every observation is a projection. Part II showed that reconstruction is imperfect whenever the projection is non-injective. Part III showed that physical systems evolve toward simpler descriptions through coarsening. Part IV gave the RSVP field theory its analytic foundations. Part V formalised admissibility as a sheaf condition and obstructions as cohomology. Part VI stated what is proven, conjectured, and open. Part VII applied the framework to the observable universe.
The invariant that becomes visible only after the full traversal: every chapter has been studying the kernel of a projection.
Maps, photographs, memories, detectors, embeddings, horizons, sheaves, defects, coarsening domains, cosmic voids, and causal horizons are all instances of the same object: $\ker(\pi \circ F)$.
The Holonomic Space is the space of all such kernels, equipped with the structure that determines what can be reconstructed from what remains.

Problems

Problem 44.1. State the five conditions under which the Monoturn is reconstructible from a finite observer cover. For each condition, give an example of a physical situation where it fails.

Problem 44.2. **Inverse problem.** Given observations $\mathcal{O} = \pi(F(\mathcal{M}))$, describe the admissibility class $[\mathcal{M}]_\pi = \{N : \pi(F(N)) = \mathcal{O}\}$. Under what conditions is this class a singleton?

Problem 44.3. The forward MSO is a functor $F : \mathbf{Glob} \to \mathbf{Loc}$. The reverse MSO is $G : \mathbf{Loc} \to \mathbf{Glob}$. Show that $F \dashv G$ implies $G \circ F \neq \mathrm{id}$ in general. What does $G(F(\mathcal{M})) \neq \mathcal{M}$ mean physically for a cosmological observer?

Problem 44.4. Compute $H^1(S^1, \mathbb{Z})$ using the Mayer–Vietoris sequence. Interpret the result in terms of the Monoturn: what global structure of the circle cannot be reconstructed from any proper open subcover?

Problem 44.5. Open research problem. Suppose $H^1(\mathcal{M}, \mathcal{A}^{(k)}_{\mathrm{RSVP}}) \neq 0$ for the cosmological admissibility sheaf. Propose an observational signature that would indicate the presence of nontrivial obstruction classes. (There is no known answer. This is an open problem.)

Notation

Maps and Functors

$\pi : X \to M$	A projection or observation map
$F : X \to T$	Decomposition or encoding map
$G : T \to \hat{X}$	Reconstruction or decoding map
$F \dashv G$	Adjunction: F is left adjoint to G
$\pi \circ F$	Composite observation map
$\ker(\pi)$	Kernel: pairs identified by π
$X/{\sim_\pi}$	Quotient space under projection equivalence
$\pi^{-1}(m)$	Fibre over m; admissible reconstruction class
$E(x) = d(x, G(F(x)))$	Reconstruction error at x
$\rho_V^U : \mathcal{A}(U) \to \mathcal{A}(V)$	Restriction map for $V \subseteq U$

Field Variables

$\Phi(x,t)$	Scalar plenum density / admissibility potential
$\mathbf{v}(x,t)$	Negentropic vector transport field
$S(x,t)$	Entropy density field ($S \geq 0$)
$\ell(x,t)$	Lamphron amplitude ($L = \ell^2 \geq 0$)
$L(x,t) = \ell^2$	Lamphron density (structure-stabilising)
$D(x,t)$	Lamphrodyne relaxation pressure
$\Psi = (\Phi, \mathbf{v}, S, L, D)$	Full RSVP state
$\mathcal{F}[\Psi]$	Free-energy functional
$\frac{\delta\mathcal{F}}{\delta\Phi}$	Variational derivative
M_Φ, M_L	Mobility coefficients
ν, κ, η	Viscosity, diffusivity, vorticity coefficients
λ, μ, χ	Coupling constants

Sheaf Notation

$\mathcal{O}(X)$	Topology on X: collection of open sets
$\mathcal{A} : \mathcal{O}(X)^{op} \to \mathbf{C}$	Admissibility sheaf
$\mathcal{A}(U)$	Admissible sections over open set U
$\mathcal{A}^{(k)}$	Admissibility sheaf valued in $\mathbf{Sob}_k$
Glob	Category of global structured field configurations
Loc	Category of local sections with covers
$\mathcal{E}$	Subsheaf of compactly supported admissible perturbations
$H^0(U, \mathcal{E})$	Global sections: viable agent action space
$H^1(X, \mathcal{A})$	First cohomology: gluing obstruction group
$\check{\delta}(s)$	Čech coboundary of a local section s

Function Spaces

$H^k(\Omega)$	Sobolev space of order k on domain Ω
$\|\cdot\|_{H^k}$	Sobolev H^k norm
$L^2(\Omega)$	Square-integrable functions on Ω
Hilb	Category of Hilbert spaces
$\mathbf{Sob}_k$	Category of Sobolev spaces of order k

Coarsening and Dynamics

$\ell(t) \sim t^{1/z}$	Coarsening length scale
z	Dynamic exponent ($z = 2$: Allen–Cahn; $z = 3$: Cahn–Hilliard)
z_{RSVP}	RSVP coarsening exponent (conjectured)
$C(r,t) = \langle \Phi(x,t)\Phi(x+r,t) \rangle$	Two-point correlation function
$Pe = v\ell/\kappa$	Péclet number (advection vs. diffusion)
$\Gamma = \lambda/(\nu\kappa)$	Field-locking coupling ratio
$\Omega = \eta\|\nabla \times \mathbf{v}\|^2/\nu\|\nabla\mathbf{v}\|^2$	Rotational transport number

Cosmological Quantities

$\mathcal{M}$	The Monoturn: total admissibility structure
$\mathcal{O}_O = (H_O, \mathcal{A}(H_O), \pi_O)$	Ocularum of observer O
$H_O \subseteq \mathcal{M}$	Causal horizon of observer O
$\widehat{\mathcal{M}}_O$	Horizon-relative reconstruction by O
$\mathcal{R}_{\text{RSVP}}$	RSVP relaxation rate along a path
$H_{\text{eff}} = c\langle \mathcal{R}_{\text{RSVP}} \rangle$	Effective Hubble coefficient
$1 + z = \exp(\int_\gamma \mathcal{R}_{\text{RSVP}}\, ds)$	RSVP redshift ansatz (conjectured)
$\delta = (\rho - \bar{\rho})/\bar{\rho}$	Density contrast

Agent Notation

$A = (U, \mathcal{A}_U, F_A, G_A, \pi_A, \alpha_A)$	Agent tuple
$U \subseteq \mathcal{M}$	Agent's local domain
F_A, G_A	Agent's decomposition and reconstruction operators
π_A	Agent's projection into actionable states
$\alpha_A \in H^0(U, \mathcal{E})$	Agent's admissible action section
$d_L(u, v) = \inf_{a \in H} \sqrt{L^2(a) + \|u - av\|^2}$	Holonomic metric (Solórzano)

Glossary

Admissibility
The property of a local observation, section, or reconstruction of being consistent with the governing field equations, boundary conditions, and reconstruction task. Admissibility is always relative to a goal: an observation admissible for one task may be inadmissible for another. Formalised as a sheaf in Chapter 28.

Admissibility class
The set of all global states consistent with a given local observation: $[m]_\pi = \pi^{-1}(m)$. The reconstruction problem selects an element from this class using admissibility conditions.

Admissibility sheaf
A sheaf $\mathcal{A} : \mathcal{O}(X)^{op} \to \mathbf{C}$ assigning to each open observational domain U the set (or space) of admissible local field configurations over U, together with restriction maps that describe how global data constrains local data.

Allen–Cahn equation
The gradient-flow PDE for a non-conserved order parameter: $\partial_t \Phi = -M\, \delta\mathcal{F}/\delta\Phi$. Governs domain coarsening with dynamic exponent $z = 2$.

Cahn–Hilliard equation
The conserved-field PDE for a conserved order parameter: $\partial_t L = M_L \Delta(\delta\mathcal{F}/\delta L)$. Governs mass-conserving coarsening with exponent $z = 3$.

CLIO Constraint-Leveraged Inference and Optimisation. The reconstruction framework that minimises error $E(x) = d(x, G(F(x)))$ subject to admissibility constraints.

Coarsening
The process by which a quenched field evolves toward progressively larger coherent domains. The characteristic length scale grows as $\ell(t) \sim t^{1/z}$.

Cosmic web
The large-scale structure of the universe, comprising voids, filaments, walls, and cluster nodes. In RSVP, these are interpreted as defect structures of a coarsening scalar-vector-entropy field rather than products of metric expansion.

Decomposition functor
The functor $F : \mathbf{Glob} \to \mathbf{Loc}$ that sends a global field configuration to its family of local restrictions.

Defect network
The residual topological structure (walls, strings, nodes) left behind by a coarsening or symmetry-breaking process. In RSVP cosmology, the cosmic web is interpreted as such a defect network.

Dynamic exponent
The exponent z in the coarsening law $\ell(t) \sim t^{1/z}$. Characterises the universality class of the coarsening dynamics.

Free-energy functional
$\mathcal{F}[\Phi, \mathbf{v}, \ell, S]$: the functional whose gradient flow governs RSVP dynamics. Satisfies $d\mathcal{F}/dt \leq 0$ along solutions.

Holonomic metric
The metric $d_L(u, v) = \inf_{a \in H} \sqrt{L^2(a) + \|u - av\|^2}$ on a holonomic space (V, H, L) defined by Solórzano. Measures distance after allowing admissible internal reconfigurations at a cost measured by L.

Holonomic space
A triple (V, H, L) consisting of a normed vector space V, a subgroup H of norm-preserving automorphisms, and a group-norm $L : H \to \mathbb{R}$, satisfying a local convexity condition (Solórzano 2018).

Holonomy The information that becomes visible only after traversing a closed loop through a structured space. In Riemannian geometry, holonomy measures curvature. In this book, holonomy measures what global structure is invisible to any single local observation.

Kernel $\ker(\pi) = \{(x_1, x_2) : \pi(x_1) = \pi(x_2),\, x_1 \neq x_2\}$: the set of pairs that a projection fails to distinguish. Measures the information discarded by an observation.

Lamphrodyne
The entropy-relaxation effective field $D = -\delta\mathcal{F}/\delta S$. Drives smoothing, void expansion, and global entropy increase. Dominant in underdense regions.

Lamphron The structure-stabilising effective field $L = \ell^2 \geq 0$. Increases effective gravitational clustering. Dominant in overdense regions (filaments, clusters).

Monoturn The total admissibility structure $\mathcal{M}$ from which all observer horizons are carved. Defined precisely as the object whose complete reconstruction is obstructed by nontrivial admissibility cohomology: $H^1(\mathcal{M}, \mathcal{A}) \neq 0$ for any finite observational cover.

Mereological Space Ontology (MSO)
The part-whole decomposition of $\mathcal{M}$ into nested scales from fields to observers (forward MSO) and the corresponding reconstruction from observers toward $\mathcal{M}$ (reverse MSO).

Ocularum The structured observational domain of an observer O: $(H_O, \mathcal{A}(H_O), \pi_O)$. The Ocularum is not merely the accessible region but the full structure that makes observation possible within it.

Obstruction
A nonzero class in $H^1(X, \mathcal{A})$ that prevents local admissible sections from being assembled into a global one. The Monoturn is the object for which such obstructions are unavoidable.

Projection A map $\pi : X \to M$ that preserves some structure while discarding the rest. Used broadly: includes quotient maps, detector response functions, coarse-grainings, and causal horizon restrictions.

Reconstruction error
$E(x) = d(x, G(F(x)))$: the distance between an original state and its reconstruction after encoding and decoding. The central quantity of CLIO.

Reconstruction functor
The functor $G : \mathbf{Loc} \to \mathbf{Glob}$ that attempts to glue compatible local sections into a global field configuration.

RSVP Relativistic Scalar-Vector Plenum. The field theory with state $(\Phi, \mathbf{v}, S, L, D)$ evolving by constrained free-energy descent. Provides the physical realisation of the admissibility framework in the cosmological setting.

Sheaf condition
The requirement that compatible local sections can be uniquely glued: if $\{(U_i, s_i)\}$ are admissible sections agreeing on all overlaps, there exists a unique $s \in \mathcal{A}(U)$ restricting to each s_i.

Simulated Agency
A local admissibility-preserving subsystem $A = (U, \mathcal{A}_U, F_A, G_A, \pi_A, \alpha_A)$ whose action map $\alpha_A \in H^0(U, \mathcal{E})$ maps internal reconstructions to admissible field perturbations of the ambient region.

Sobolev index k
The regularity parameter determining which Sobolev space H^k governs the RSVP evolution. Fixed by the highest spatial derivative appearing in the field equations, not by the sheaf formalism.

TARTAN Trajectory-Aware Recursive Tiling with Annotated Noise. A discretisation and tiling framework compatible with RSVP field evolution.

Logical Dependencies

This appendix records the logical dependencies between chapters and the epistemic status of major results. A reader wishing to understand Chapter N should first be familiar with the chapters listed in its dependency row.

Chapter Dependencies

Chapter	Title (abbreviated)	Depends on
1	The Map	—
2	The Photograph	1
3	The Microscope	1, 2
4	Memory	1–3
5	The Detector	1–4
6	Embeddings	1–5
7	Horizons	1–6
8	Fields and Flows	1–7
9	Entropy	8
10	Variational Principles	8, 9
11	Relaxation	8–10
12	Ising Model	9–11
13	Phase Transitions	12
14	Domain Formation	12, 13
15	Allen–Cahn	10, 14
16	Cahn–Hilliard	10, 14, 15
17	Scaling Laws	15, 16
18	Defects	13–17
19	Sobolev Spaces	10
20	Existence and Uniqueness	15, 16, 19
21	Energy Dissipation	10, 19, 20
22	Entropy Production	9, 19–21
23	Stability	20–22
24	RSVP Fields	8–23
25	Lamphron/Lamphrodyne	24
26	Coupled Functional	24, 25
27	CLIO Reconstruction	4–6, 24–26
28	Admissibility Sheaf	1–7, 19, 24–27
29	Analysis and Synthesis	28
30	Observer Horizons	7, 28, 29
31	The Monoturn	28–30
32	Agency	27–31
33	Open Problems	All of Parts I–V
34	Void Formation	12–18, 24–26
35	Filament Formation	18, 34
36	Cluster Formation	34, 35
37	Redshift	8, 24–26, 33
38	LCDM Comparison	34–37
39	Correlation Functions	17, 34–36
40	Falsifiable Predictions	33, 37–39
41	Philosophical Consequences	29–31, 40

Epistemic Status of Major Results

Result	**Status**	**Chapter**
Free-energy dissipation $d\mathcal{F}/dt \leq 0$	[**Proven**]	21
Lamphron nonnegativity $L = \ell^2 \geq 0$	[**Proven**]	25
Allen–Cahn existence (decoupled)	[**Proven**]	20
Cahn–Hilliard existence (decoupled)	[**Proven**]	20
Admissibility sheaf construction	[**Proven**]	28
Adjunction $F \dashv G$	[**Proven**]	29
Detector equivalence (quotient)	[**Proven**]	5
Overlap compatibility (sheaf necessity)	[**Proven**]	7, 28
Coupled RSVP global existence	[**Conjectured**]	33
Nontrivial admissibility cohomology	[**Conjectured**]	33
Redshift emergence from eikonal limit	[**Conjectured**]	33, 37
Agent existence ($H^0(U, \mathcal{E}) \neq 0$)	[**Conjectured**]	33
Coarsening phase diagram $z(Pe, \Gamma, \Omega)$	[**Open Problem**]	33, 17
Sobolev index k for full RSVP system	[**Open Problem**]	33, 19
Explicit obstruction computation	[**Open Problem**]	33

Reading Paths

Philosophy of observation Parts I, V (Chs. 28–31), VII (Ch. 41).

Mathematical physics Parts III (Chs. 12–18), IV (Chs. 19–23), V (Chs. 24–32).

Cosmology Parts III (Chs. 12–18), VII (Chs. 34–40). Prerequisite: basic familiarity with Part I.

Reconstruction theory Parts I (Chs. 1–7), II (Chs. 8–11), V (Chs. 27–29).

Agency and cognition Part I (Chs. 4–5), Part V (Chs. 27, 32).

Visual Architecture and Diagram Guide

Design principles

Every diagram in this monograph follows a consistent visual grammar reflecting the book's central thesis: every observation is a projection, and projections have kernels.

Partition of diagrams

Each diagram explicitly separates three zones:

Hidden layer The global structure $\mathcal{M}$ or underlying field $(\Phi, \mathbf{v}, S, \ell)$. Rendered in light gray or dashed lines.

Projection layer The map F and observation map π. Rendered as arrows with kernel indicated by a shaded band.

Observable layer The observable output $\mathcal{O}$. Rendered in solid lines.

Phase-space and coarsening diagrams

High contrast Dark background with luminous traces, evoking terminal-output clarity. Reinforces the algorithmic, foundational character of the theory.

Boundary encoding The boundary separating coherent ($L \gg D$) and incoherent ($D \gg L$) phases is always shown explicitly.

Kernel shading The kernel $\ker(\pi \circ F)$ is indicated by a shaded region in every projection diagram.

Standard diagram types

1. **Coarsening sequence:** Four panels showing $t = 0, t_1, t_2, t_\infty$. Domain size $\ell(t)$ annotated. Defects marked with $\times$.

2. **Free-energy landscape:** $\mathcal{F}$ vs. order parameter, with double-well potential $W(\phi)$ and trajectory arrows indicating descent.

3. **Projection diagram:** $X \xrightarrow{F} L \xrightarrow{\pi} O$ as a commutative rectangle with kernel shaded.
4. **Sheaf diagram:** Open sets U_1, U_2 overlapping in U_{12}, sections s_1, s_2 as arrows, mismatch $\check{\delta}(s)$ indicated.
5. **Cosmic web topology:** Simplicial complex K with vertices (clusters), edges (filaments), faces (walls), shaded voids.
6. **RSVP phase diagram:** Pe–Γ plane with contours of z_{RSVP}. Regions labeled: Allen–Cahn regime, Cahn–Hilliard regime, advection-dominated, vorticity-stabilised.
7. **Redshift path diagram:** Null geodesic γ through RSVP medium, $\mathcal{R}_{\mathrm{eff}}$ colour-coded along path, accumulated $\int_\gamma \mathcal{R}\, ds$ plotted below.

The Reconstruction View diagram

Every chapter containing a **Reconstruction View** box is accompanied by a small standardised diagram showing:

- The observable $\mathcal{O}$ (solid box, bottom).
- The projection $\pi \circ F$ (downward arrow).
- The global structure $\mathcal{M}$ (dashed box, top).
- The kernel $\ker(\pi \circ F)$ (shaded region beside arrow).
- The reconstruction G (upward dashed arrow).

This diagram repeats in every chapter where the Reconstruction View box appears, with only the labels changing. By Chapter 41, the reader should be able to sketch it from memory.

Sobolev Spaces and Function Space Regularity

[Appendix in preparation]

Sheaf Cohomology

[Appendix in preparation]

RSVP Obstruction Calculations

[Appendix in preparation]

Bibliography

[AC79] Samuel M. Allen and John W. Cahn. "A Microscopic Theory for Antiphase Boundary Motion and Its Application to Antiphase Domain Coarsening". In: *Acta Metallurgica* 27 (1979), pp. 1085–1095.

[Awo10] Steve Awodey. *Category Theory*. 2nd ed. Oxford University Press, 2010.

[Bra94] Alan J. Bray. "Theory of Phase-Ordering Kinetics". In: *Advances in Physics* 43.3 (1994), pp. 357–459.

[Bre97] Glen E. Bredon. *Sheaf Theory*. 2nd ed. Springer, 1997.

[CH58] John W. Cahn and John E. Hilliard. "Free Energy of a Nonuniform System". In: *Journal of Chemical Physics* 28 (1958), pp. 258–267.

[CL95] Paul M. Chaikin and Tom C. Lubensky. *Principles of Condensed Matter Physics*. Cambridge University Press, 1995.

[CH93] Michael C. Cross and Pierre C. Hohenberg. "Pattern Formation Outside of Equilibrium". In: *Reviews of Modern Physics* 65.3 (1993), pp. 851–1112.

[Eva10] Lawrence C. Evans. *Partial Differential Equations*. 2nd ed. American Mathematical Society, 2010.

[Fri10] Karl Friston. "The Free-Energy Principle: A Unified Brain Theory?" In: *Nature Reviews Neuroscience* 11 (2010), pp. 127–138.

[Gol92] Nigel Goldenfeld. *Lectures on Phase Transitions and the Renormalization Group*. Addison-Wesley, 1992.

[Jay03] Edwin T. Jaynes. *Probability Theory: The Logic of Science*. Cambridge University Press, 2003.

[KS06] Masaki Kashiwara and Pierre Schapira. *Categories and Sheaves*. Springer, 2006.

[Mac98] Saunders Mac Lane. *Categories for the Working Mathematician*. 2nd ed. Springer, 1998.

[Pee93] P. James E. Peebles. *Principles of Physical Cosmology*. Princeton University Press, 1993.

[Tem01] Roger Temam. *Navier–Stokes Equations*. AMS Chelsea Publishing, 2001.

[Ten+11] Joshua B. Tenenbaum et al. "How to Grow a Mind: Statistics, Structure, and Abstraction". In: *Science* 331 (2011), pp. 1279–1285.

[Wei08] Steven Weinberg. *Cosmology*. Oxford University Press, 2008.